

# **Overexpression of CPEB3 leads to astrocyte dysfunction**

Dissertation

zur

Erlangung des Doktorgrades (Dr. rer. nat)

der

Mathematisch-Naturwissenschaftlichen Fakultät

der

Rheinischen Friedrich-Wilhelms-Universität Bonn

vorgelegt von

**Vamshidhar Reddy, Vangoor**

aus

Mahabubnagar, Indien

**Bonn, March 2013**

**Angefertigt mit Genehmigung der Mathematisch-Naturwissenschaftlichen Fakultät der  
Rheinischen Friedrich-Wilhelms-Universität Bonn**

1. Gutachter: Prof. Dr. Martin Theis
2. Gutachter: Prof. Dr. Klaus Willecke

Tag der Promotion: 08<sup>th</sup> July 2013

Erscheinungsjahr: 2013

## **Declaration**

I solemnly declare that the work submitted here is result of my own investigation, except where otherwise stated. This work has not been submitted to any other university or institute towards the partial fulfillment of any degree.

Bonn, March 2013

**Vamshidhar Reddy Vangoor**

## **Acknowledgements**

I would like to express my deepest gratitude to my supervisor Prof. Dr. Martin Theis for giving me the opportunity to perform this work in his research group and for his support throughout my PhD and giving valuable inputs and encouragement without which this work would have been not possible.

I would like to thank Prof. Dr. Christian Steinhäuser for his critical comments and suggestions during my PhD work.

I would like to thank Prof. Dr. Klaus Willecke, Prof. Dr. Walter Witke and Prof. Dr. Jochen Walter for accepting my request to be part of the doctoral committee.

I would like to thank my colleagues Dr. Peter Bedner, Jiong Zhang, Pavel Dublin, Lech Kaczmarczyk, Anja Matijevic and Joana Fischer for their co-operation and help during my stay in the lab. I would like to thank Mrs. Yvette Simons and Dr. Ines Nauroth for their help with administrative things.

I would like to thank all other members of the Institute of Cellular Neurosciences. I would like to thank the animal caretakers at the HET and at the Genetics department.

I would like to thank my colleague and wife Sada Lakshmi for her continuous support as my best friend and life partner. Last but not least, I would like to thank my parents and brother for their love and moral support. I would like to also thank my friends in Bonn for making my stay a memorable one.

# Table of Contents

<b>Abbreviations</b> .....	<b>i</b>
<b>1 Introduction</b> .....	<b>1</b>
1.1 Cytoplasmic polyadenylation element binding (CPEB) proteins.....	1
1.2 Transgenic approaches for studying gene functions .....	5
1.3 Astrocytes .....	7
1.4 Gap junctions and connexins.....	9
1.5 Adult neurogenesis .....	13
1.6 Glutamate transporters and glutamine synthetase .....	15
1.7 Astrocyte dysfunction in Epilepsy .....	16
<b>2 Aim of the thesis</b> .....	<b>20</b>
<b>3. Materials and Methods</b> .....	<b>21</b>
<b>3.1 Materials</b> .....	<b>21</b>
3.1.1 Solutions and reagents (ready-to-use) .....	21
3.1.2 Kits used .....	21
3.1.3 Buffers and solutions .....	22
3.1.3.1 Western blotting (WB) buffers .....	22
3.1.3.2 Buffers for SDS-PAGE gel .....	23
3.1.3.3 Buffers for Immunofluorescence.....	23
3.1.3.4 Solutions for stainings .....	24
3.1.3.5 Solutions for genotyping .....	24
3.1.3.6 Solutions for bacterial cultures .....	25
3.1.4 Antibodies .....	26
3.1.4.1 Primary antibodies.....	26
3.1.4.2 Secondary antibodies.....	26
3.1.5 Restriction enzymes .....	27
3.1.6 Expression vectors.....	27
3.1.7 Competent cells .....	27
3.1.8 Lab devices .....	27
3.1.9 General lab materials.....	28
<b>3.2 Methods</b> .....	<b>29</b>
<b>3.2.1 Cell culture</b> .....	<b>29</b>
3.2.1.1 Primary astrocyte cell culture .....	29
3.2.1.2 Transfection.....	29
<b>3.2.2 RNA isolation and reverse transcription PCR from primary astrocytes in culture</b> .....	<b>29</b>
3.2.2.1 RNA purification .....	29
3.2.2.2 Reverse transcription PCR .....	30
<b>3.2.3 Immunocytochemistry</b> .....	<b>31</b>

3.2.3.1 Staining for CPEBs in primary astrocytes.....	31
3.2.3.2 Triple staining of primary cultures .....	32
<b>3.2.4 Generation of vectors for transgenic mice .....</b>	<b>32</b>
3.2.4.1 3' RACE of CPEB3 .....	32
3.2.4.2 Generation of vectors .....	33
3.2.4.3 Cloning of short and long UTRs of CPEB3 into pMM vector.....	34
3.2.4.4 Cloning of CPEB3d and CPEB3aKD into pMM403-400 vector.....	35
<b>3.2.5 Generation of CPEB3-GFAP transgenic mice.....</b>	<b>35</b>
3.2.5.1 Cloning .....	35
3.2.5.2 Construct preparation for zygote injection .....	35
3.2.5.3 Isolation of genomic DNA from mouse tail tips .....	36
3.2.5.4 Genotyping PCR.....	36
3.2.5.5 Breedings.....	37
3.2.5.6 Doxycycline treatment .....	37
<b>3.2.6 Immunohistochemistry .....</b>	<b>37</b>
3.2.6.1 Perfusion fixation .....	37
3.2.6.2 Cryoprotection and sectioning.....	38
3.2.6.3 Staining procedure.....	38
3.2.6.4 TUNEL staining .....	38
3.2.6.5 Nissl staining .....	39
3.2.6.6 Image acquisition and processing.....	39
3.2.6.7 Quantification .....	40
3.2.6.8 Electrophysiology and biocytin visualization .....	40
<b>3.2.7 Western blotting .....</b>	<b>41</b>
3.2.7.1 Sample preparation.....	41
3.2.7.2 SDS-PAGE, blotting and detection .....	41
3.2.7.3 Quantification.....	42
<b>3.2.8 RNA isolation and real time PCR.....</b>	<b>43</b>
3.2.8.1 RNA preparation from mouse brain.....	43
3.2.8.2 RNA purification and reverse transcription .....	43
3.2.8.3 Real time PCR.....	43
<b>3.2.9 Generation of luciferase vectors.....</b>	<b>44</b>
3.2.9.1 GS 3' RACE .....	44
3.2.9.2 Luciferase vectors.....	45
3.2.9.2.1 Isolation and cloning of WT and MUT 3' UTR of GS.....	45
3.2.9.2.2 Isolation and cloning of WT 3' UTR of Cx30.....	46
<b>3.2.10 Generation of the CPEB3a-FLAG vector .....</b>	<b>46</b>
<b>3.2.11 RNA Co-immunoprecipitation or pulldown .....</b>	<b>46</b>
3.2.11.1 HeLa cell culture and transfection.....	46
3.2.11.2 Co-IP assay .....	47
3.2.11.3 RNA extraction and reverse transcription .....	47
3.2.11.4 Real time PCR.....	48

<b>4. Results</b> .....	<b>49</b>
<b>4.1 Expression of CPEBs in primary astrocyte cultures</b> .....	<b>49</b>
4.1.1 Expression pattern of CPEB isoforms.....	49
4.1.2 Localization of CPEBs in astrocytes.....	50
4.1.3 Cx43 and GFAP downregulation.....	51
<b>4.2 Generation of CPEB3-GFAP transgenic mice</b> .....	<b>52</b>
4.2.1 Transgenic mouse generation.....	52
4.2.2 Genotyping of mice.....	53
4.2.3 Screening of lines.....	53
<b>4.3 Characterization of CPEB3-GFAP transgenic mice</b> .....	<b>54</b>
4.3.1 Expression of CPEB3 across brain regions.....	54
4.3.2 Localization of CPEB3 within astrocytes.....	55
4.3.3 Developmental deficit in CPEB3-GFAP mice.....	55
4.3.4 Doxycycline treatment.....	56
4.3.5 Extent of CPEB3 overexpression in astrocytes.....	57
4.3.6 Specificity of CPEB3 expression.....	57
4.3.7 Increase in GFAP immunoreactivity.....	58
4.3.8 No change in GFAP protein levels.....	59
4.3.9 CPEB3 overexpression did not affect the number of astrocytes.....	60
4.3.10 TUNEL staining.....	61
<b>4.4 Putative astrocytic mRNA targets</b> .....	<b>62</b>
<b>4.5 Interaction of CPEB3 with target mRNAs</b> .....	<b>63</b>
4.5.1 Co-IP of Cx43 mRNA.....	63
4.5.2 Co-IP of Cx30 mRNA.....	64
4.5.3 Co-IP of GS mRNA.....	65
<b>4.6 CPEB3 downregulates major astrocytic connexins</b> .....	<b>66</b>
4.6.1 Downregulation of Cx43.....	66
4.6.2 Downregulation of Cx30.....	67
<b>4.7 Role of CPEB3 in adult neurogenesis</b> .....	<b>70</b>
4.7.1 Reduced proliferation.....	70
4.7.2 Decreased number of granule neurons.....	71
4.7.3 Reduction in the number of BLBP positive cells.....	72
<b>4.8 Analysis of other targets in CPEB3 mice</b> .....	<b>73</b>
4.8.1 Downregulation of GS.....	73
4.8.2 Downregulation of GLT-1.....	74
<b>4.9 No significant change in the transcript levels of CPEB3 targets</b> .....	<b>75</b>
<b>4.10 Endogenous expression of CPEB3 in WT and transgenic mice</b> .....	<b>76</b>
<b>4.11 CPEB3 constructs for transgenic mice</b> .....	<b>77</b>
4.11.1 Investigation of the 3' end of CPEB3.....	78

4.11.2 Constructs generated with 3' regulatory elements of CPEB3.....	78
4.11.3 CPEB3d and CPEB3aKD constructs for transgenic mice.....	79
<b>5 Discussion .....</b>	<b>80</b>
5.1 Expression of CPEBs in astrocytes .....	80
5.2 CPEB3-GFAP transgenic mice .....	80
5.3 Bimodal impact on GFAP protein expression.....	82
5.4 Downregulation of astrocytic connexins by CPEB3 .....	82
5.5 Downregulation of GLT-1 and GS.....	85
5.6 CPEB3 regulation does not induce cell death or affects astrocyte identity.....	86
5.7 Upregulation of CPEB3 leads to astrocyte dysfunction .....	87
5.8 Regulation of CPEB3 activity .....	87
<b>6 Future outlook .....</b>	<b>89</b>
<b>7 Summary .....</b>	<b>92</b>
<b>8 References .....</b>	<b>93</b>
<b>9 Appendix .....</b>	<b>112</b>
I. Preparation of Competent cells for transformation.....	112
II. pMM403-400 vector map .....	113
<b>List of Figures .....</b>	<b>114</b>
<b>List of Tables.....</b>	<b>116</b>
<b>Curriculum Vitae .....</b>	<b>117</b>



## Abbreviations

µg	microgram
µl	microlitre
µM	micromolar
µm	micrometer
mM	millimolar
mg	milligram
nM	nanomolar
pm	picomoles
APS	Ammonium persulfate
BCA	Bicinchonic acid assay
Biocytin	N-biotinyl-L-lysine
bp	base pairs
CA1	Cornu Ammonis I
CamKII	Ca <sup>2+</sup> /Calmodulin dependent protein kinase II
CNS	Central nervous system
CPE	Cytoplasmic polyadenylation element
CPEB	Cytoplasmic polyadenylation element binding protein
Cx43	Connexin 43
Cx30	Connexin 30
CSF	Cerebrospinal fluid
DEPC	Diethylpyrocarbonate
DKO	Double knockout
DOX	Doxycycline
DT	Double transgenic
EAAT	Excitatory amino-acid transporter
ECL	Enhanced chemiluminescence
EDTA	Ethylene diaminetetraacetic acid
FAM	Fluorescein amidite
FITC	Fluorescein isothiocyanate
GABA	γ-aminobutyric acid
GAPDH	Glyceraldehyde-3-phosphate dehydrogenase
GFAP	Glial fibrillary acidic protein
GFP	Green fluorescent protein
GS	Glutamine Synthetase
H	Hour
HC	Hippocampus
HCs	Hemichannels
Iba1	Ionized calcium binding adaptor molecule 1
IF	Immunofluorescence
IHC	Immunohistochemistry
KO	Knockout
LB	Luria Bertani
Min	minutes
MUT	mutant
MTLE	mesial temporal lobe epilepsy
NeuN	neuronal nuclei antigen
NGS	Normal goat serum
NP40	Nonidet P-40

ORF	Open reading frame
PBS	Phosphate buffered saline
PFA	Paraformaldehyde
PN	Postnatal
PKA	Protein kinase A
PVDF	Polyvinylidene fluoride
RT	Room temperature
RACE	Rapid Amplification of cDNA ends
SDS	Sodium dodecyl sulfate
SDS-PAGE	Sodium dodecyl sulfate - polyacrylamide gel electrophoresis
Sec	Seconds
SOE-PCR	Splicing by overlapping extension – PCR
SO	Stratum Oriens
SLm	Stratum Lacunosum moleculare
SP	Stratum pyramidale
SR	Stratum radiatum
STAT3	Signal transducer and activator of transcription
TAMRA	Tetramethyl rhodamine
TBST	Tris-buffered saline and Tween20
TetO	Tetracycline operator
TE	Tris-EDTA
TEMED	Tetramethylethylenediamine
TRITC	Tetramethyl rhodamine isothiocyanate
TTA	Tetracycline transactivator
TUNEL	Terminal deoxynucleotidyl transferase dUTP nick end labeling
TLE	Temporal lobe epilepsy
UTR	Untranslated region
WB	Western Blot
WT	wild type

## **Amino acids**

Alanine - A  
 Serine – S

# 1 Introduction

Local protein synthesis is a key cellular mechanism required for several functions, in specifying the formation of axis and body pattern (Bashirullah et al., 1998), in responding to synaptic stimulation and modifying the neuronal synapses (Steward and Schuman, 2003) and also in the cell cycle (Groisman et al., 2000). The mRNAs involved in this process have to be transported and regulated locally. This process of transport and protein synthesis to the respective sites is regulated by mRNA-binding proteins (Wells, 2006). Many of these proteins bind to the regulatory elements in the 3' untranslated region (UTR) of the responsive mRNAs (Wells, 2006). Zip-code binding protein1 (ZBP1), a member of the heterogeneous nuclear ribo-nucleoprotein (hnRNP) family was found to bind the 3' UTR of  $\beta$ -actin mRNA in neurons and regulate its transport and translation (Huttelmaier et al., 2005). Similarly, Fragile X mental retardation protein (FMRP), hnRNPA2, Staufen1 and Staufen2 are other RNA binding proteins which are involved in mRNA transport in neurons (Eberhart et al., 1996; Shan et al., 2003; Kiebler et al., 2005). FMRP regulates metabotropic glutamate receptor (mGluR) dependent long term depression, a form of activity-induced, protein synthesis-dependent synaptic plasticity (Huber et al., 2002). The target mRNAs localized in the distinct compartments of the neuronal cell bodies are either translated upon external stimuli or kept in an inactive state (Wells, 2006). One class of mRNA-binding proteins which regulate translation by binding to the 3' regulatory elements of the target mRNAs are Cytoplasmic Polyadenylation Element Binding (CPEB) proteins.

## 1.1 Cytoplasmic polyadenylation element binding (CPEB) proteins

CPEBs are RNA binding proteins which recognize and bind to a *cis* element named cytoplasmic polyadenylation element (CPE) located upstream of the hexanucleotide (poly (A), AAUAAA) sequence at varying distances in the 3' UTR (McGrew and Richter, 1990). Structurally, CPEBs contain an N-terminal regulatory domain, two RNA recognition motifs and a zinc finger domain required for RNA recognition and binding (Fig. 1) (Hake and Richter, 1994; Stebbins-Boaz et al., 1996; Hake et al., 1998; Theis et al., 2003b).



Figure 1: CPEB general domain structure. CPEB proteins contain an N-terminal regulatory domain (Reg domain) and a C-terminal RNA binding domain which consists of two RNA recognition motifs (RRM) (RRM1 and RRM2) and a Zinc finger domain (Znf).

The general consensus CPE sequence is UUUUUAU (Mendez and Richter, 2001), in addition there are variable CPE sequences reported, as UUUUUAU (McGrew and Richter, 1990; Du and Richter, 2005) or UUUUAACA (Barkoff et al., 2000). Upon binding to the CPE-containing mRNAs, CPEBs regulate translation of the bound mRNA. CPEB is a key factor that regulates the process of cytoplasmic polyadenylation by elongating the poly(A) tails upon external stimuli, thus ensuing translation (Groisman et al., 2001). The founding member of the CPEB family, CPEB1, on which much of the studies were carried out is involved in key cellular processes either via translational activation (elongation of poly(A) tail) or translational repression of the target mRNAs (Mendez and Richter, 2001; Richter, 2007). Recently it was shown that the number of CPEs present, the distance between CPEs, and the distance between CPE and the poly(A) signal on a specific mRNA have a strong impact on the translation of mRNA, determining whether it is being translated or repressed by CPEB1 (Pique et al., 2008). In mammalian cells, CPEB1 was shown in a complex with stress granules, where the mRNAs can be stored until translated or these stored mRNAs can be degraded by recruiting dcp1 in so-called P bodies (Wilczynska et al., 2005).

So far, different mechanisms were proposed by which CPEB1 regulates its target mRNA, which were reviewed in detail recently (Villalba et al., 2011). In *Xenopus* oocytes, CPEB1 binds the mRNAs containing CPEs and keeps them translationally dormant in a complex containing maskin and eukaryotic initiation factor (eIF4E) (Mendez and Richter, 2001). The CPEB binding protein maskin prevents the interaction of mRNA-cap binding factor eIF4E with another translational initiation factor (eIF4G) by binding at the region normally occupied by eIF4G (Stebbins-Boaz et al., 1999). Upon oocyte maturation, CPEB1 is activated with progesterone by phosphorylation at serine 174 via Eg2 kinase, a member of the Aurora kinase family (Mendez et al., 2000a; Mendez et al., 2000b). Apart from CPEB1 phosphorylation, the cytoplasmic polyadenylation complex requires other factors, namely the cytoplasmic polyadenylation and specificity factor (CPSF) (Dickson et al., 1999) and poly (A) polymerase (PAP) (Gebauer and Richter, 1995) for translational activation. Upon CPEB1 phosphorylation, CPSF is recruited to the hexanucleotide and elongates the poly (A) tail, but also disrupts the maskin-eIF4E association and results in the interaction of eIF4G with eIF4E. The eIF4G/eIF4E complex then recruits the 43S ribosome at the start codon, resulting in translation of the bound mRNA (Cao and Richter, 2002; Richter and Lorenz, 2002).

In neurons, CPEB1 regulates the translation very similar to early *Xenopus* development (Wu et al., 1998; Huang et al., 2002) and directs the transport of the specific target mRNA (Huang et al., 2003). The CPE-containing mRNAs, maskin and CPEB1 are packed into a ribonucleoprotein (RNP) complex and transported to dendrites along microtubules (Huang et al., 2003). As depicted in Fig. 2, N-methyl-D-aspartate (NMDA) receptor stimulation at synapses activates Aurora A kinase which then phosphorylates CPEB1. This leads to the elongation of the poly (A) tail followed by the disruption of the maskin interaction with eIF4E and the translation of bound mRNA (Richter and Lorenz, 2002). The translation of the alpha subunit of the calcium/calmodulin-dependent protein kinase II ( $\alpha$ -CamKII) mRNA containing two CPEs is regulated by CPEBs (Wu et al., 1998; Wells et al., 2000; Huang et al., 2002). It was also shown that Calmodulin dependent kinase II (CamKII) can phosphorylate Thr171 of mouse CPEB1 (Atkins et al., 2004) indicating a positive feedback loop. Another maskin like protein named neuroguidin which interacts with CPEB1 is expressed in the mammalian CNS and present in the complex that inhibits translation in a CPE dependent manner (Jung et al., 2006).

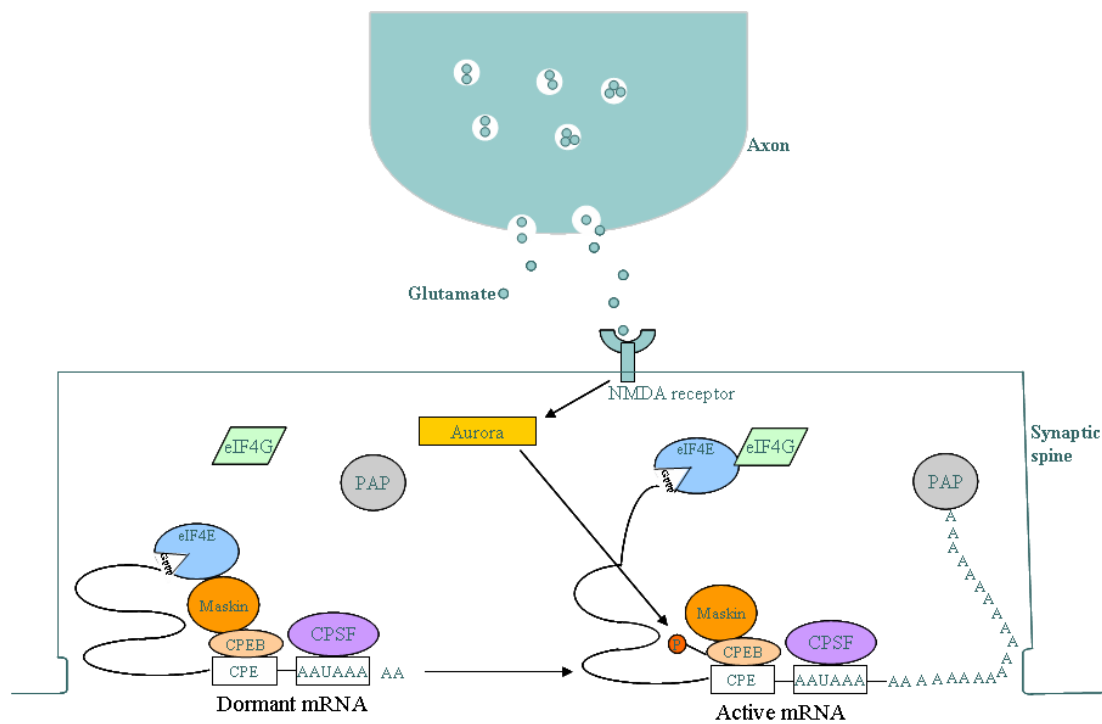


Figure 2: A model of synapse-specific translational control. CPEB1 in the non-phosphorylated state is inactive and keeps the mRNA dormant. Upon activation via glutamate (shown as small circles), the NMDA receptor activates Aurora kinase which in turn phosphorylates CPEB1 interacting with CPE. Recent findings indicate CamKII $\alpha$  might also phosphorylate CPEB1 (Atkins et al., 2004). The hexanucleotide (AAUAAA) binding protein CPSF probably gets stabilized by this modification of CPEB1 and attracts poly (A) polymerase (PAP) which then catalyzes polyadenylation at the end of mRNA. This further enables maskin (CPEB1 associated protein) to dissociate from eIF4E, a cap binding factor and allowing eIF4G to bind eIF4E, which then initiates translation. Adapted and modified from Richter and Lorenz (2002).

In *Xenopus* oocytes, CPEB1 regulates the localization of cyclinB1 mRNA to the mitotic apparatus and involves in oocyte maturation during embryonic cell cycle (Groisman et al., 2000; Groisman et al., 2002). CPEB1 knockout (KO) mice have deficits in germ cell development, where CPEB1 regulates the mRNAs in the synaptonemal complex (Tay and Richter, 2001; Tay et al., 2003). CPEB1 KO mice exhibited deficits with some forms of long term potentiation (LTP) dependent on protein synthesis, whereas long term depression (LTD) was only weakly affected (Alarcon et al., 2004). Further, these mice showed alterations in their behavioural pattern related to hippocampus-dependent tasks (Berger-Sweeney et al., 2006). Moreover, CPEB1 is present at the post synaptic density (PSD) (Wu et al., 1998) and regulates the translation of tissue plasminogen activator (tPA) mRNA (Shin et al., 2004), a serine protease involved in LTP. Studies carried out on embryonic fibroblasts (MEFs) derived from CPEB1 KO mice show that CPEB1 is involved in controlling cellular senescence by regulating the translation of myc mRNA (Groisman et al., 2006).

The mild deficits observed in LTP of the CPEB1 KO mouse could be due to a compensatory effect of the other members of the CPEB family (CPEB2-4) (Alarcon et al., 2004). These include the murine CPEB2, which was initially discovered on mouse chromosome 5 and is abundantly expressed in testis (Kurihara et al., 2003). It was also reported in mouse brain (Theis et al., 2003b; Hagele et al., 2009) (Turimella et al., in preparation). CPEB3 and CPEB4 were discovered in mouse brain along with the expression of mCPEB2 in brain (Theis et al., 2003b). CPEB3 and CPEB4 are close mouse homologues of the human cDNAs encoding KIAA0490 and KIAA1673. CPEB1 and CPEB2-4 were reported as structurally distinct classes of proteins across and within phyla (Mendez and Richter, 2001). CPEB (2-4) lack the Aurora A kinase phosphorylation site present in CPEB1. CPEB (2-4) contain putative phosphorylation sites for various kinases in their so-called B-region (Fig. 3) for cyclic AMP dependent protein kinase (PKA), CamKII and p70S6 kinase, a serine threonine kinase which acts on components involved in translation (Gingras et al., 2001; Theis et al., 2003b). Alternative splicing has led to several isoforms for each CPEB which were described in the mouse hippocampus: mCPEB1 contains three isoforms called CPEB1-N (full length isoform) (Gebauer and Richter, 1996), CPEB1- $\Delta$ 5 (with a 5 amino acid deletion; (Wilczynska et al., 2005), and CPEB1- $\Delta$ 17 (with a 17 amino acid deletion; Turimella et al., in revision). For mCPEB2, four isoforms were described in brain: 2a, 2a\*, 2c & 2c\* (Turimella et al., in revision). Similarly, mCPEB3 and 4 each contain four different splice isoforms, named as 3a, 3b, 3c and 3d for CPEB3 (Fig. 3) and similarly 4a, 4b, 4c and 4d for CPEB4. The ‘a’ and ‘c’

isoforms of CPEB3 and 4 contain the putative phosphorylation sites (with the B region) and are specifically upregulated after kainate injection in the principal cell layers of the mouse hippocampus (Theis et al., 2003b).

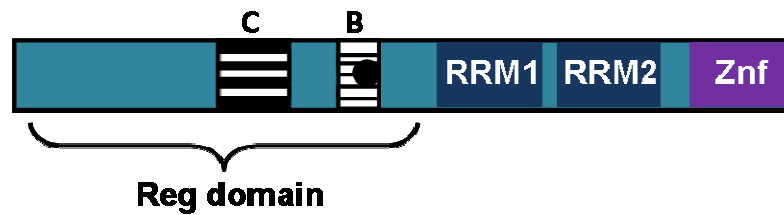


Figure 3: CPEB3 domain structure with the B (hatched box with dark circle, dark circle represents the putative phosphorylation sites present) and C (striated box) regions labelled in the regulatory domain. Reg domain: regulatory domain, RRM1: RNA recognition motif 1, RRM2: RNA recognition motif 2, Znf: Zinc finger.

In neurons, CPEB3 and CPEB4 were found in the postsynaptic density (PSD) fractions and CPEB3 was shown to repress the basal translation of GluR2 mRNA, an  $\alpha$ -amino-3-hydroxy-5-methyl-4-isoxazolepropionic acid (AMPA) receptor subunit (Huang et al., 2006). Recently, CPEB3 was reported to affect the stability of mRNAs by interacting with Tob, which functions as mRNA decay factor (Hosoda et al., 2011).

Apart from the expression and the functional role of CPEB proteins in *Xenopus* oocytes and neurons of the mouse hippocampus, CPEBs are also expressed in other cell types. Recent reports show the expression of CPEB1 in rat primary astrocytes in culture, where it regulates  $\beta$ -catenin translation, a protein localized at the leading edge of migrating astrocytes (Jones et al., 2008). In rat primary astrocytes, CPEB1 co-localizes with cyclin B1 and Aurora A kinase in centrosome fractions, where CPEB1 repressed the translation of cyclin B1 mRNA until phosphorylated by Aurora kinase (Kim et al., 2011). Upon phosphorylation, the repression is abolished and leads to an increase in cyclin B1 protein and progression into mitosis (Kim et al., 2011). These results show the importance of local protein synthesis of various target mRNAs required for different processes in astrocytes. Much less information is available for the expression and function of CPEB (2-4) in astrocytes.

## 1.2 Transgenic approaches for studying gene functions

One of the most important ways for evaluating gene function *in vivo* is by molecular genetic manipulation. Various techniques have been developed which involve either disruption of an endogenous gene via gene targeting in embryonic stem (ES) cells or introducing a gene into the mouse germline via transgenic approaches. By analyzing the phenotype of the mutant or the transgenic mice, knowledge about the gene functions during mammalian development as

well as molecular insight into certain human diseases can be gained (Smithies, 1993). Despite success, the conventional transgenic approaches have limitations due to the fact that most genes are disrupted or expressed throughout the life span of the recipient animal, and these manipulations are present not only in the adult stage but also during embryonic development. So, the ectopic expression, overexpression or disruption of these genes has often led to embryonic lethality which prevents studying the function of these genes in adult tissues (Gao et al., 1999). To overcome these problems, new approaches have been developed for genetic manipulation of target genes that allow stringent temporal and spatial control (Gingrich and Roder, 1998).

One of the most powerful approaches is overexpression of the gene of interest in genetically engineered mice to investigate the functional role of the gene *in vivo*. The Tetracycline (Tet)-inducible expression system is the most prominent inducible system used, which allows to rapidly and reversibly switch the transgene expression on or off in a specific cell type or tissue(s) at any time of the animal development (Sun et al., 2007). The Tet system uses the bacterial Tet resistance operon to reversibly turn the gene expression on or off (Fig. 4). There are two basic variants of the Tet-inducible expression system: the Tet transactivator (tTA) (Tet-off) system (Gossen and Bujard, 1992) and the reverse tTA (rtTA) (Tet-on) system (Gossen et al., 1995). tTA is a fusion protein of the DNA binding domain of the Tet repressor (TetR) and the herpes simplex virus VP16 transactivator protein (Gossen and Bujard, 1992). Expression of tTA is controlled by a promoter that can be used to direct cell type specific expression. For instance, the human glial fibrillary acidic protein (hGFAP) promoter was used to drive the expression of transgene specifically in hippocampal astrocytes (Fiacco et al., 2007). tTA binds and activates a promoter that contains several Tet-operator (tetO) sites coupled to a minimal cytomegalovirus (CMV) promoter. The TetO-CMV promoter is placed at the 5' of the transgene whose expression is to be regulated. Tet (or doxycycline (Dox)) binds to tTA and turns off gene activation by preventing the binding of tTA to tetO and this is referred to as tet-off system. The other variant, the Tet-on system (Fig. 4), contains rtTA, in which the TetR domain of tTA is mutated and the binding of tTA to tetO occurs only in the presence of Dox (Gossen et al., 1995).



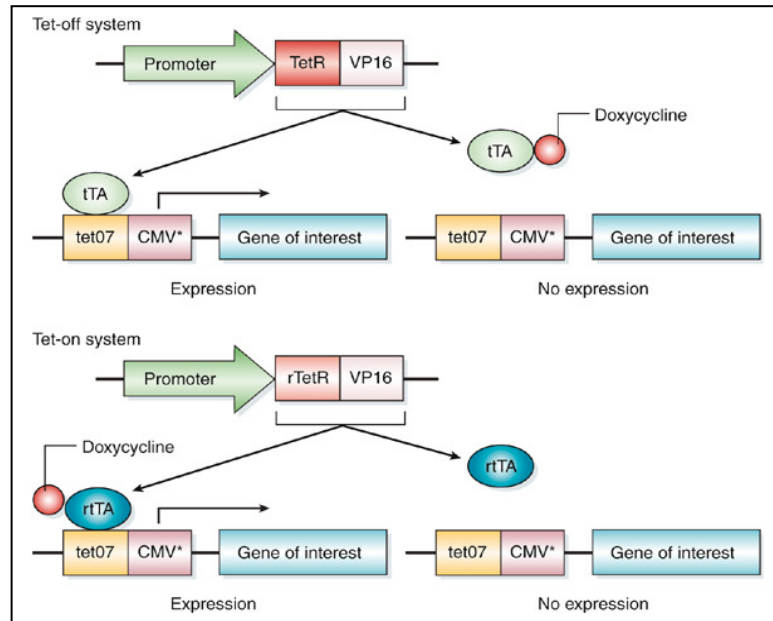


Figure 4: Schematic showing the Tet based inducible gene expression. In the Tet-Off system in which the tTA contains the TetR and herpes simplex virus VP16 domain, tTA recognizes and binds to the seven tetO (tetO7) domains connected to a minimal cytomegalovirus (CMV) promoter in the absence of doxycycline and activates gene expression. In the tet-on system, mutated tTA (rtTA) binds to the tetO7 only in the presence of doxycycline to activate gene expression, adapted from Kohan, 2008.

### 1.3 Astrocytes

Astrocytes are star shaped cells with multiple fine processes, which comprise approximately 70-80 % of the neuroglial cells in the mammalian central nervous system (CNS). Structurally mature astrocytes in grey matter are called protoplasmic astrocytes which are spherical and bushy whereas in white matter, fibrous astrocytes with process-bearing and less bushy appearance are often observed (Kimelberg and Nedergaard, 2010). Another important type of astroglial cells are radial glia. These cells are characterized by elongated processes and an ovoid cell body. Radial glia cells are neural stem cells and generate neurons at early embryonic stages, a common feature of the developing brain. Radial glia cells assist in neuronal migration and lateron, they mature or transform into stellate astrocytes (Schmechel and Rakic, 1979), whereas Müller glia in retina and Bergmann glia in cerebellum retain the radial glial morphology (Verkhatsky and Butt, 2007). Not only in the embryonic stage but also in adult neurogenesis radial glia cells with stem cell properties in the subgranular zone in the adult dentate gyrus and subventricular zone give rise to neurons and glial cells (see below) (Kempermann et al., 2004).

Star shaped	Elongated or radial
Fibrous astrocytes in white matter	Bergmann glia in the cerebellum
Protoplasmic astrocytes in grey matter	Muller glia across the retina

Table 1: Classification of mature astrocytes.

Most astrocytes express an intermediate filament called glial fibrillary acidic protein (GFAP) (Eng et al., 1971; Bignami et al., 1972). The expression of GFAP in astrocytes varies between regions i.e., cerebellum (all Bergmann glia express GFAP), cortex (only 15% of astrocytes are GFAP positive) and hippocampus (all express GFAP) (Verkhatsky and Butt, 2007). GFAP negative astrocytes which are morphologically similar to astrocytes can be identified using antibodies against glutamine synthetase (GS), a glutamate-glutamine converting enzyme specifically expressed by astrocytes and also by S100 $\beta$ , a calcium binding protein (Nishiyama et al., 2005). However, S100 $\beta$  and GS were also reported in other cell types: S100 $\beta$  in up to 20% of NG2 cells (Karram et al., 2008; Nishiyama et al., 2009), and GS in oligodendrocytes (Tansey et al., 1991; Polito and Reynolds, 2005). Recently aldehyde dehydrogenase 1 family, member L1 (Aldh1L1) was identified as an astrocyte specific marker from microarray studies performed on isolated astrocytes (Cahoy et al., 2008). A BAC Aldh1L1-EGFP transgenic mouse expressed GFP specifically in astrocytes (Cahoy et al., 2008).

Astrocytic processes form endfeet on blood vessels and the pial surface (Butt and Ransom, 1989) and cover intraparenchymal capillaries (Peters et al., 1991). The protoplasmic astrocytes in grey matter form separate domains with their elaborated processes, thereby forming structurally individual units (Nedergaard et al., 2003; Bushong et al., 2004). Within these micro-anatomical domains, these cells establish contact with blood vessels and neuronal membranes. This type of micro-architectural organisation of astrocytes is conserved in mammals and is basically similar between humans and rodents (Oberheim et al., 2009). Furthermore, astrocytes are integrated into syncytia by forming gap junctions with the aid of connexins that are localized on their peripheral processes (see below). Gap junctions formed by connexins facilitate intercellular diffusion of small molecules and are involved in long-range signalling (Giaume and Venance, 1998). With an efficient domain organisation and by establishing contacts with other cells, astrocytes are involved in several key functions. One such important function is the neuron-astrocyte communication with the aid of intracellular astrocytic Ca<sup>2+</sup> signalling, where astrocytes integrate and process synaptic information and control synaptic transmission and plasticity by releasing gliotransmitters (Perea et al., 2009). This release of transmitters by astrocytes leads to a paracrine action on astrocytes which supports inter-astrocytic Ca<sup>2+</sup> signal propagation, thereby regulating neuronal excitability and synaptic transmission (Guthrie et al., 1999). Astrocytes *in vivo* display Ca<sup>2+</sup> elevations triggered by physiological external stimuli and also respond to neuronal activity (Wang et al., 2006; Perea et al., 2009).

Some of the important functions of astrocytes are summarized in the table 2:

#	Function	Description	References
1	Potassium buffering	Involved in extracellular $[k^+]_o$ ion homeostasis	(Orkand et al., 1966) (Wallraff et al., 2006)
2	Astrocyte receptor functions	Astrocytes express mainly metabotropic receptors which act by intracellular $Ca^{2+}$ or cAMP.	(Kimelberg and Nedergaard, 2010)
3	Control of $[H^+]_o$ .	pH control of extracellular space by different transporting enzymes ( $H^+$ and $HCO_3^-$ )	(Kimelberg et al., 1979)
4	Glutamate and GABA ( $\gamma$ -aminobutyric acid) uptake	Clearance of glutamate and GABA	(Martinez-Hernandez et al., 1977) (Schousboe et al., 1977) (Levi et al., 1983)
5	Cerebral blood flow control	Regulate blood flow with their end-feet processes surrounding blood vessels. Prostaglandin $E_2$ ( $PGE_2$ ) released by astrocytes is a key vasodilator.	(Zonta et al., 2003) (Takano et al., 2006) (Gordon et al., 2007)
6	Water transport	AQP4 specifically expressed at astrocytic perivascular processes regulates water transport.	(Nielsen et al., 1997)
7	Antioxidant functions	Antioxidants such as glutathione are present in astrocytes.	(Aschner, 2000)
8	Astrocyte-neuronal lactate shuttle (ANLS)	Astrocytes support neurons by supplying lactate as substrate (lactate shuttle hypothesis).	(Pellerin and Magistretti, 1996)
9.	Tripartiate synapse	Astrocytes are involved along with neurons in controlling brain function.	(Halassa et al., 2007)

Table 2: Functions of astrocytes.

### 1.4 Gap junctions and connexins

Gap junctions are cell-cell contacts that provide intercellular communication by connecting the cytoplasm of two cells. These gap junctions occur as gap-junctional plaques (Fig. 5a) and can contain up to thousands of single gap-junctional channels (Kumar and Gilula, 1996). Depending on their molecular composition, three different types of gap junction channels have been described: 1) homomeric / homotypic, 2) heterotypic and 3) heteromeric. Homotypic gap junctions contain two identical types of hemichannels and heterotypic channels contain two different hemichannels, whereas homomeric hemichannels are composed of identical connexins and heteromeric are composed of different connexins in a hemichannel (Sohl et al., 2005). So far, 20 different connexin genes in mouse and 21 genes in the human genome have been described (Sohl and Willecke, 2003). Connexins (abbreviated as Cx, followed by their molecular mass in kilodaltons (kDa)) are expressed in most cell types of lower and higher vertebrates during development as well as in the adult stage (Sohl et al., 2004). These gap junctions allow passive diffusion of small molecules such as: second

messengers (Bedner et al., 2012),  $K^+$  (Wallraff et al., 2006), glucose (Rouach et al., 2008),  $Na^+$  (Langer et al., 2012) with a size exclusion limit of about 1,000 daltons.

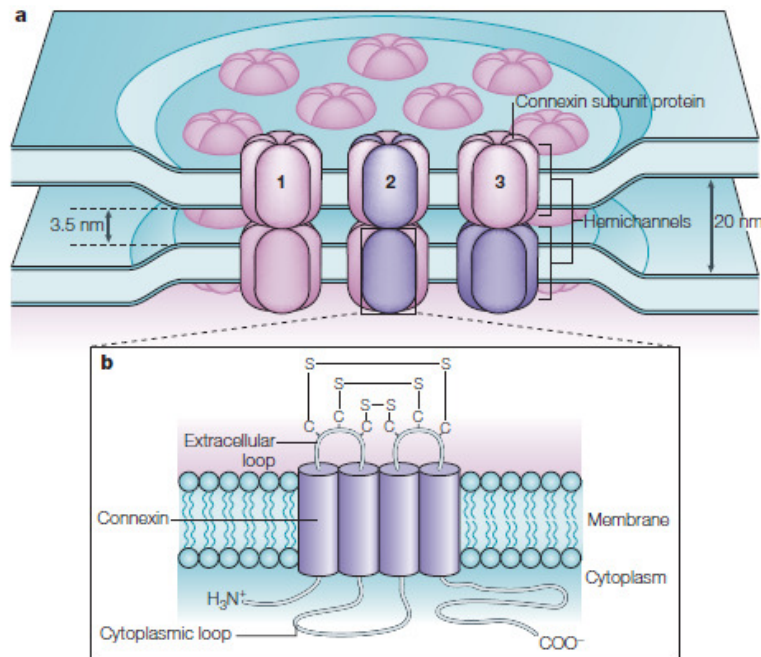


Figure 5: Gap-junctional plaque – Molecular organization and schematic topology.

a) Hemichannels of two neighbouring cells with plasma membranes near to each other can join together to form gap junction channels. Each channel consists of two hemichannels (also termed connexons), each of which contains an assembly of six subunits of connexin proteins. b) Connexins contain four membrane-spanning domains, three cytoplasmic loops, two extracellular loops, a cytoplasmic loop and one amino- and one carboxy-terminal region. Connexin proteins are membrane spanning and share three conserved extracellular cysteine residues that are important for docking. S-S represents disulphide bonds in the extracellular domains of these proteins, adapted from Söhl et al (2005).

Apart from forming gap junctional channels between cells, connexins can also function as hemichannels (HCs) which are involved in the exchange of ions and molecules not only between cells but also with the external medium, thereby supporting both autocrine and paracrine actions (Spray et al., 2006; Giaume and Theis, 2010). HCs are closed under normal conditions but are opened during pathological states by various factors such as exposure to pro-inflammatory agents (Retamal et al., 2007), with reduced extracellular concentrations of  $Ca^{+2}$  or  $Mg^{+2}$  ions as observed in the ischemic brain (Orellana et al., 2009) and with moderate increase in the intracellular  $Ca^{+2}$  concentration (Orellana et al., 2012).

Invertebrates express innexins which mediate similar gap junctional coupling as connexins in vertebrates. Around 25 distinct innexins have been identified so far (Scemes et al., 2009; Fushiki et al., 2010). These innexins are evolutionary distinct from connexins, and the junctions formed by innexins are distinct from the junctions formed by connexins (Larsen,

1977). The homologues of innexins in vertebrates are named pannexins, which show 20% sequence similarity to innexins (Shestopalov and Panchin, 2008; D'Hondt et al., 2009; Scemes et al., 2009). So far, three different pannexin genes (named Panx1, Panx2 and Panx3) have been described in mammals (Baranova et al., 2004; Scemes et al., 2007). Pannexins were shown to form gap junctions when expressed in *Xenopus* oocytes (Bruzzone et al., 2003). Recent studies indicate that glycosylation of the pannexin extracellular loop prevents the docking of hemichannels of neighbouring cells (Boassa et al., 2007). Similar to connexins, pannexins are also reported to form HCs which exhibit similar unitary conductance and pharmacology as connexins (Giaume and Theis, 2010). However in studies performed on astrocyte cultures, pannexins were shown to form nonselective, high-conductance plasmalemmal channels that are permeable to ATP (Iglesias et al., 2009).

Connexins are expressed in most of the cell types in brain and form functional gap junction channels. Neurons mainly express three different types of connexins namely Cx36, Cx45 and Cx57 depending on the region (Sohl et al., 2005). Cx36 expression is mainly observed in interneurons in deep cerebellar nuclei during early development (Degen et al., 2004). In the hippocampus, Cx36 was shown to mediate gap junctional coupling between hippocampal interneurons (Venance et al., 2000). From reporter gene studies, Cx45 was reported to be expressed highly during embryogenesis and up to two weeks after birth and afterwards is restricted to the thalamus, cerebellum and the pyramidal neurons of the CA3 region of the hippocampus (Maxeiner et al., 2003). In kainate injection studies, Cx45 was found to play a role in neuronal homeostasis and cell survival (Condorelli et al., 2003). Cx57 was thought to have a role in electrical and tracer coupling between horizontal cells of the retina (Hombach et al., 2004). Neuronal connexins are required to build gap junctions which facilitate fast oscillatory networks and synchronisation (Bennett and Zukin, 2004). At gap junctions which undergo activity dependent plasticity, CamKII interacts with and phosphorylates Cx36, showing a possible pathway for plasticity of electrical synapses (Alev et al., 2008).

The major connexins expressed in oligodendrocytes are Cx32, Cx47 and Cx29 (Nagy et al., 2003; Odermatt et al., 2003; Eiberger et al., 2006). Cx32 expression is observed during myelin development, axonal regeneration and Wallerian degeneration (Sohl et al., 2004). Cx29 protein was detected in internodal and juxta-paranodal regions of small myelin sheaths of oligodendrocytes in the CNS whereas Cx32 was localized to large myelin fibers (Altevogt et al., 2002; Theis et al., 2005). Cx47 is strongly expressed in the somata of oligodendrocytes

and is co-localized with Cx32 and also with the astrocytic Cx43, suggesting that Cx47 might be on the oligodendroglial side and involved in the formation of oligodendrocyte-astrocyte gap junctions (Altevogt and Paul, 2004; Nagy et al., 2004). Similarly, Cx32 is expressed on the oligodendritic side together with Cx30 and Cx26 on the astroglial side. Astrocytes not only form gap junctions between astrocytes (astrocyte-astrocyte or A/A gap junctions) but also form heterocellular junctions with oligodendrocytes (astrocyte-oligodendrocyte or A/O gap junctions). This type of intercellular gap junctional communication with other cell types is termed panglial coupling (Nagy et al., 2003; Nagy and Rash, 2003; Theis et al., 2005).

Among the astroglial connexins, Cx43 and Cx30 are the major gap junctional proteins (Dermietzel et al., 2000; Bedner et al., 2012). Cx43 knockout (KO) mice do not survive postnatally due to cardiac malfunction (Reaume et al., 1995). *In vitro* studies performed on Cx43 deficient astrocyte cultures from these KO mice showed an impaired growth, decreased tracer coupling and reduced saturation density, all of which indicate the importance of Cx43 in gap junctional coupling and growth (Naus et al., 1997; Theis et al., 2004; Magnotti et al., 2011). Residual coupling was observed in astrocyte cultures of Cx43KO mice probably through other connexin proteins present in cultures namely Cx26, Cx30, Cx40, Cx45 and Cx46 (Kunzelmann et al., 1999; Dermietzel et al., 2000). Specific deletion of Cx43 using the Cre/loxP system in astrocytes led to only a 50% reduction in the tracer coupling (Theis et al., 2003a; Wallraff et al., 2006). The remaining coupling could be influenced by the compensatory up-regulation of Cx30 in mice lacking Cx43 (Theis et al., 2003a; Nakase et al., 2004), Cx30 contributes only 20% of the coupling between astrocytes (Gosejacob et al., 2011). In double knock out mice lacking Cx43 and Cx30 in astrocytes, a complete inhibition of tracer coupling was observed (Wallraff et al., 2006; Rouach et al., 2008). Using reporter gene studies a low abundance of Cx30 was observed in the cerebral cortex and the hippocampus (Gosejacob et al., 2011), whereas in thalamus, cerebellum and leptomeningeal cells Cx30 is highly expressed (Nagy et al., 2004; Theis et al., 2005). The gap junctional plaques near by the blood vessels are composed of Cx30 in most of the brain areas (Rouach et al., 2008). Another connexin is Cx26 which localizes abundantly in perivascular, sub-pial and subependymal areas and co-localizes with the astrocytic marker GFAP (Mercier and Hatton, 2001; Nagy et al., 2004). Conversely, reporter studies from Cx26 BAC transgenic mice concluded that Cx26 is not expressed in neurons or in glia but is restricted to the meninges in both embryonic and adult brain (Filippov et al., 2003). Recent reports indicated the expression of Cx26 mRNA in radial glia like cells (Kunze et al., 2009). The expression of Cx26 in

astrocytes was not yet clearly elucidated and was a matter of debate until recently, when widespread Cx26 expression was found in the thalamus (Nagy et al., 2011).

Astrocytic connexins are involved in spatial buffering of ions. Studies performed on DKO mice lacking Cx43 and Cx30 showed that astrocytic gap junctions are required for extracellular K<sup>+</sup> clearance (Wallraff et al., 2006). The coupling-deficient astrocytes in DKO mice showed a reduced threshold for generation of spontaneous and induced epileptiform events (Wallraff et al., 2006). A recent study performed on DKO mice showed that astroglial connexins were also involved in clearance of extracellular glutamate and K<sup>+</sup> during synaptic activity by modulating the astroglial clearance rate and extracellular space volume (Pannasch et al., 2011). Astroglial networks in the hippocampus formed mainly by Cx43 and Cx30 are involved in the supply of glucose and its metabolites to neurons in an activity-dependent manner (Rouach et al., 2008). These studies prove the important role of astrocytic connexins in controlling neuronal activity.

The C-terminus of Cx43 interacts with  $\beta$ -catenin and moreover the C-terminus of Cx43 localizes in the nucleus where it might be involved in regulating the gene expression (Theis et al., 2005). Cx43 3' UTR contains regulatory elements such as microRNA binding sites and CPEs by which it can be regulated post-transcriptionally. The 3' UTR of Cx43 possesses binding sites for miRNA-206 and miRNA-1 (miRNAs are 20-21 short nucleotide sequences which bind to mRNAs and regulate their translation). While miRNA-206 regulates Cx43 expression during skeletal muscle development (Anderson et al., 2006) and miR-1 regulates Cx43 expression in viral myocarditis (Xu et al., 2012).

## 1.5 Adult neurogenesis

In adult brains of mammals, neurogenesis takes place at two locations: in the subgranular zone (SGZ) of the dentate gyrus in the hippocampus and in the subventricular zone (SVZ) of the lateral ventricles (Fig. 6), which was also observed in humans (Eriksson et al., 1998; Curtis et al., 2007). Adult neurogenesis depends on several physiological and pathological conditions at different levels, which includes proliferation of adult neural stem cells (NSCs), differentiation and fate determination of progenitors, as well as on the maturation, survival and integration of newborn neurons. These NSCs might be involved in various functions of the olfactory bulb and the hippocampus both of which are important for learning and memory (Zhao et al., 2008). It was recently shown that ablation of adult neurogenesis in hippocampus

leads to impairment of spatial memory in mice (Clelland et al., 2009). Neurogenesis in mammalian brain regions other than SVZ and SGZ remains controversial (Gould, 2007).

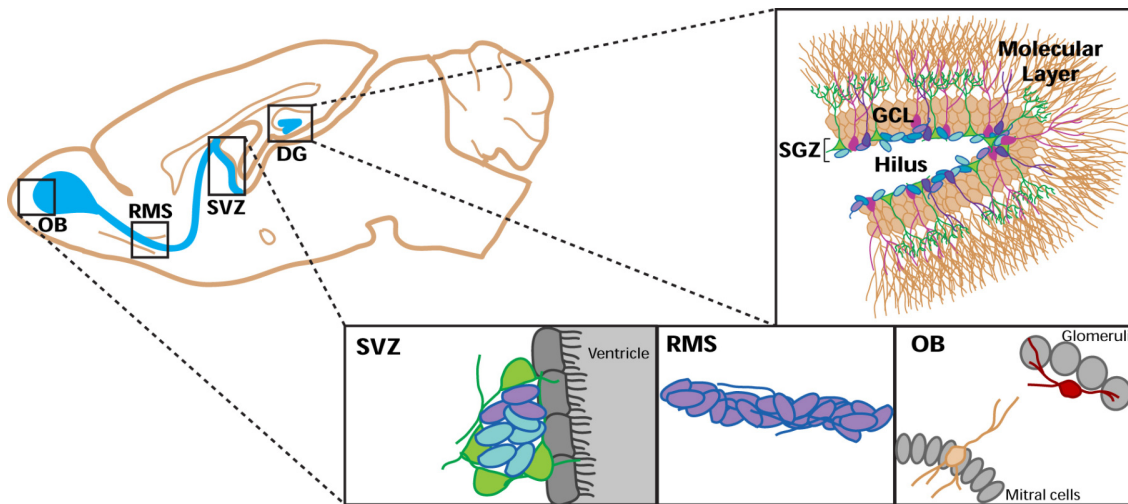


Figure 6: Schematic depicting adult neurogenesis in mammals: Adult neurogenesis mainly occurs in the subventricular zone (SVZ) and in the subgranular zone (SGZ) of the dentate gyrus. Image with a sagittal view of the mouse brain. Blue colour represents the active neurogenic niches. In the SVZ, stem cells (green) give rise to transit amplifying cells (light blue) and neuroblasts (purple), and reside on the wall in the lateral ventricle just below the ependymal layer (grey). These neuroblasts migrate to the olfactory bulb through the rostral migratory stream (RMS) where these cells are functionally integrated as granule (peach) and periglomerular (red) neurons. In the SGZ, the stem cells (green) are clustered at the base of the hippocampal dentate gyrus (DG) granule cell layer (GCL) and give rise to transit amplifying cells (light blue). Neuroblasts (blue) and newborn neurons (purple) arise from these stem cells and are eventually transformed to granule cell neurons. These mature neurons are located in the GCL and extend their radial processes to the molecular layer to receive cortical input; adapted from Johnson et al, (2009).

In the SGZ of the DG, astrocytes with radial glia (RG)-like morphology expressing GFAP and nestin are considered as stem cells which eventually give rise to new neurons (Kempermann et al., 2004). These cells extend long processes over the GCL and display electrophysiologically a passive current pattern (Fukuda et al., 2003; Huttmann et al., 2003). These cells play an important role in neurogenesis; they promote neuronal differentiation of the adult progenitor cells from hippocampus and also aid in the integration of newborn neurons into the neuronal networks with functional synaptic transmission *in vitro* (Song et al., 2002). Wnt signalling pathway blockade prevents neurogenic activity of astrocytes *in vitro* and SGZ neurogenesis *in vivo*, suggesting that RG-like cells may act via Wnt signalling in promoting neurogenesis (Lie et al., 2005). Other possible signalling pathways regulating adult neurogenesis are Notch (Ninkovic and Gotz, 2007), Sonic hedgehog (Shh) (Favaro et al., 2009), and signalling by bone morphogenetic proteins (BMPs) (Colak et al., 2008) which was reviewed in detail recently (Morrens et al., 2011). Adult neurogenesis in the DG of the



hippocampus requires astrocytic connexin expression in RG-like cells (Kunze et al., 2009) and Cx43 expression is also required in radial glia for neuronal migration (Cina et al., 2009).

## 1.6 Glutamate transporters and glutamine synthetase

One of the important roles of astrocytes is the maintenance and modulation of glutamergic and GABAergic neurotransmission (Schousboe, 2003), and astrocytes are considered as a sink for the extracellularly released glutamate. In the mammalian CNS L-glutamate is the major excitatory neurotransmitter which contributes to fast synaptic neurotransmission, complex physiological processes such as learning and memory, plasticity and cell death (Dingledine et al., 1999). The extracellularly released glutamate activates different ionotropic and metabotropic glutamate receptors for fast excitatory as well as for slower modulatory effects on neurotransmission (Shigeri et al., 2004). The extracellular glutamate concentration is controlled via various Na<sup>+</sup>-dependent high-affinity glutamate transporters (excitatory aminoacid transporters, EAATs) to prevent excitotoxicity and cell death. These EAATs are expressed on the plasma membranes of neurons and glial cells and aid in removing the glutamate rapidly from the extracellular space (Danbolt, 2001; Balcar, 2002). So far, five different Na<sup>+</sup>-dependent high-affinity glutamate transporters have been identified namely: EAAT1-EAAT5 (Sheldon and Robinson, 2007) which are expressed in different cell types. GLAST and GLT-1 are the two transporters which are primarily expressed by astrocytes (Rothstein et al., 1994; Lehre et al., 1995), these are also called EAAT1 and EAAT2 respectively (Arriza et al., 1994). EAAT3 is expressed on the somatodendritic compartments of the neurons, particularly in pyramidal cells of the hippocampus and cortex, whereas EAAT4, another neuronal transporter is expressed in the Purkinje neurons of the cerebellum (Rothstein et al., 1994). EAAT5 is expressed in the retina (Arriza et al., 1997). With quantitative electron microscopy, both GLAST and GLT-1 were found to be enriched mainly on the astrocytic processes near neuronal synaptic termini (Lehre et al., 1995) where the synaptically released glutamate is taken up by astrocytes through these transporters (Lehre and Danbolt, 1998; Gegelashvili et al., 2000). From gene knock out studies in mice, GLAST and GLT-1 were found to be the essential transporters in extracellular glutamate clearance (Rothstein et al., 1996; Tanaka et al., 1997). Either a loss or alteration in the expression of glutamate transporters has been observed in several neurodegenerative disorders such as Amyotrophic lateral sclerosis (ALS), Huntington's disease, Parkinson disease and Alzheimer's disease (Sheldon and Robinson, 2007). By using anti-sense oligonucleotide mediated knockdown of glutamate transporters, it was shown that neurodegeneration was associated

with loss of transporter expression (Rothstein et al., 1996) and mice lacking GLT-1 showed lethal spontaneous seizures and susceptibility to acute cortical injury (Tanaka et al., 1997).

The glutamate that is released synaptically is taken up by astrocytes via glutamate transporters and converted rapidly into glutamine by the enzyme glutamine synthetase (GS) (Martinez-Hernandez et al., 1977). GS is the major component of the glutamate-glutamine cycle controlled by astrocytes, where the glutamate is converted into glutamine and transported back to neurons and repackaged into synaptic vesicles (Hertz and Zielke, 2004). GS is mainly expressed by astrocytes both *in vitro* and *in vivo* and is localized to the fine processes surrounding neuronal excitatory synapses (Martinez-Hernandez et al., 1977; Derouiche and Frotscher, 1991). Variations in GS expression lead to disturbances in neuronal functions (Suarez et al., 2002). Glial GS was shown to be involved in different brain pathologies where GS expression was either upregulated or downregulated (Suarez et al., 2002). Loss of GS expression is observed in the perisynaptic processes of astrocytes of the cerebral cortex in patients with Alzheimer's disease in the vicinity of senile plaques (Robinson, 2001). GS is also reduced under conditions of glucose deprivation (Rosier et al., 1996). Conversely increased GS expression is observed after ischemia *in vivo* (Petito et al., 1992) and after chronic hypoxia (Sher and Hu, 1990). In patients with mesial temporal lobe epilepsy (MTLE), an increased extracellular glutamate concentration was observed which made neurons hyperexcitable, together with loss of GS (Eid et al., 2008b). The regulation of GS activity is crucial in maintaining extracellular glutamate levels and thereby preventing the adverse effects of hyperexcitability and excitotoxicity of neurons.

## 1.7 Astrocyte dysfunction in Epilepsy

Epilepsy is a chronic neurological disorder which affects about 1% of the world population. It is a condition which is characterized by the periodic and unpredictable occurrence of seizures which are due to the hypersynchronous activity of the neurons. Changes in the neuronal properties have been attributed to the induced seizure activity in humans or in experimental models of epilepsy (Steinhäuser and Seifert, 2002). MTLE is one of the most common types of epilepsy which often is medically-intractable and surgical removal of the sclerotic hippocampus is considered for seizure control in some patients. Sclerosis in the hippocampus is characterized by loss of neurons in specific areas of the hippocampus (CA1, CA3 and hilus of dentate gyrus), glial and microvasculature proliferation, and synaptic reorganization (Blumcke et al., 1999). Apart from neuronal loss, a hallmark of the sclerotic hippocampus is

the hypertrophy of glial cells, characterized by increased GFAP immunoreactivity with long and thick processes (Binder and Steinhäuser, 2006). Many recent studies indicate that astrocyte dysfunction is a crucial aspect contributing to epilepsy (Fig. 7). The astrocytic gap junction proteins Cx43 and Cx30 are required for glucose trafficking and transport of energetic metabolites to neurons from blood to maintain synaptic transmission (Rouach et al., 2008). The delivery of glucose with the syncytium formed by astrocytic gap junctions is required to sustain epileptiform activity (Giaume et al., 2010). This would indicate a pro-epileptic function of connexins. On the other hand, the lack of astrocytic connexins led to impaired  $K^+$  buffering, spontaneous epileptiform activity and reduced threshold to elicit hyperactivity (Wallraff et al., 2006). This would indicate an anti-epileptic function of connexins. Using transcriptome analysis, a decrease in connexin transcripts was shown in a model with disruption of the blood-brain barrier (BBB) and albumin-dependent generation of epileptic seizures (Cacheaux et al., 2009). Conversely, patients with pharmacoresistant MTLE and hippocampal sclerosis (HS) show an increased immunoreactivity for Cx43 protein and also increased transcript levels (Naus et al., 1991; Fonseca et al., 2002; Collignon et al., 2006). The authors proposed that this upregulation of Cx43 might have increased seizure spread and the progression of MTLE.

The expression of the glutamate transporters (GLAST and GLT-1) is altered in patients with epilepsy and also in other brain disorders (Seifert et al., 2006); one of the proposed mechanisms is the reduced clearance of extracellular glutamate by glutamate transporters expressed by astrocytes. Increased extracellular glutamate found in human epileptic tissue can induce seizure activity and neuronal cell death (Glass and Dragunow, 1995). Contrasting results about the expression of glutamate transporters were reported in patients suffering from HS and TLE. Tessler et al., (1999) have reported no difference in the expression of GLAST and GLT-1 in tissue from patients with HS using *in situ* hybridisation and Western blotting (Tessler et al., 1999), whereas other groups have reported a reduction in GLT-1 levels in the hilus and CA1 region associated with neuronal loss in HS patients (Mathern et al., 1999; Proper et al., 2002). Increased GLAST expression was found in CA2 and CA3 regions of the sclerotic hippocampus (Mathern et al., 1999). Downregulation of both the transporters GLAST and GLT-1 in the hippocampal CA1 region was also reported from other studies where the authors speculated the decrease in the transporter expression might be either an adaptive response to neuronal death or a causative event (Sarac et al., 2009). The enzyme encoding protein GS that is expressed in astrocytes was reported to be deficient in patients

with MTLE, which was thought to be the underlying reason for an increase in extracellular glutamate levels (Eid et al., 2008b). In experimental models, it was found that pharmacological inhibition of GS induced recurrent seizure activity and rat brain pathology resembling human HS (Eid et al., 2008a). But, in a recent study performed on the pilocarpine model of TLE in rats, no reduction in the number of GS positive cells and the GS containing cell volume was observed, rather a redistribution of the enzyme was reported at both intracellular and tissue levels in the epileptic hippocampus (Papageorgiou et al., 2011). Synaptic GABA release as well as regulation of the inhibitory synaptic strength is mainly controlled by the glial glutamate-glutamine cycle (Liang et al., 2006). In addition epileptiform activity is maintained by glutamine transported to neurons (Tani et al., 2010). So, the loss of GS leads to reduced glutamine availability to neurons and further reduced GABA release from interneurons and subsequently decreased inhibition.

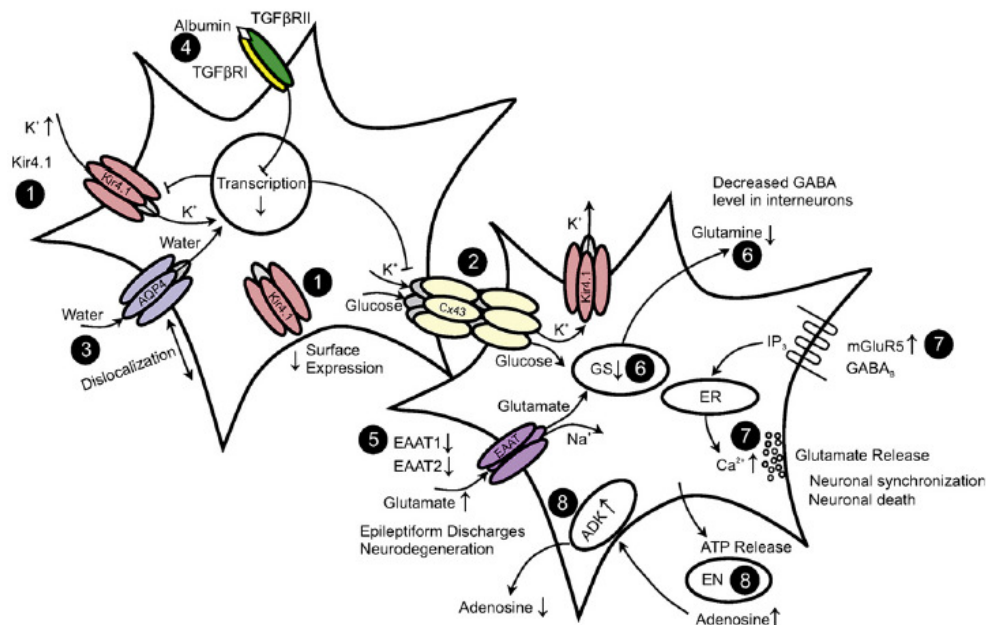


Figure 7: Astrocyte dysfunction in epilepsy: 1) Increased extracellular  $K^+$  concentration results in seizure activity. Reduced expression of Kir channels in human and experimental epilepsy lead to decreased  $K^+$  uptake. 2) Spatial redistribution of  $K^+$  is mediated by gap junctions. 3) Impaired  $K^+$  buffering is also due to displaced water channels. 4) Blood-brain barrier disruption, albumin uptake and TGF $\beta$  activation results in Cx43, Cx30 and Kir4.1 downregulation and impaired  $K^+$  buffering. 5) The glutamate uptake by astrocytes is thought to be impaired in human epilepsy, as the glutamate transporters EAAT1 and EAAT2 are downregulated. 6) The glutamate converting enzyme GS expressed by astrocytes is downregulated in patients with epilepsy. This loss of GS leads to increased glutamate levels extracellularly, and reduced availability of glutamine which leads to reduced inhibition as a result of decreased release of GABA by interneurons. 7) mGluR5 activation leads to increase in intracellular  $Ca^{2+}$ . Increased mGluR5 levels in epileptic patients were observed which can lead to increased glutamate release. 8) ATP release, ectonucleotidases and adenosine kinase (ADK) regulate the levels of ambient adenosine. In epilepsy, seizure activity leads to increased ADK levels and reduced adenosine concentration; adapted and modified from Seifert and Steinhäuser, (2011).

The expression of inward rectifying potassium channel (Kir) channels which are responsible for spatial buffering of  $K^+$  was downregulated in patients with MTLE, leading to impaired  $K^+$

buffering and enhanced susceptibility to seizures (Seifert and Steinhäuser, 2011). Using molecular and functional analyses, the main subunit of Kir channels in astrocytes was shown to be Kir 4.1 (Olsen and Sontheimer, 2008; Seifert et al., 2009). Genetic downregulation of Kir 4.1 led to decreased ability of glutamate and  $K^+$  clearance from the extracellular space both *in vitro* (Kucheryavykh et al., 2007) and *in vivo* (Djukic et al., 2007) and moreover mice with astrocytic deletion of Kir 4.1 exhibited seizures (Djukic et al., 2007). Another astrocytic protein, aquaporin4 (AQP4), which forms a water channel and localizes at the astrocytic end feet contacting the capillaries, is co-localized with Kir 4.1 (Higashi et al., 2001; Badaut et al., 2002). Impaired  $K^+$  buffering and increased seizure duration was observed in mice with AQP4 deletion (Binder et al., 2006). In patients with MTLE and HS a loss of AQP4 at the vasculature associated with astrocyte endfeet was observed by immunostaining (Eid et al., 2005). Dystrophin is required for the membrane anchoring of AQP4 (Amiry-Moghaddam et al., 2003). The loss of AQP4 at the endfeet is due to the loss of the dystrophin anchoring complex whose expression was also found to be absent at the perivascular end feet in the MTLE hippocampus (Eid et al., 2005). Dislocation of water channels and also the decreased expression of Kir channels in astrocytes would explain the impaired  $K^+$  buffering and increased seizure susceptibility observed in MTLE (figure 6) (Seifert and Steinhäuser, 2011). It is still unclear whether the alterations in the expression levels of the various mRNAs leading to dysfunctional astrocytes in epileptic condition are the causative factors or rather a compensatory phenomenon. Further studies are required. Interestingly, Cx43, Cx30, GLT-1, GLAST, GS, dystrophin and AQP4 all have CPEs in their 3' UTRs. Thus a change in expression of CPEBs in astrocytes could be responsible for dysfunction of many typical astrocytic proteins and be a key player in astrocyte dysfunction in epilepsy.

## 2 Aim of the thesis

Little information is available about the expression pattern and the possible role of CPEB 2-4 in astroglial cells. Astrocyte dysfunction is increasingly considered as a key aspect in the progression of epilepsy (Seifert and Steinhäuser, 2011). Several mRNAs which are involved in key cellular functions of astrocytes are dysregulated in epilepsy and possess binding sites for CPEBs and thus could be potential CPEB targets. The main aims of this thesis work were to investigate the following 4 questions:

### 1. What is the expression pattern of CPEBs in astrocytes?

The expression pattern of CPEBs is well characterized in neurons (Theis et al., 2003b; Richter, 2007), whereas the role of CPEBs in astrocytes is less explored. Recently expression of CPEB1 was also observed in primary astrocytes in culture (Jones et al., 2008), but the expression of other CPEBs i.e., CPEB 2-4 was not investigated in astrocytes. In the present study the expression of CPEB1-4 was studied in detail using primary astrocyte cultures.

### 2. What is the impact of astrocytic overexpression of CPEB3?

CPEB3 in neurons acts as a basal repressor of GluR2 protein (Huang et al., 2006). In mice overexpressing CPEB3 in neurons, GluR2 protein levels were downregulated (Kaczmarczyk, Unpublished). To investigate the functional role of CPEB3 in astrocytes transgenic mice were generated using the Tet-Off system where the CPEB3-EGFP transgene was specifically expressed in astrocytes driven by the GFAP promoter.

### 3. Which targets can be regulated by CPEB3 in astrocytes?

Several mRNAs expressed in astrocytes (Cx43, Cx30, GS, GLT-1) contain CPEs in their 3' UTRs and thus can be regulated by CPEB3. These proteins are involved in key cellular functions of astrocytes and are de-regulated in epilepsy (Seifert et al., 2010). Using mice overexpressing CPEB3 in astrocytes, studies were performed to identify its potential targets and investigate a possible role of CPEB3 in epilepsy.

### 4. Is the interaction of CPEB3 with target mRNAs CPE dependent?

CPEB1 binds to CPEs present in the 3' UTR of target mRNAs. Studies were performed to check if CPEB3 is interacting with its target mRNA in a CPE dependent manner. For this purpose, various vectors were generated containing the 3' UTR regions with and without CPEs. By using RNA co-immunoprecipitation and real time PCR, the interaction of CPEB3 with its target mRNAs were studied.

### 3. Materials and Methods

#### 3.1 Materials

##### 3.1.1 Solutions and reagents (ready-to-use)

2-Mercaptoethanol  
 Aqua polymount  
 Acetic acid  
 Acrylamide solution (Rotiphorese Gel 30 (37, 5:1)  
 CepetorKH (1mg/ml)  
 Chloroform  
 DNase/RNase free water  
 DNase free RNasin  
 Dimethyl sulfoxide (DMSO)  
 Ethanol  
 Ethidium bromide (10mg/ml)  
 Entellan  
 Gene expression master mix  
 Isopropanol  
 Ketamin 10%  
 Methanol  
 Normal goat serum (NGS)  
 Permafluor  
 Qiazol  
 Restore western blot stripping buffer  
 Roti-liquid barrier marker  
 SOC medium  
 Sucrose  
 Superscript III reverse transcriptase  
 Supersignal west dura extended duration substrate  
 Tissue-tek (O.C.T compound)  
 TritonX-100  
 Trizol reagent  
 Tween-20  
 TEMED

##### 3.1.2 Kits used

Product Name	Company
One Taq polymerase	New England Biolabs
Accuprime Taq DNA polymerase system	Invitrogen
Advantage 2 polymerase kit	Clontech
Advantage HD polymerase kit	Clontech
Advantage high fidelity PCR kit	Clontech
RNase free DNase kit	Qiagen
Endofree plasmid maxi kit	Qiagen
Fast-link DNA ligation kit	Epicentre
Gel and PCR cleanup kit	Promega
Go taq flexi DNA polymerase	Promega

Hipure plasmid filter midiprep kit	Invitrogen
Infusion PCR cloning kit	Clontech
Marathon ready cDNA kit	Clontech
Miniprep kit	Promega
Pierce BCA protein assay kit	Thermo scientific
RQ1 RNase-free DNase kit	Promega
Rneasy plus mini	Qiagen
TOPO-XL-PCR Cloning kit	Invitrogen
TUNEL staining kit	Invitrogen

### 3.1.3 Buffers and solutions

#### 3.1.3.1 Western blotting (WB) buffers

Buffer	Contents and preparation	Final concentration
Lysis buffer (modified RIPA buffer)	6.05 g Tris 8.76 g NaCl 5 ml Nonidet P-40 (NP40) 5 g sodium deoxycholate (NaDOC) 10 ml TritonX-100 Contents (without NP40 & Triton) were dissolved in 700 ml of deionized water (dH <sub>2</sub> O). pH was adjusted to 7.5. Later NP40 & Triton were added and volume adjusted to 1 L with dH <sub>2</sub> O, aliquoted and stored at -20°C.	50 mM 150 mM 0.5% 0.5% 1% pH 7.5
APS	0.05 g of APS was dissolved in 500 µl of dH <sub>2</sub> O. Always prepared before use.	10%
Resolving gel buffer	27.23 g of Tris base was dissolved in 80 ml of dH <sub>2</sub> O. Adjusted the pH to 8.8. Volume adjusted to 150 ml with dH <sub>2</sub> O. Stored at 4°C	1.5 M pH 8.8
Stacking gel buffer	6.05 g Tris base was dissolved in 60 ml dH <sub>2</sub> O. Adjusted the pH to 6.8. Volume adjusted to 100 ml with dH <sub>2</sub> O. Stored at 4°C.	0.5 M pH 6.8
SDS	10 g of SDS pellets were dissolved in 100 ml of dH <sub>2</sub> O.	10%
10x Tris-glycine SDS buffer (WB running buffer)	30.3 g Tris base 144.0 g glycine 10 g SDS pellet. Contents were dissolved in 1 l of dH <sub>2</sub> O, stored at 4°C.	25 mM 192 mM 0.1% pH 8.3
1x WB running buffer	50 ml of 10x WB running buffer Volume was adjusted to 450 ml with dH <sub>2</sub> O.	1x
10x Tris-glycine buffer (transfer buffer)	30.3 g Tris base 144.0 g glycine Contents were dissolved in 1 l of dH <sub>2</sub> O, stored at 4°C.	25 mM 192 mM pH 8.3
1x Transfer buffer	50 ml of 10x transfer buffer 100 ml of methanol Volume adjusted to 500 ml with dH <sub>2</sub> O	1x 20% methanol



10x TBS-T (Tris-buffered saline and Tween-20)	30.3 g Tris base, 87.7 g NaCl Contents were dissolved in 900 ml dH <sub>2</sub> O. Adjusted pH to 7.4. 5 ml of Tween-20 was added. Volume was adjusted to 1 l.	25 mM 150 mM 0.05% pH – 7.4
1x WB wash buffer	50 ml of 10x TBS-T Volume adjusted to 450 ml with dH <sub>2</sub> O.	1x
3x Sample buffer	0.77 g Tris HCL (pH 6.8) 2 g SDS 1.54 g DTT 10 ml glycerol 10 µl bromophenol blue Contents were dissolved in 100 ml dH <sub>2</sub> O, aliquoted 1 ml each and stored at -20°C.	50 mM 2% (w/v) 100 mM 10% (v/v) 0.01% (w/v)
Blocking buffer	5 g of milk powder was dissolved in 100 ml of 1x TBS-T	5% milk powder
Antibody solution	2.5 g of milk powder was dissolved in 100ml of 1x TBS-T	2.5% milk powder

### 3.1.3.2 Buffers for SDS-PAGE gel

Amounts used to prepare 2 gels. Contents were added in the order mentioned.

#	Contents	10% Resolving gel	12% Resolving gel	4% Stacking gel
1	H <sub>2</sub> O	6.15 ml	6.8 ml	6.1 ml
2	Buffer	3.75 ml (1.5 M Tris pH 8.8)	5 ml (1.5 M Tris pH 8.8)	2.5 ml (0.5 M Tris pH 6.8)
3	SDS (10%)	150 µl	200 µl	100 µl
4	Acrylamide	4.95 ml	8 ml	1.3 ml
5	APS (10%)	75 µl	100 µl	50 µl
6	TEMED	7.5 µl	10 µl	10 µl
	Total	20 ml	20 ml	10 ml

### 3.1.3.3 Buffers for Immunofluorescence

Buffers	Contents and preparation	Final concentration
0.1 M Phosphate buffered saline (PBS) 10x pH – 7.4	2.04 g NaH <sub>2</sub> PO <sub>4</sub> 14.77 g Na <sub>2</sub> HPO <sub>4</sub> ·2H <sub>2</sub> O 87.6 g NaCl All contents were dissolved in dH <sub>2</sub> O and pH adjusted to 7.4	17 mM 3 mM 1.5 mM
1x PBS with sodium azide (0.01%)	1x PBS 0.1 g of NaN <sub>3</sub> dissolved in 1 l dH <sub>2</sub> O and pH adjusted to 7.4	1x PBS 0.01% NaN <sub>3</sub>
Paraformaldehyde (PFA)	40 gm of PFA was dissolved in 800 ml of dH <sub>2</sub> O and heated to 60° C. Solution was cleared by adding 1 M NaOH, allowed it to cool down and then 100 ml of 1x PBS was added. Adjusted pH to 7.4, volume adjusted	4%

	to 1 l and filtered, aliquoted and stored at -20° C.	
PFA with sucrose	5 g of sucrose was dissolved in 100 ml of 4% PFA, aliquoted and stored at -20°C	4% PFA 5% sucrose
Cryoprotection solution	30 g of sucrose dissolved in 100 ml of 1x PBS.	30% sucrose in 1x PBS
Crystal violet solution (Nissl staining)	1.25 g dissolved in 500 ml dH <sub>2</sub> O. Later 1.5 ml of acetic acid was added and filtered.	0.25%

### 3.1.3.4 Solutions for stainings

Solution	Contents
Blocking solution for primary astrocyte cultures (PACs)	5% NGS in 1x PBS (pH 7.4)
Permeabilization solution (PACs)	0.5% TritonX-100 in 1x PBS (pH 7.4)
Primary antibody solution (for PACs)	Diluted in solution with 2.5% NGS in 1x PBS (pH 7.4)
Secondary antibody solution (for PACs)	Diluted in 1x PBS
Blocking solution for mouse brain sections	10% NGS, 0.4% TritonX-100 in 1x PBS (pH 7.4)
Primary antibody solution	Diluted in 5 % NGS, 0.1% TritonX-100 in 1x PBS (pH 7.4)
Secondary antibody solution	Diluted in 1x PBS
Blocking for biocytin visualization	10% NGS, 2% TritonX-100 in 1x PBS (pH 7.4)
Primary antibody solution for biocytin	Diluted in 2% NGS, 0.1% TritonX-100 in 1x PBS (pH 7.4)
Nuclei staining – Hoechst (1 mg/ml)	Diluted 1:10 or 1:100 in dH <sub>2</sub> O
Nuclei staining – DRAQ5	Diluted 1:1000 in 1x PBS

### 3.1.3.5 Solutions for genotyping

Solution	Contents and preparation	Final concentration
Laird buffer	6.057 g Tris (pH 8.5) 5.84 g NaCl were first dissolved in dH <sub>2</sub> O, pH was adjusted to 8.5, 0.73 g EDTA 1 g SDS Contents were dissolved and volume adjusted to 500 ml	100 mM 200 mM  5 mM 0.2%
Proteinase-K	Stock (20 mg/ml) dissolved in dH <sub>2</sub> O	50 µg
70% Ethanol	70 ml of absolute ethanol was dissolved with 30 ml of dH <sub>2</sub> O	70%
TBE buffer (10x)	121.1 g Tris 51.35 g boric acid 3.72 g EDTA Contents were dissolved in 1 l dH <sub>2</sub> O.	1 M 0.83 M 10 mM
TBE buffer (1x)	100 ml of 10x TBE was adjusted to 1 l using dH <sub>2</sub> O.	1x

**3.1.3.6 Solutions for bacterial cultures**

<b>Solution</b>	<b>Contents and preparation</b>	<b>Final concentration</b>
LB agar (Lennox)	35 g dissolved in 1 l of dH <sub>2</sub> O. Sterilized by autoclaving at 121°C, 15 lbs pressure for 20 min. (appropriate antibiotics were added before pouring plates)	---
LB medium (Lennox)	20 g dissolved in 1 l of dH <sub>2</sub> O and sterilized.	---
Ampicillin	10 g of Ampicillin dissolved in 100 ml of dH <sub>2</sub> O. Sterile filtered, aliquoted and stored at -20°C.	100 µg/ml
Kanamycin	5 g of Kanamycin dissolved in 100 ml of dH <sub>2</sub> O. Sterile filtered, aliquoted and stored at -20°C.	50 µg/ml

**3.1.3.7 RNA Co-immunoprecipitation buffers**

<b>Buffer</b>	<b>Preparation</b>	<b>Final concentration</b>
NaCl	2.92 g was dissolved in 50 ml of RNase/DNase free water	1 M
HEPES	0.60 g was dissolved in 50 ml of RNase/DNase free water	0.5 M
EDTA	0.73 g was dissolved in 50 ml of RNase/DNase free water. Adjusted pH to 8 with 1M NaOH	0.5 M
TritonX-100	5 ml of TritonX-100 was dissolved in 25 ml of RNase/DNase free water	20%
RNA-FLAG lysis buffer	1 ml 10 ml 3 ml 1.25 ml, volume adjusted to 50 ml with RNase/DNase free water and filtered using sterile filters. 200 U/ml RNasin, complete mini without EDTA (Roche) 1 tablet/ 10 ml of lysis buffer, 1µg tRNA/ 1 ml lysis buffer were added before using.	10 mM HEPES 200 mM NaCl 30 mM EDTA 0.5% Triton X-100
RNA-FLAG wash buffer	1 ml 25 ml 3 ml 1.25 ml, volume adjusted to 50 ml with RNase/DNase free water and filtered using sterile filters. 100 U/ml RNasin, complete mini without EDTA (Roche) one tablet/ 50 ml of wash buffer were added before using.	10 mM HEPES 200 mM NaCl 30 mM EDTA 0.5% TritonX-100
RNA-FLAG blocking buffer	RNA-FLAG lysis buffer (without RNasin and complete mini tablet).	1 µg tRNA 30 µl beads 3% BSA per 0.5 ml of lysis buffer

### 3.1.4 Antibodies

#### 3.1.4.1 Primary antibodies

Name	Species	Dilution		Company
		WB	IHC	
FLAG epitope	Mouse	1:1000	--	Sigma Aldrich
BLBP	Rabbit	--	1:500	Abcam
CPEB1 serum	Rabbit	--	1:500	Eurogentec
CEPB2 serum	Rabbit	--	1:500	Eurogentec
CEPB3 serum	Rabbit	--	1:500	Eurogentec
CPEB3	Rabbit	--	1:1000	Abcam
CPEB4	Rabbit	--	1:500	Eurogentec
CPEB1 PA*	Rabbit	--	1:100	Eurogentec
CPEB2 PA*	Rabbit	--	1:250	Eurogentec
CPEB4 PA*	Rabbit	--	1:100	Eurogentec
β-Actin	Mouse	1:5000	--	Sigma Aldrich
GFP	Rabbit	--	1:1000	Synaptic systems
GFP	Chicken	--	1:500	Abcam
GFP (FITC coupled)	Rabbit	--	1:500	Invitrogen
GFP	Mouse	1:1000	--	Clontech
GFAP	Mouse	1:1000	1:500	Millipore
Glutamine synthetase	Mouse	1:1000	1:500	Millipore
GLT-1	Guinea pig	1:1000	1:500	Millipore
Ki67	Rabbit	--	1:500	Novocasta
Connexin43	Rabbit	1:2000	1:1000	Sigma Aldrich
Connexin30	Rabbit	1:250	1:500	Invitrogen
S100β	Rabbit	--	1:3000	Abcam
Iba1	Rabbit	--	1:500	Alamone labs
NG2	Rabbit	--	1:250	Millipore
NeuN	Mouse	--	1:500	Millipore
Prox1	Rabbit	--	1:2500	Chemicon
Tubulin	Mouse	1:10,000	--	Sigma Aldrich

\*purified antibody

#### 3.1.4.2 Secondary antibodies

Name	Species	Application	Dilution	Company
Anti mouse HRP	Sheep	WB	1:10,000	GE Healthcare
Anti rabbit HRP	Donkey	WB	1:10,000	GE Healthcare
Anti guinea pig HRP	Goat	WB	1:5000	Abcam
Alexa fluor 488	Goat anti mouse	IHC/ICC	1:500	Molecular probes
Alexa fluor 488	Goat anti rabbit	IHC/ICC	1:500	Molecular probes
Alexa fluor 488	Goat anti chicken	IHC/ICC	1:500	Molecular probes
Alexa fluor 594	Goat anti mouse	IHC/ICC	1:500	Molecular probes
Alexa fluor 594	Goat anti rabbit	IHC/ICC	1:500	Molecular probes
Cy3 coupled	Goat anti guinea pig	IHC/ICC	1:500	Dianova
Alexa fluor 647	Goat anti rabbit	IHC/ICC	1:500	Molecular probes
Alexa fluor 647	Goat anti mouse	IHC/ICC	1:500	Molecular probes

### 3.1.5 Restriction enzymes

Enzyme	Recognition sequence (5' to 3')	Source
<i>EcoRI</i>	G <sup>1</sup> AATTC	NEB
<i>EcoRV</i>	GAT <sup>1</sup> ATC	NEB
<i>HindIII</i>	A <sup>1</sup> AGCTT	NEB
<i>MfeI</i>	C <sup>1</sup> AATTG	NEB
<i>SalI</i>	G <sup>1</sup> TCGAC	NEB
<i>SfiI</i>	GGCCNNNN <sup>1</sup> NGGCC	NEB
<i>XbaI</i>	T <sup>1</sup> CTAGA	NEB

### 3.1.6 Expression vectors

Vector	Company
PCR-XL topo vector	Invitrogen
pEGFP-N1	Clontech
pGL4.75	Promega
p3XFLAG-CMV-7.1 expression vector	Sigma
pMM403-400	Provided by Dr. Martin Theis

### 3.1.7 Competent *E. coli*

Self made competent *E. coli* (Appendix I)  
 Top10 chemically competent *E. coli* (Invitrogen)  
 Fusion blue competent cells (Clontech)

### 3.1.8 Lab devices

Device	Company
ABI 7900HT fast real time PCR system	Applied Biosystems, Darmstadt, Germany
Axiophot	Carl Zeiss, Carlzeiss microimaging GmbH, Göttingen, Germany
Binocular	Moticam, Xiamen, China
Centrifuges	Eppendorf GmbH, Wesseling, Germany
Cryostat	Microm HM560, ThermoScientific
Gel electrophoresis chamber	Biorad, Munich, Germany
Genegnome syngene bioimaging	Synaptics ltd. Cambridge, England
GeneFlash syngene bioimaging	Synaptics ltd. Cambridge, England
Heat block	VWR, Darmstadt, Germany
Incubator	BINDER, USA
Leica TCS confocal	Leica Microsystems, Wetzlar, Germany
Nanophotometer Pearl	Implen GmbH, München, Germany
Novex Minicell WB module	Invitrogen, Darmstadt, Germany
Olympus (FLUOVIEW FV1000) confocal	Olympus, Hamburg, Germany
PCR machines (MyCycler thermal cycler)	Biorad, München, Germany
Table top small centrifuge	VWR, Darmstadt, Germany
Table top centrifuge (Centrifuge5424)	Eppendorf GmbH, Wesseling, Germany
Centrifuge (15ml and 50ml falcons)	HERAEUS LABOFUGE centrifuge, Thermo Fisher Scientific, Schwerte, Germany
Cooling centrifuge	HERAEUS Fresco17 centrifuge,

---

Hybridization oven	Thermo Fisher Scientific, Schwerte, Germany
pH meter	Labnet International Inc., Edison, USA
Refrigerators (4°C and -20°C)	Mettler Toledo, Giessen, Germany
Refrigerators (-80°C)	Liebherr GmbH, Biberach, Germany
Rotator mixer	Thermo Fisher Scientific, Schwerte, Germany
Shaker	Grant-Bio, UK
Shaking incubator (GFL)	Heidolph Rotomax 120
Shaking water bath	Progen Scientific, London, England
Vibratome (VT1000S)	Memmert GmbH, Schwabach, Germany
Vortexer	Leica, Nussloch, Germany
Mini-Protean 3 cell (WB)	VWR, Darmstadt, Germany
WB power supply	Biorad, Munich, Germany
Weigh balance	Biorad, Munich, Germany
Water bath	ACCULAB, Sartorius group
	P-D Industriegesellschaft GmbH, Germany

---

### 3.1.9 General lab materials

---

Material	Company
Agarose	Invitrogen
Cell culture materials	Grenier Bio-one,/Millipore, Germany
Cell scrapers, Tubes	Sarstedt, Germany
Gloves	Ansell ltd, Staffordshire, UK
Mice surgery equipment	Fine Science Tools (F.S.T), Heidelberg, Germany
Microscopic slides	Thermo Fisher Scientific
Pasteur pipettes	Carl-Roth, Karlsruhe, Germany
Pipette tips	Greiner Bio-one
Pipettes, PCR tubes	BRAND, Wertheim, Germany
PVDF membrane	Millipore, Germany
Sterile filters	Millipore
Syringes, Venofix safety	Braun, Melsungen, Germany
Whatman paper	Whatman International, Maidstone, UK

---

## **3.2 Methods**

### **3.2.1 Cell culture**

#### **3.2.1.1 Primary astrocyte cell culture**

Primary astrocyte cultures were prepared as described previously (Derouiche and Frotscher, 2001). Briefly, cortical astrocytes were isolated from 2-4 day old rat pups. The tissue was dissociated using trypsin (Gibco/Invitrogen, Darmstadt, Germany) and cells were plated in 75 cm<sup>2</sup> tissue culture flasks (Sarstedt, Nümbrecht, Germany) with Dulbecco Modified Eagle Medium (DMEM, Sigma-Aldrich, Munich, Germany) supplemented with FCS (10%, Sigma-Aldrich) and incubated at 37°C with 5% CO<sub>2</sub>. Medium was exchanged after 5 days and later on regularly at 2-3 day intervals, but only with DMEM. After 8-14 days, cells were shaken for 18 hrs in a shaking incubator (Heidolph Instruments, Germany) at 37°C/250 rpm, and the adherent cells were re-plated (McCarthy and de Vellis, 1980) onto 10 cm or 6-well plates for further experiments. At least 95% of these cells in culture were type I astrocytes (McCarthy and de Vellis, 1980).

#### **3.2.1.2 Transfection**

Primary astrocytes were transiently transfected using Lipofectamine 2000 (Invitrogen) or Fugene (Roche, Mannheim, Germany) as per the manufacturer instructions. Briefly, cells were plated in a 6-well plate 24-48 hrs before transfection with poly-L-lysine (PLL, Sigma) coated 12 mm coverslips (Carl Roth, Karlsruhe, Germany), care was taken not to overgrow the cultures before transfection. For each well, 680 µl of the DMEM without serum was mixed with DNA and Lipofectamine (5 µl Lipofectamine:4 µg DNA). After 5 hrs medium was replaced with medium containing serum. For Fugene, 680 µl of the DMEM with serum was mixed with DNA and fugene (6 µl Fugene:2 µg DNA) complex and were used for transfection. After 48 hrs of transfection, the cells were fixed for further stainings.

### **3.2.2 RNA isolation and reverse transcription PCR from primary astrocytes in culture**

#### **3.2.2.1 RNA purification**

For extracting RNA, cells were grown in 10 cm dish until 90% confluent. The medium was removed and the cells were washed 3 times with 1x PBS. Using 1ml Trizol reagent (Invitrogen) / dish, cells were scraped and collected into a 2 ml tube and frozen immediately

on dry ice and stored at  $-80^{\circ}\text{C}$  until further use. 250  $\mu\text{l}$  of chloroform was added to each tube and vigorously shaken followed by centrifuging at 10,000  $\times g/10\text{ min}/4^{\circ}\text{C}$ . The aqueous upper layer was taken into a new tube and 500  $\mu\text{l}$  of isopropanol was added and incubated on ice for 10 min and then centrifuged at 10,000  $\times g/10\text{ min}/4^{\circ}\text{C}$ . Supernatant was removed and the pellet was washed with 75% ethanol at 7500  $\times g/5\text{ min}/4^{\circ}\text{C}$ . The supernatant was removed and the pellet was air dried for 5 min and dissolved in 20  $\mu\text{l}$  of DEPC water. The RNA samples were stored at  $-20^{\circ}\text{C}$ . DNase treatment was done using RQ1 RNase-free DNase kit (Promega, Madison, USA) as per the manufacturer instructions.

### 3.2.2.2 Reverse transcription PCR

For reverse transcription, Omniscript Reverse Transcription kit (Qiagen, Hilden, Germany) was used according to manufacturer instructions and the reaction mix used is in table 3.

Components	Amount
10x RT buffer	2 $\mu\text{l}$
dNTP (5 mM each)	2 $\mu\text{l}$
Oligo dT primer (50 $\mu\text{M}$ )	0.4 $\mu\text{l}$
RNase inhibitor (40 U/ $\mu\text{l}$ )	0.25 $\mu\text{l}$
Omniscript reverse transcriptase	1 $\mu\text{l}$
RNase free water	8.6 $\mu\text{l}$
Total	15 $\mu\text{l}$

Table 3: Reverse transcription reaction mix for astrocyte cultures.

5  $\mu\text{l}$  of template RNA was used for each reverse transcription reaction. Samples were incubated at  $37^{\circ}\text{C}$  for 1 hr. The cDNA samples were used for PCR with primers specific to identify the splice isoforms of each CPEB (Table 4). Accuprime DNA polymerase system (Invitrogen) was used for the PCR amplification as per manufacturer instructions. The primers used are in table 4 and the program used is in table 5.

#	Type	Sequence	Gene
1	forward	5'-AGGCCATCTGGGCTCAGCGGG-3'	CPEB1
	reverse	5'-GGATTGGTTAACACCTTCCGTGTTTTTGGC-3'	
2	forward	5'-ATGTGTTTCAGGACAGACAATAGTAACA-3'	CPEB2
	reverse	5'-CAAGCTATCATCTATTGGAAATAGGGAAGA-3'	
3	forward	5'-GGATATGATCAGGACTGATCATGAGCCTCTGAAAG-3'	CPEB3
	reverse	5'-CCATGGCTGTCATCCAAGAAGGCGTC-3'	
4	forward	5'-CCCAGGACATTTGACATGCACTCATTG-3'	CPEB4
	reverse	5'-CAGACCACTGTGAAGAGGCTGGTCCCCACGG-3'	
5	forward	5'-CGTGGGCCGCCCTAGGCACCA-3'	$\beta$ -actin
	reverse	5'-CGGTTGTCCTTAGGGTTCAGAGGGG-3'	

Table 4: Primer sequences of CPEBs (1-4).  $\beta$ -actin served as a positive control.



Initial denaturation	94°C for 30 sec	
Denaturation	94°C for 30 sec	
Annealing	55°C for 30 sec for CPEB2 & CPEB3	} 30x
	58°C for 30 sec for CPEB1, CPEB4 and $\beta$ -actin	
Extension	68°C for 1 min	
Final extension	68°C for 20 min	
Hold	4°C	

Table 5: PCR program for CPEB isoforms.

The PCR amplified products were separated on 1.5% agarose gel, and the respective bands for each CPEB were excised from the gel. The DNA was purified from excised bands using a gel extraction kit (Promega) according to manufacturer instructions. Later, the PCR products were cloned into the PCR-XL-TOPO vector (Invitrogen) as per the manufacturer instructions. The cloned products were transformed with Top10 chemically competent *E. coli* (Invitrogen) and plated onto LB agar plates with kanamycin (50  $\mu$ g/ml) as selection marker and incubated at 37°C overnight. Single colonies were picked and grown overnight in LB medium with kanamycin (50  $\mu$ g/ml) in a shaking incubator at 250 rpm/37°C. DNA was isolated with a Miniprep kit (Promega) according to manufacturer instructions. The PCR-XL-TOPO cloned CPEB inserts were analyzed by restriction digestion with *EcoRI* enzyme (NEB, Frankfurt, Germany), as *EcoRI* flanks the cloning site (and is used to verify the size of the cloned PCR product). Minipreps were sequence analyzed (Qiagen sequencing services) to identify the isoforms for each CPEB.

### 3.2.3 Immunocytochemistry

#### 3.2.3.1 Staining for CPEBs in primary astrocytes

For immunofluorescence, primary astrocytes were grown for 2-3 days on 12 mm coverslips coated with PLL (Sigma) in 6 well plates. The medium was removed, washed twice with 1x PBS and fixed with 4% PFA in 1x PBS (pH 7.4) with 5% sucrose for 20 min at room temperature (RT). Cells were washed twice with 1x PBS for 5 min each, permeabilized with 0.5% TritonX-100 (Applichem, Darmstadt, Germany) for 5 min at RT and washed twice quickly. Blocking was done with 5% normal goat serum (NGS) in 1x PBS (pH 7.4) for 1 hr at RT and then incubated with primary antibodies in antibody solution (2.5% NGS in 1x PBS) (pH 7.4) at 4°C overnight. The primary antibodies used were CPEB (custom made purified antibodies or serum (Eurogentec, Cologne, Germany) for CPEB1 (dilution 1:100), CPEB2 (1:250), CPEB4 (1:100) and for CPEB3 (1:100, Abcam, Cambridge, UK) and GFAP (1:500,

Millipore, Germany). The cells were washed three times with 1x PBS for 5 min at RT each and incubated with respective secondary antibodies in 1x PBS for 1 hr at RT. It was followed by washes with 1x PBS and nuclei staining with Hoechst (1:10, Invitrogen) in dH<sub>2</sub>O water for 10 min at RT. After washing with 1x PBS, coverslips with cells were mounted onto microscopic slides (Thermo Fisher Scientific, Schwerte, Germany) using Permafluor (Thermo Fisher Scientific) mounting medium. Slides were dried and images were taken with Axiophot microscope (Carl Zeiss, Göttingen, Germany) with 20x and 40x objectives.

### **3.2.3.2 Triple staining of primary cultures**

Cells were prepared as described in 3.2.3.1 and incubated with primary antibodies directed to Cx43 (1:1000, rabbit polyclonal, Sigma) and GFAP (1:500, mouse monoclonal, Millipore) diluted in 2.5% NGS in 1x PBS (pH 7.4) for 2 hr at RT. After washes, cells were incubated with respective secondary antibodies: Alexa594 (1:500, goat anti-rabbit, Invitrogen) and Alexa647 (1:500, goat anti-mouse, Invitrogen) in 1x PBS for 1.5 hr at RT. Cells were washed with 1x PBS for 3 times 5 min each and incubated with GFP antibody (1:500, FITC coupled) for 2 hr at RT, followed by washes with 1x PBS. Nuclear staining and mounting were done as mentioned in 3.2.3.1.

## **3.2.4 Generation of vectors for transgenic mice**

### **3.2.4.1 3' RACE of CPEB3**

Rapid amplification of cDNA ends (RACE) experiments were done to determine the 3' end of CPEB3. Marathon Ready cDNA kit (Clontech) was used as per the manufacturer instructions. Gene specific primers of 23-28 nt length with a GC content of 40-60% and melting temperature higher than or equal to 70°C were designed for the touchdown PCR (Don et al., 1991; Roux, 1995). Four forward primers were designed which bind approximately 1.6 kb, 1 kb, 535 bp and 300 bp upstream of the 3' end of the CPEB3 UTR as per the sequence information obtained from Ensembl ([www.ensembl.org](http://www.ensembl.org)). The primer sequences are in table 6.

<b>Primer name</b>	<b>Sequence</b>
1.6 kb	5' -GGGTTTCCCCTGGACCCTTTGGTAA- 3'
1 kb	5' -GACTCCACTTGGTGCTGAGGGCTGT- 3'
535 bp	5' -GCAGACTTTAGACATTGTGCTCACAG- 3'
300 bp	5' -GGGAGGGACTTTCATATCTGGTCAA- 3'

Table 6: Primer used for CPEB3 RACE.

Advantage 2 polymerase (Clontech) was used for the PCR and the PCR program used is described in table 7.

Initial denaturation	94°C for 1 min		
Denaturation	94°C for 30 sec	}	40x
Annealing and extension	68°C for 3 min		
Final extension	68°C for 20 min		
Hold	4°C		

Table 7: PCR program for CPEB3 RACE.

Electrophoresis of the PCR products was done on 1.2% agarose gels. In cases when smear (which indicates non specific products) was observed, a nested PCR was done using the PCR product from 535 bp as a template. The 300 bp primer and nested adapter primer (RACE kit) were used with a touchdown PCR program as in table 8.

Initial denaturation	94°C for 1 min		
Denaturation	94°C for 5 sec	}	5x
Annealing and extension	72°C for 3 min		
Denaturation	94°C for 5 sec	}	5x
Annealing and extension	70°C for 3 min		
Denaturation	94°C for 5 sec	}	25x
Annealing and extension	68°C for 3 min		
Final extension	68°C for 20 min		
Hold	4°C		

Table 8: Touchdown PCR program for CPEB3 RACE.

After electrophoresis, PCR products were excised from the agarose gel and DNA was purified and cloned into PCR-XL-TOPO vector (Invitrogen) and transformed as described in 3.2.2.2. The minipreps from the RACE PCR were sequence analysed.

### 3.2.4.2 Generation of vectors

Expression vectors were generated using PCR based, infusion and conventional cloning strategies (Sambrook and Russell, 2001). Vectors for transgenic mice were generated by cloning the sequences of different CPEB3 forms using infusion cloning technology (Clontech) as per the manufacturer’s instructions. These vectors were further used for zygote injection to generate transgenic mice.

### 3.2.4.3 Cloning of short and long UTRs of CPEB3 into pMM vector

Following the identification of the 3' ends of CPEB3 by RACE, the two full length 3' UTRs (shortUTR and longUTR) were isolated and cloned: For cloning the shortUTR (0.9 kb, shUTR) and longUTR (3.5 kb lgUTR) fragments of CPEB3, infusion cloning was performed. Inserts were cloned into the *Mfe*I site of the pMM403-400 vector (Appendix II). CPEB3-EGFP-pMM vector was digested with *Mfe*I (NEB) and run on 1 % agarose gel, excised the respective band and DNA was purified using gel extraction kit (Promega). Simultaneously, the inserts were PCR amplified using Advantage HD polymerase (Clontech) using a two step program as described in table 9.

Initial denaturation	98°C for 30 sec	
Denaturation	98°C for 10 sec	} 35x
Annealing and extension	68°C for 1 min for shUTR 68°C for 3 min 40 sec for lgUTR	
Final extension	68°C for 20 min	
Hold	4°C	

Table 9: Two step PCR program for infusion cloning.

The primers used for amplifying CPEB3sh/lgUTR with *Mfe*I flanking sites are in table 10.

Vector		Primer sequence
shUTR	forward	5' -AAAATGAATGCAATTGAGGCCGCCACAGCTACAAGTACTGG- 3'
	reverse	5' -TTAACAACAACAATTGGGATATAAAAATTTATTGCATGCAG- 3'
lgUTR	forward	5' -AAAATGAATGCAATTGAGGCCGCCACAGCTACAAGTACTGG- 3'
	reverse	5' -TAACAACAACAATTGCACGTTCTGCTCATTCTGTCGTTTTATTATCC- 3'

Table 10: Primer sequences for CPEB3sh and lgUTR amplification.

The PCR amplified UTR inserts with *Mfe*I overhangs were purified after electrophoresis and ligated with the purified vector as per the manual from infusion cloning. The ligated vectors were transformed with Fusion blue competent cells (Clontech) as per the manual, and plated onto LB plates containing ampicillin (100 µg/ml) antibiotic and incubated at 37°C overnight. Single colonies were picked and inoculated each in 2 ml LB medium with ampicillin (100 µg/ml), incubated at 37°C/overnight/250 rpm in a shaking incubator. DNA was isolated using Miniprep kit (Promega). The cloning was verified by restriction digestion with *Sfi*I and by sequencing (Qiagen).

#### 3.2.4.4 Cloning of CPEB3d and CPEB3aKD into pMM403-400 vector

The CPEB3d isoform, which lacks the B-region containing putative phosphorylation sites for PKA, S6kinase and CamKII (Theis et al., 2003b), was cloned into the unique *EcoRV* site of the pMM403-400 vector. CPEB3aKD is the kinase dead form of CPEB3a (full length isoform), which was generated by mutating two serines (S419 and S420) in the phosphorylation site. These two serines were mutated to alanines using the Splicing on Overlapping Extension (SOE) PCR (Sambrook and Russell, 2001) strategy. This mutated form was later cloned into the *EcoRV* site of pMM403-400 vector (Appendix II) using infusion cloning (Clontech). These two vectors were tagged with EGFP at the 3' end of the CPEB3 coding region. The pMM403-400 vector was digested with *EcoRV* restriction enzyme (NEB) and was purified after electrophoresis. The inserts (CPEB3d, CPEB3aKD) were PCR amplified using a two step program (as described in the Methods section 3.2.4.3) using Advantage HD polymerase and primers flanking with *EcoRV* restriction enzyme sites are: 5'-GCG GAT CCT GCG GAT ATC TCA GCG CCC CTT CTC CGC G -3' (forward) and 5'-GTG TGA TGG ATG GAT ATC TTA CTT GTA CAG CTC GTC -3' (reverse). These PCR amplified products with the *EcoRV* overhangs were purified from agarose gel after electrophoresis and ligated with the vector as described in the infusion cloning manual. Later fusion blue competent cells (Clontech) were transformed with the ligated products; the same procedure was followed as described in 3.2.4.3 Methods section.

### 3.2.5 Generation of CPEB3-GFAP transgenic mice

Handling and maintenance of the animals was according to the rules and regulations of federal law (University of Bonn, Germany). All the animals were housed under 12 hr day and night cycle.

#### 3.2.5.1 Cloning

CPEB3-EGFP transgene was cloned into the *EcoRV* sites of the pMM403-400 vector (Appendix II) inframe with the tetracycline operator (TetO) sequences (generated by Dr. Martin Theis).

#### 3.2.5.2 Construct preparation for zygote injection

The CPEB3-pMM403-400 plasmid was linearized with *SfiI* and the DNA fragments were separated by electrophoresis on 1% agarose gel, after clear separation the right band was excised. This DNA product was purified from gel using gel extraction kit (Promega) and

eluted in injection buffer (provided by House for Experimental Therapy (HET)). The purified DNA was injected into the male pronuclei of zygote (Injection was performed at the HET, University Hospital Bonn, Germany).

### 3.2.5.3 Isolation of genomic DNA from mouse tail tips

Lysis of mouse tail tips was done in Laird buffer (Laird et al., 1991) supplemented with 50 µg Proteinase-K/ ml at 55°C overnight in a water bath with agitation. The DNA was precipitated in isopropanol (one volume) by centrifuging at 13,500 rpm/10 min/RT. DNA pellet was washed in 70% ethanol in de-ionized water by centrifuging at 13,500 rpm/8 min/RT, air dried and eluted in an appropriate volume of TE buffer.

### 3.2.5.4 Genotyping PCR

To determine the presence of transgene, tail tip DNA was used as a template and PCR was performed with the primers specific to the TetO and tetracycline controlled transactivator (tTA) sequences. Primer sequences used are shown in table 11.

PCR	Primer name	Primer sequence
TetO	tetO-A/B (forward)	5' -GCGGCCGCAACTCTCG- 3'
	tetO-A (reverse)	5' -TCAAAACAGCGTGGATGGCGTCTC- 3'
	tetO-B (reverse)	5' -GATCGGTCCCGGTGTCTTCTATG- 3'
tTA	tTA-A1 (forward)	5' -GCGCTGTGGGGCATTCTTACTTTAG- 3'
	tTA-A2 (reverse)	5' -CCGCCAGCCCCGCCTCTTC- 3'
	tTA-B1 (forward)	5' -TAGAAGGGGAAAGCTGGCAAGATT- 3'
	tTA-B2 (reverse)	5' -CCGCGGGGAGAAAGGAC- 3'

Table 11: Primer sequences for genotyping (TetO and tTA) PCR.

The reaction mix used for genotyping PCR was as in table 12.

dH <sub>2</sub> O	14,8 µl
5x Promega PCR buffer	5,0 µl
MgCl <sub>2</sub> 25 mM	1,0 µl
dNTP's 2.5 mM each	1,0 µl
Primer 1 (10 µM)	1,0 µl
Primer 2 (10 µM)	1,0 µl
GoTaq Flexi DNA polymerase	0,2 µl
DNA template (tail tip DNA)	1,0 µl
Total	25 µl

Table 12: Reaction mix for genotyping PCR.

The program for both the genotyping PCRs (TetO and tTA) is in table 13.

Initial denaturation	94°C for 3 min	
Denaturation	94°C for 30 sec	} 30x
Annealing	62°C for 1 min	
Extension	72°C for 2 min (5 sec increase per cycle)	
Final extension	72°C for 10 min	
Hold	8°C	

Table 13: PCR program for genotyping.

The PCR products were run on a 1.5% agarose gel and the size was estimated with reference to the 1 kb marker (Invitrogen).

**3.2.5.5 Breedings**

After zygote injection, the mouse litters were screened for positive founders carrying the transgene (TetO-CPEB3) by genotyping (Methods 3.2.5.4). The positive TetO-CPEB3 mice were further bred with hGFAP-tTA mice (Pascual et al., 2005; Fiacco et al., 2007) and the litters were screened for double transgenics (DT) by genotyping.

**3.2.5.6 Doxycycline treatment**

CPEB3-GFAP mice were given doxycycline (Dox) (a derivative of tetracycline) in their food at a concentration of 650 mg doxycycline/kg of the food (Altromin, Lage, Germany). Dox was given up to postnatal 21-28 days to the mice. After removing Dox from the food, mice were analyzed after 7 weeks.

**3.2.6 Immunohistochemistry**

All the experiments with CPEB3-GFAP mice were performed 7 weeks after removal of Dox from the food, which was given during birth and until 3 - 4 weeks of age. Mice were aged p70 - p75 at the time of analysis.

**3.2.6.1 Perfusion fixation**

Mice were anesthetized with a 2:3 ratio of Ketamin (10%, Medistar, Aschberg, Germany) and Cepetor-KH (1 mg/ml, cp-pharma, Burgdorf, Germany) intraperitoneally. The abdomen was cut open removing the diaphragm and thoracic cavity was opened. The left atrium was cut for the blood to flow. Following insertion of a 25G needle (Braun, Melsungen, Germany) into the left ventricle, 30 ml of 1x PBS (pH 7.4) was injected to remove blood and fixation was done

by perfusing with 30 ml of 4% PFA in 1x PBS (pH 7.4). Brains were isolated and stored in 4% PFA 1x PBS (pH 7.4) overnight at 4°C.

### 3.2.6.2 Cryoprotection and sectioning

After 24 hr of fixation, cryoprotection was done by soaking the brains in 30% sucrose in 1x PBS (pH 7.4) at 4°C (at least for 48 hr). Brains were embedded in Tissue-tek (Sakura, Netherlands), frozen and stored at -80°C. Forty µm thick, free floating coronal sections were cut using a cryostat (Microm HM560, Thermo Fisher Scientific) and slices were collected in 1x PBS with 0.01 % sodium azide (for longer preservation of tissue) and stored at 4°C.

### 3.2.6.3 Staining procedure

For staining, sections were washed three times in 1x PBS for 10 min each and blocked with blocking solution (10% NGS, 0.4% TritonX-100 in 1x PBS (pH 7.4)) for 2 hr at RT and incubated in appropriate primary antibodies diluted in blocking solution (5% NGS, 0.1% TritonX-100 in 1x PBS (pH 7.4)) overnight at 4°C with gentle shaking. Primary antibodies used were: rabbit GFP (1:1000 dilution, Synaptic Systems), chicken GFP (1:500, Abcam), mouse GFAP (1:500, Millipore), mouse GS (1:500, Millipore), rabbit Cx43 (1:1000, Sigma), rabbit S100β (1:3000, Abcam), rabbit Iba1 (1:500, Alamone labs), rabbit NG2 (1:250, Millipore), mouse NeuN (1:200, Millipore), rabbit Cx30 (1:500, Invitrogen), rabbit BLBP (1:500, Abcam), rabbit Ki-67 (1:500, Novocastra) and rabbit Prox1 (1:2500, Chemicon). For Ki-67 staining, sections were incubated with primary antibody for 48 hr at 4°C with gentle shaking. Sections were washed three times in 1x PBS and then incubated with the appropriate secondary antibodies diluted in 1x PBS (pH 7.4) for 1.5 hr at RT. Sections were washed 3 times with 1x PBS, 10 min each and stained for nuclei with Hoechst (1:100 in dH<sub>2</sub>O, Invitrogen) by incubating for 10 min at RT, followed by washes for 3 times with 1x PBS, 10 min each, and mounted using Permafluor (Thermo Fisher Scientific) onto microscopic slides. For double immunofluorescence, the same procedure was followed with appropriate primary and secondary antibodies.

### 3.2.6.4 TUNEL staining

To estimate if there was any cell death caused due to the overexpression of CPEB3 in astrocytes, Terminal deoxynucleotidyl transferase dUTP nick end labeling (TUNEL) staining was performed. Mouse brains were isolated after cervical dislocation, cerebellum and frontal brain was cut off and placed facedown in a cryomold (Sakura, Netherlands) and covered with



Tissue-tek. The cryomold was placed in a styrofoam box containing liquid nitrogen for 5-10 min for fast freezing. Later the brains were stored at -80°C. Fourteen µm thick sections were taken onto Superfrost object slides (Thermo Fisher Scientific) allowed to air dry and stored at -80°C.

For labelling of TUNEL positive cells, the Click-it TUNEL Alexa Fluor Imaging Assay (Invitrogen) was used and the manufacturer instructions were followed with some modifications. Sections were fixed with acetone for 2 min at RT, slides were air dried and a barrier (Roti-Liquid Barrier Marker, Roth) was applied around the section, followed by a wash with 1x PBS. For GFAP staining, sections were blocked with 5% NGS, 0.125% TritonX-100 in 1x PBS (pH 7.4) for 1 hr at RT and incubated with mouse GFAP antibody (1:400) in 2% NGS, 0.125% TritonX-100 in 1x PBS (pH 7.4) for 1hr at RT. The sections were washed three times for 5 min each with 1x PBS followed by incubation with goat anti mouse Alexa fluor 488 (1:500) secondary antibody in 2% NGS, 0.125 % TritonX-100 in 1x PBS (pH 7.4) for 1 hr at RT. Sections were washed three times with 1x PBS for 5 min each, followed by staining for nuclei with Draq5 (1:1000, Biostatus ltd, Leicestershire, UK) in 1x PBS for 10 min at RT followed by two short washes, drying of the sections and mounting using Aqua polymount (Polysciences Inc, USA) mounting medium.

### 3.2.6.5 Nissl staining

Fourty µm thick, free floating sections were collected in 1x PBS (pH 7.4) after perfusion fixation and cryoprotection as described in Methods section 3.2.6.1, 3.2.6.2. Sections were mounted onto Superfrost object slides (Thermo Fischer Scientific) and allowed to dry completely for approximately 1 hr at RT. Sections were washed with dH<sub>2</sub>O for 2 min at RT and stained with crystal violet solution (0.25%) at 70°C for 10 min in a hybridization oven (Labnet International Inc., Edison, USA). Crystal violet was preheated at 70°C. Later sections were washed first with 70% ethanol, then 96% ethanol and with isopropanol each for 30 sec at RT. The slides were dried and mounted using Entellan (Merck, Darmstadt, Germany). Images were taken with a 30x objective of a binocular microscope (Moticam, Xiamen, China) with Motic Images Plus 2.0ML software.

### 3.2.6.6 Image acquisition and processing

All the images except the Nissl stained were acquired using 10x, 20x or 40x objectives of an Axiophot microscope (Carl Zeiss). For higher resolution, images were taken using 20x or 40x

objectives of a Leica TCS confocal (Leica Microsystems) or Olympus confocal (FLUOVIEW FV1000, Olympus, Hamburg, Germany) microscopes. Image processing and quantification was done using the ImageJ software (Rasband, 1997-2011; Abramoff et al., 2004).

### 3.2.6.7 Quantification

The overexpression of CPEB3-EGFP was quantified by taking 1-in-5 series sections with a total number of 4 sections/mice (8 hippocampi/mouse). The total number of GFP positive and GFP/GFAP, GFP/S100 $\beta$  co-localized cells were counted using ImageJ, in one view field of the Cornu Ammonis area 1 (CA1) region of the hippocampus taken with the 20x objective of the Axiophot microscope (Carl Zeiss). Similar quantification was performed for GFP/Iba1 and GFP/NG2 co-localizations. Quantification of the stainings related to adult neurogenesis (Ki-67, Prox1 and BLBP positive cells) was performed by Mr. Jiong Zhang in the institute, as previously described (Kunze et al., 2009).

### 3.2.6.8 Electrophysiology and biocytin visualization

Electrophysiology on these mice was performed by Dr. Peter Bedner in the institute, where the diffusion of the tracer N-biotinyl-L-lysine (biocytin; Sigma, Germany) between astrocytes was analyzed as described previously (Theis et al., 2003a; Wallraff et al., 2004; Wallraff et al., 2006). Mice were anesthetized with Isofluran, decapitated and the brains were isolated quickly and 200  $\mu$ m thick transversal sections of the hippocampus were cut on a vibratome (VT1000S; Leica). Single astrocytes from acute brain slices of CPEB3-GFAP mice were injected with biocytin after electrophysiological characterization by their passive current pattern (Wallraff et al., 2004). Cells from the CA1 region of the hippocampus were selected for biocytin injection.

After electrophysiology, sections were fixed in 4% PFA in 1x PBS overnight at 4°C, washed three times in 1x PBS for 10 min each and blocked for 2 hr at RT with 10% NGS/2% TritonX-100 in 1x PBS (pH 7.4). Sections were incubated with Cy3-coupled streptavidin (1:300 dilution) in 2% NGS/ 0.1% TritonX-100 in 1x PBS (pH 7.4) overnight at 4°C. Sections were washed with 1x PBS three times and stained for nuclei with Hoechst (1:10 dilution in dH<sub>2</sub>O) for 10 min at RT. Sections were washed briefly and mounted onto slides using Permafluor (Thermo Fisher Scientific) and allowed to dry. Stacks were made using the Axiophot microscope (Carl Zeiss) with a 20x objective and the extent of coupling was estimated by counting the number of cells positive for biocytin. For double labelling with

GFP antibody, the sections were co-incubated with GFP (1:1000) and Cy3-coupled streptavidin with the same conditions as described above. After washing, the sections were incubated with Alexa fluor 488 (1:500) secondary antibody in 1x PBS (pH 7.4) for 1.5 hr at RT followed by washing, nuclei staining and mounting as described in Methods section 3.2.6.3. Cells which were positive for GFP were considered in the quantification. A Student t-test was used to test for significant differences in the extent of coupling between the DT and control mice.

### **3.2.7 Western blotting**

#### **3.2.7.1 Sample preparation**

Mice were sacrificed by cervical dislocation, and the brain was isolated and cut into two halves. One half was used for immunostaining, fixed in 4% PFA/1x PBS (pH 7.4) at 4°C for 24 hr and cryoprotected with 30% sucrose in 1x PBS at 4°C for a minimum of 48 hr. From the second half, the cerebellum was harvested into a 1.5 ml Eppendorf tube and frozen in liquid nitrogen. The olfactory bulbs and the frontal cortex were cut off, and by placing the brain on the coronally cut side, the hippocampus and cortex were separated carefully and collected into a tube and frozen immediately in liquid nitrogen and stored at -80°C until further use. Lysis buffer (50 mM Tris, 150 mM NaCl, 0.5% NP-40, 0.5% NaDOC, 1% TritonX-100, pH 7.5) supplemented with complete mini tablet (1 tablet/10 ml, Roche) was used to lyse the tissue. A volume of 350 µl lysis buffer for hippocampus, 500 µl for both cortex and cerebellum was aliquoted into a prechilled tube. Tissue was transferred and lysed using a pestle until no further homogenization was possible. A 27G (Braun) 1 ml needle was used to further disrupt the tissue. The lysed samples were incubated on ice for 30 min followed by centrifugation for 30 min/10,000 g/4°C. Supernatant was aliquoted into a new prechilled tube. The concentration of the protein was estimated using a BCA kit (Thermo scientific) as per the manufacturer's instructions.

#### **3.2.7.2 SDS-PAGE, blotting and detection**

A 10% or 12% SDS polyacrylamide resolving gel and 4% stacking gel (self made) were used for electrophoresis. Thirty µg of protein each was used, samples were denatured in 3x loading dye at 65°C for 10 min, after that samples were spin briefly and loaded onto respective gels. The proteins were separated for 15 min at 80 V and 1 hr and 15 min at 160 V with running buffer (1x Tris-glycine-SDS). Novex (Invitrogen) standard was loaded along with the samples

to estimate the size based on separation of proteins. Separated proteins were transferred onto 0.45  $\mu\text{m}$  polyvinylidene fluoride (PVDF) membrane (Immobilon-P Transfer membrane, Millipore) which was activated by soaking in methanol for 1min and washed briefly by transfer buffer (1x Tris-glycine buffer with 20% methanol). Blotting was done for 2 hr at 50 V with transfer buffer. Membranes were blocked in 5% milk powder (Carl Roth)/1x Tris-buffered saline with Tween-20 (TBS-T) for 1 hr at RT and incubated with primary antibodies diluted in 2.5% milk/1x TBS-T overnight at 4°C. Primary antibodies used were rabbit Cx43 (1:1000, Sigma), rabbit Cx30 (1:250, Invitrogen), mouse GS (1:1000), mouse GFAP (1:1000, Millipore), guinea pig GLT-1 (1:1000, Millipore), mouse GFP (1:1000, Clontech) and mouse tubulin (1:10,000, Sigma). Membranes were washed three times with 1x TBS-T and incubated with horseradish peroxidase (HRP)-coupled secondary antibodies diluted in 2.5% milk/1x TBS-T for 1 hr at RT. Secondary antibodies used were anti-mouse HRP (1:10,000, GE Healthcare, Munich, Germany), anti-rabbit HRP (1:10,000, GE healthcare) and anti-guinea pig (1:5000, Abcam). After washing three times, blots were developed using ECL substrates (Supersignal West Dura extended duration substrate, Thermo scientific) using the Genegnome imaging device (Syngene bioimaging, Synoptics ltd, Cambridge, England). For Cx30, 50  $\mu\text{g}$  of the protein was loaded and after separation of proteins the membrane was blocked as explained above and incubated with primary antibodies diluted in 5% milk/1x TBS-T for 48 hr at 4°C. For probing with tubulin antibody, blots were stripped (Restore Western Blot stripping buffer, Thermo scientific) for 15 min at RT followed by washing 3 times each with 1x TBS-T for 10 min and blocking as described above, followed by incubating with the primary antibody (tubulin, 1:10,000) diluted in 2.5% milk/1x TBS-T overnight at 4°C. The same procedure as described above was followed for incubation with secondary antibodies.

### 3.2.7.3 Quantification

To quantify differences in the protein levels between transgenic and control mice, the blots were probed with tubulin as a loading control. The intensity of the bands was measured using the Gene tools software of Genegnome (Syngene bioimaging). After subtracting the background value for each band, the values from the target proteins were normalized to the values from their respective loading controls (tubulin). Significance was tested using the Student's t-test and p value less than 0.05 was considered as significant. Error bars are shown as standard errors of the mean (SEM).

### 3.2.8 RNA isolation and real time PCR

#### 3.2.8.1 RNA preparation from mouse brain

Tissue was harvested from mouse brains was as described in Methods section 3.2.7.1 and stored at -80°C.

#### 3.2.8.2 RNA purification and reverse transcription

Hippocampi were lysed in a 2 ml tube using Qiazol (Qiagen) with a pestle. A 27G 1 ml syringe (Braun) was used to further disrupt the small chunks of tissue until the mixture was homogenous. Samples were incubated at RT for 5 min, 200 µl of chloroform was added and tubes were shaken vigorously. The samples were centrifuged at 12,000 g/15 min/4°C and the aqueous phase was transferred into a new 1.5 ml tube containing 600 µl of 70% ethanol and mixed well. RNA was isolated using the RNeasy plus mini kit (Qiagen) according to the manufacturer’s protocol, 30 µl of RNase free water was used to elute the RNA (provided in the kit). On column DNase (provided in the kit) treatment was done for the samples as described in the kit. Concentration of RNA was determined by Nanophotometer Pearl (Implen GmbH, Munich, Germany). Reverse transcription was done by taking equal amounts of RNA by Superscript III reverse transcriptase (Invitrogen) according to the manufacturer protocol. The reverse transcription reaction mix is described in table 14.

Contents	Amount
5x first strand buffer	4 µl
DTT	1 µl
dNTP	1 µl
Random hexamers	1 µl
Superscript III reverse transcriptase	1 µl
RNasin (40 U/µl)	1 µl
DEPC dH <sub>2</sub> O	1 µl
Total	10 µl

Table 14: Reverse transcription reaction mix for RNA from mouse brain.

Ten µl of equal amounts of RNA template were used for reverse transcription reaction. The program for reverse transcription was: 50°C for 2 hr, 75°C for 20 min and after termination the products were kept at 4°C.

#### 3.2.8.3 Real time PCR

After the reverse transcription reaction, a real time PCR was performed using a Gene Expression Master Mix (Applied Biosystems, Darmstadt, Germany). 0.5 µl of cDNA was used as template in 12.5 µl total reaction volume. Ten µM of each primer and 5 µM probe

mix were prepared and 0.5 µl of this primer probe mix was used for real time PCR. Each reaction was done in triplicates. The reactions were carried out in optical 384-well reaction PCR plates (Applied Biosystems) in 7900HT Fast Real Time PCR System (Applied Biosystems). The PCR program used was at 50°C for 2 min, 95°C for 10 min, 95°C for 15 sec and 60°C for 1 min with 40 repetitions. Premixed *taqman* primers for β-actin and GLT-1 (Applied Biosystems) were provided by Dr. Gerald Seifert in the institute. All probes were labeled at 5' with fluorescein amidite (FAM) and at 3' end with carboxytetramethylrhodamine (TAMRA), except for β-actin where the quencher is non fluorescent. For each reaction, the critical threshold cycle ( $C_t$ ) value was determined using SDS 5.0 software (Applied Biosystems). The data was analyzed with the  $\Delta\Delta C_t$  method, using GAPDH and β-actin as reference genes. The efficiency of the different gene specific primers used was calculated by performing real time PCR (as mentioned above) with serial dilutions (100 ng, 10 ng, 1 ng, 0.1 ng, 0.01 ng, 0.001 ng) of mouse brain cDNA template. The  $C_t$  values were plotted against the concentration and the slope and correlation co-efficient were estimated. Primers and probe sequences used for each gene are described in table 15.

#	Type	Oligonucleotide sequence	Target
1	Forward	5'-TTTGACTTCAGCCTCCAAGGA- 3'	Cx43
	Reverse	5' -TCTGGGCACCTCTCTTTCACTTA- 3'	
	Probe	5' -TTCCACCACTTTGGCGTGCCG- 3'	
2	Forward	5' -CGTACACCAGCAGCATTCTT- 3'	Cx30
	Reverse	5' -ACCCATTGTAGAGGAAGTAGAACACAT-3'	
	Probe	5' -CGCATCATCTTTCGAAGCCGCCT- 3'	
3	Forward	5' -GAGAAGGACTGCGCTGCAA- 3'	GS
	Reverse	5' -CCACTCAGGTAACTCTTCCACACA- 3'	
	Probe	5' -CCGTACCCTGGACTGTGAGCCCAA- 3'	
4	Forward	5' -AGCTGTTCTGTCTACACTCCTGTTACTC- 3'	S100β
	Reverse	5' -CCTTCTCCAGCTCGGACATC- 3'	
	Probe	5' -ACACTGAAGCCAGAGAGGACTCCAGCA- 3'	
5	Forward	5' -CGACAGTCAGCCGCATCTT- 3'	GAPDH
	Reverse	5' -CCGTTGACTCCGACCTTCAC- 3'	
	Probe	5' -CGTCGCCAGCCGAGCCACA- 3'	

Table 15: Real time PCR primers and probe sequences of transcripts.

### 3.2.9 Generation of luciferase vectors

#### 3.2.9.1 GS 3' RACE

RACE (Clontech) was performed to identify the 3' end of the GS mRNA according to manufacturer instructions. Touchdown PCR was performed as mentioned in the Methods section 3.2.4.1. Primers were binding at 230 bp (RaceGS1), 369 bp (RaceGS2) and 617 bp (RaceGS3) upstream of 3' UTR end (sequence obtained from ensemble.org). Sequences of primers used were as in table 16.

Primer	Sequence
RaceGS1	5' -GTAAACACACCCCCACCTCCATCCCAGCC- 3'
RaceGS2	5' -CAATGTCTCCCTCCACTTGGCTCTTAGGG- 3'
RaceGS3	5' -CCAGGCTTAGGTTTAGGGGATGCGTATAC- 3'

Table 16: Primers for GS 3' RACE.

### 3.2.9.2 Luciferase vectors

For studying functional interactions between CPEB3 and its target proteins, luciferase expressing plasmids were generated. pGL4.75 [*hRluc*/CMV] was generated by replacing the renilla luciferase open reading frame (ORF) with firefly luciferase ORF (done by Lech Kaczmarczyk, IZN). The distal UTR sequences of the corresponding targets with CPEs were cloned into luciferase reporter plasmid.

#### 3.2.9.2.1 Isolation and cloning of WT and MUT 3' UTR of GS

The GS distal 3' UTR of 281 bp length was isolated which contains a CPE (wildtype, WT) from mouse brain cDNA (Clontech) with primers containing flanking restriction enzyme sites for *XbaI* and *SalI*. Advantage HF polymerase (Clontech) was used as per the manufacturer's instructions. The PCR program used is described in table 17.

Initial denaturation	94°C for 1 min	
Denaturation	94°C for 5 sec	} 35x
Annealing	45°C for 30 sec	
Extension	68°C for 1 min	
Final extension	68°C for 20 min	
Hold	4°C	

Table 17: PCR program for generating luciferase vectors.

The PCR product was run on a gel and the DNA was purified using a gel extraction kit (Promega) and cloned into the PCR-XL-TOPO vector (Invitrogen). The minipreps were verified by sequencing (Qiagen). The mutant (MUT) version was generated by mutating the CPEs using an SOE PCR-based strategy (Sambrook and Russell, 2001) and cloned into the PCR-XL-TOPO vector as above. Both the WT and MUT versions were sequence verified (Qiagen). The inserts were isolated from the PCR-XL-TOPO vector by digesting with *XbaI* and *SalI* enzymes; similarly, the luciferase vector was linearized using the same enzymes. They were separated on an agarose gel and DNA was purified using a gel extraction kit (Promega). The inserts and the vector were ligated with Fast-link ligase (Epicentre, Madison,

WI, USA) as per manufacturer’s instruction to obtain a GSWT-pGL and GSMUT-pGL vectors of GS 3' UTR. The primers used are shown in table 18.

Primer	Sequences
GSCPE left	5' -TCTAGAGACTGTTACTTTCCTTCTG- 3'
GS CPE right	5' -GTCGACGGAACCACAAAGAAACAAGTCAG- 3'
GS MUT up	5' -CTTTTTTTTTTTTCGGCCATAGTAAACACACCCCC- 3'
GS MUT down	5' -GGGGGTGTGTTTACTATGGCCGAAAAAAAAAAG- 3'

Table 18: Primers used for generating GS luciferase vectors.

### 3.2.9.2.2 Isolation and cloning of WT 3' UTR of Cx30

A Cx30 3'UTR fragment (WT) of 183 bp length was isolated from mouse brain cDNA (Clontech) using primers shown in table 19. Primers were flanked by sites for the restriction enzymes *XbaI* at the 5' end and *SalI* at the 3' end. Advantage HF polymerase (Clontech) was used as per the manufacturer’s instructions. The PCR program used was identical to the one described in Methods section 3.9.2.1, except for the annealing temperature, which was set to 49°C, and the same procedure was followed as described in 3.9.2.1.

Primer	Sequence
Cx30lt_sh	5' -TCTAGAGTTTAATGAGCTAGTGTGTGCTC- 3'
Cx30UTR_rt	5' -GTCGACGAAGCAACAGGGTCAAGCTTTATTGGC- 3'

Table 19: Primers used for generating Cx30 luciferase vectors.

### 3.2.10 Generation of the CPEB3a-FLAG vector

The ORF of CPEB3a was cloned downstream of the 3x FLAG sequence in a p3XFLAG-CMV-7.1 expression vector. Primers were designed as per the instructions in the infusion cloning manual (Clontech) with flanking restriction enzymes *HindIII* at 5' and *EcoRI* at 3' end.

### 3.2.11 RNA Co-immunoprecipitation or pulldown

To study the interaction between CPEB3 protein and the target mRNAs containing CPEs, RNA Co-immunoprecipitation (Co-IP) experiments were performed.

#### 3.2.11.1 HeLa cell culture and transfection

HeLa cells were maintained regularly in DMEM medium supplemented with 10% FCS, Penstrep (100 u/ml) at 37°C with 5% CO<sub>2</sub>. Cells were trypsinised at 48 hr intervals and replated in 75 cm<sup>2</sup> tissue culture flasks. HeLa cells were plated (1.7x10<sup>6</sup> cells/10 cm dish) 24 hr before transfection. Cells were allowed to grow until they reach 70-80% confluency. Cells were co-transfected with bait (CPEB3a-FLAG, CPEB1-FLAG (vector provided by Dr. Martin



Theis) or FLAG-GFP) and prey (luciferase constructs with WT or MUT CPEs) plasmids with lipid-based transfection using Lipofectamine 2000 (Invitrogen) according to the manufacturer's instructions. For each pulldown experiment, 6 µg of bait and 2 µg of prey plasmid DNA was used for transfection. Transfection was done using medium without serum, medium was exchanged with medium containing serum 5 hr after transfection. The transfected cells were used for further analysis after 24 hr.

### 3.2.11.2 Co-IP assay

Co-IP was performed to determine the interaction of CPEB3 with the target mRNAs (Cx43, Cx30 and GS) using FLAG antibody. Cells were harvested 24 hr post transfection, medium was removed and cells were washed twice with ice cold 1x PBS. The cell lysate was obtained by scraping in ice-cold lysis buffer (1 ml/10 cm dish) (10 mM HEPES pH 7.4, 200 mM NaCl, 30 mM EDTA, 0.5% TritonX-100) with RNasin (200 U/ml), Roche complete mini tablet (1 tablet/10 ml), tRNA (1 µg tRNA/ml) and taken into a pre-chilled 1.5 ml tube. The cell lysate was passed through a 27G needle (Braun) for 5-6 times for obtaining a homogenized lysate and was centrifuged at 16,000 g/4°C/20 min. Protein A sepharose beads (Invitrogen) were used for pre-clearing, 60 µl beads were first equilibrated in 1 ml of lysis buffer (without additives) by centrifuging at 6,000 g/4°C for 1 min, the buffer was removed and 1 ml of the supernatant from the centrifuged lysate was added to the beads and incubated at 4°C/1 hr by rotating at 12 rpm (Rotator mixer, Grant-Bio). To capture immunoprecipitated complexes protein G-Dyna beads (Invitrogen) were used, beads were first equilibrated with lysis buffer (without additives) and blocked (1 µg of tRNA/30 µl of beads/0.5 ml of lysis buffer with 3% BSA) for 1 hr on ice. Later the pre-cleared lysates were incubated for 2-4 hr/4°C/12 rpm with 10 µl of anti-FLAG mouse monoclonal antibody (Sigma) and Protein G-Dyna beads (Invitrogen) mixture. Thirty µl of the sample were taken to determine the amount of input material. Then the beads were washed (1 ml/tube) for 5-6 times/5 min each with ice cold wash buffer (10 mM HEPES pH 7.4; 500 mM NaCl; 30 mM EDTA; 0.5% TritonX-100 with 100 U of RNasin and one complete mini tablet /50 ml of wash buffer). 350 µl of RLT buffer (RNeasy mini kit, Qiagen) was added to the beads and stored at -20°C.

### 3.2.11.3 RNA extraction and reverse transcription

The CPEB3 bound mRNA was extracted from the co-immunoprecipitate. Reverse transcription was performed by using Superscript III (Invitrogen). RNA was extracted from both the pull down samples and inputs using an RNeasy plus mini kit (Qiagen) following

manufacturers instructions. For reverse transcription reaction, equal amounts of RNA were used with Superscript III reverse transcriptase (Invitrogen) according to manufacturer’s instructions. The reverse transcription reaction mix used for RNA Co-IP is in table 20.

Contents	Amount
5x first strand buffer	4 µl
DTT	1 µl
dNTP	1 µl
Random hexamers	1 µl
Superscript III reverse transcriptase	1 µl
RNasin (40 U/µl)	1 µl
DEPC dH <sub>2</sub> O	1 µl
Total	10 µl

Table 20: Reverse transcription reaction mix for RNA extracted from Co-IP samples.

For pulldowns, 10 µl of RNA template was used for the reverse transcription reaction. For the inputs, the concentration was determined using Nanophotometer (Implen GmbH), and equal amounts of RNA were taken. Reaction conditions were the same as mentioned in the Methods section 3.2.8.2.

### 3.2.11.4 Real time PCR

To measure the enrichment of the co-immunoprecipitated mRNAs, *Taqman* (Applied Biosystems) based quantitative real time PCR for luciferase was performed. After reverse transcription reaction, a *Taqman* reaction was performed using a Gene Expression Master Mix (Applied Biosystems). Each reaction was done in triplicate. The reactions were carried out in Optical 384-Well Reaction PCR plates (Applied Biosystems) using a 7900HT Fast Real Time PCR System (Applied Biosystems). The reaction mix and PCR conditions used were identical to the conditions mentioned in 3.2.8.3 except that 60 repetitions were carried out. Human GAPDH was used as reference gene. Data was analyzed using the  $\Delta\Delta C_t$  method and the retention of mRNA by the bait proteins was calculated using normalized input mRNA values. The primers and probe sequences used for real time PCR are shown in table 21.

#	Type	Oligonucleotide sequence	Target	Species
1	Forward	5' - CCAATTCAGCGGGAGCC - 3'	Luciferase	Firefly
	Reverse	5' - TTCGACGCAGGTGTCGC - 3'		
	Probe	5' - TGTTGGGGTGTGGAGCAAGATGGAT - 3'		
2	Forward	5' - AAGATGCGGCTGACTGTGC - 3'	GAPDH	Human
	Reverse	5' - GTGAAGGTCGGAGTCAACGG - 3'		
	Probe	5' - TGTGGCTCGGCTGGCGACG - 3'		

Table 21: *Taqman* primer and probe sequences used for real time PCR of RNA Co-IP samples.

## 4. Results

### 4.1 Expression of CPEBs in primary astrocyte cultures

In order to investigate the role of CPEBs in astrocytes, the expression pattern of different CPEBs (1-4) was studied in primary astrocyte cultures.

#### 4.1.1 Expression pattern of CPEB isoforms

For investigating the expression pattern of CPEBs in astrocytes, RNA was harvested from rat primary astrocyte cultures and reverse transcription PCR was done. For each CPEB, primers flanking the alternatively spliced region were used to differentiate between splice isoforms. All CPEB transcripts i.e. CPEB (1-4) were expressed in primary astrocyte cultures. The different bands observed for each CPEB represent splice isoforms of the respective CPEB (Fig. 8). These PCR products were subcloned and analyzed by sequencing. Table 22 summarizes different splice isoforms observed for each CPEB and their relative abundance. For CPEB1 predominantly the  $\Delta 5$  type (Wilczynska et al., 2005) was observed. For CPEB2 and CPEB3, isoforms lacking the B-region which contain the putative phosphorylation sites for various kinases as CamKII, S6-kinase and PKA (Theis et al., 2003b) were more abundantly expressed. For CPEB4, only the isoforms lacking the B-region were observed. The isoforms containing the B-region were more abundantly expressed in the principal neuronal cell layers of the mouse hippocampus (Theis et al., 2003b). The presence of B-region lacking isoforms is consistent with the results obtained from single cell reverse transcription PCR data (Turimella et al., in revision; Vangoor et al., in revision).

CPEB	Isoforms
CPEB1	15x - $\Delta 5$
	1x - $\Delta 17$
	8x - 2d
CPEB2	3x - 2a
	2x - 2c
	1x - 2b
	11x - 3d
CPEB3	2x - 3b
	2x - 3c
	1x - 3a
CPEB4	11x - 4d
	5x - 4b

Table 22: Distribution of CPEB isoforms, for each CPEB 16 minipreps were sequence analyzed.

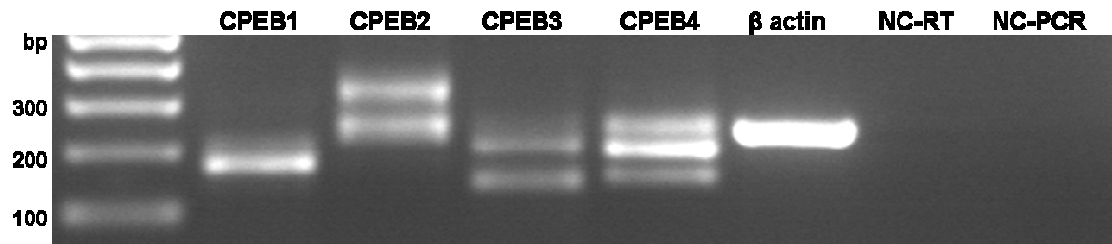


Figure 8: RT-PCR for CPEBs on primary astrocyte cultures for CPEBs. Representative image showing CPEB 1-4 transcripts in cultured astrocytes (n=3 experiments). The different bands represent splice isoforms of CPEBs.  $\beta$  actin was used as a positive control. bp: base pairs, NC-RT: negative control reverse transcription PCR, PC-RT: positive control reverse transcription PCR.

#### 4.1.2 Localization of CPEBs in astrocytes

Primary astrocytes were stained with antibodies specific for each CPEB (1-4) to visualize the localization of the endogenous CPEB proteins. All CPEBs were localized in the cytoplasm (Fig. 9). For CPEB1, 2 and 4 a diffuse localization in the cytoplasm and also in the processes was observed, whereas CPEB3 protein was found to be enriched more in the processes than in the cytoplasm (Fig. 9g, shown by arrows). A similar pattern of localization was observed for CPEB3 in primary hippocampal neurons (Huang et al., 2006). The presence of CPEB3 in the distal processes might give a clue about its possible role in modulating local protein synthesis. Together with nonradioactive *in situ* hybridization showing CPEB3 and CPEB4 mRNA in GFAP positive cells of the hippocampus (Theis et al., unpublished; Vangoor et al, in revision), single cell reverse transcription PCR for CPEBs 2-4 in astrocytes of acute hippocampal slices (Turimella et al., unpublished; Vangoor et al., in revision) and FACS purification of fluorescently labeled astrocytes from Cx43kiECFP mice followed by real time PCR for CPEBs 2-4 (Kaczmarczyk et al., unpublished; Vangoor et al., in revision), it can be concluded that CPEBs 1-4 are present in astrocyte cultures, while CPEBs 2-4 are expressed in astrocytes of the mouse brain.

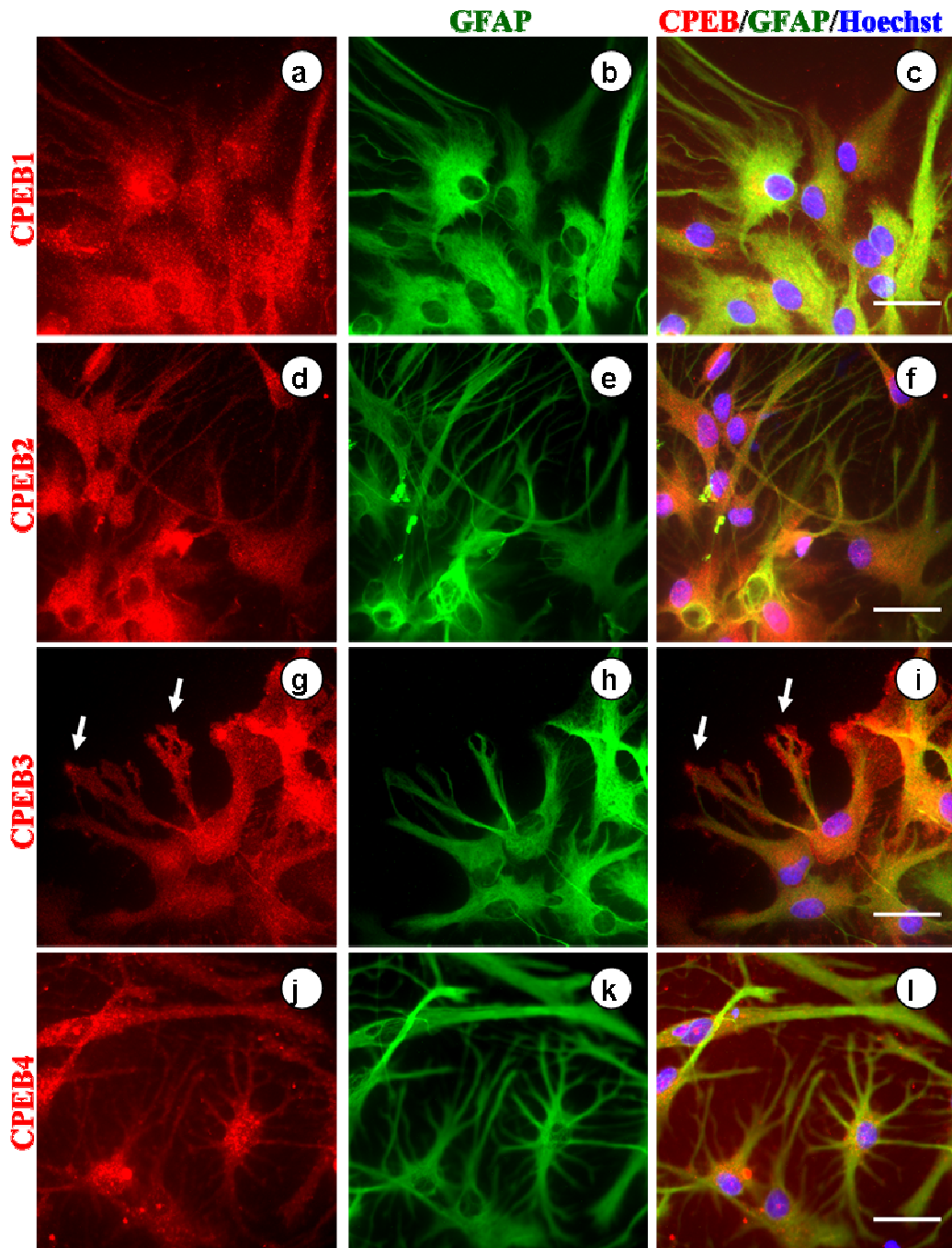


Figure 9: Staining for different CPEB (1-4) proteins in primary astrocyte cultures shows the localization of endogenous CPEB proteins. CPEB (red), GFAP (green), Hoechst (blue). CPEB1 (a-c), CPEB2 (d-f), CPEB3 (g-i) and CPEB4 (j-l). Scale bar, 20  $\mu$ m.

#### 4.1.3 Cx43 and GFAP downregulation

To study if CPEB3 has any negative impact on the astrocytic target proteins, primary astrocytes were transfected with a CPEB3-EGFP fusion vector. A reduction in the immunoreactivity for Cx43 and GFAP was observed when the cells were transfected with CPEB3. Specifically, the cells overexpressing CPEB3 had reduced levels of Cx43 (Fig. 10), together where the expression was normal in the neighboring untransfected cells; this gives a

hint that CPEB3 could regulate the basal translation of Cx43 in astrocytes. Cx43 mRNA contains two CPEs in its 3' UTR. CPEB3 was also shown to regulate the basal translation of GluR2 in neurons (Huang et al., 2006). The immunoreactivity for GFAP was also reduced in those cells overexpressing CPEB3 (Fig. 10) (n= 20 cells from two independent transfection experiments).

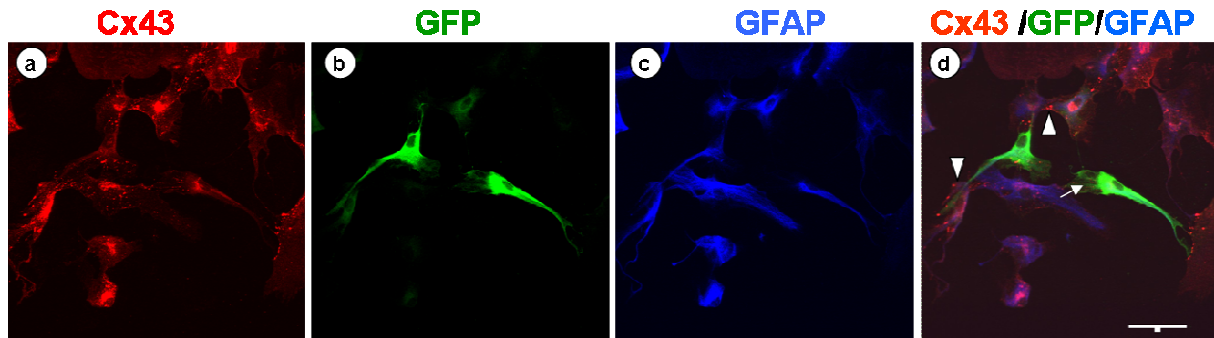


Figure 10: Representative picture showing decreased Cx43 (a) and GFAP (c) expression in cells overexpressing CPEB3 (b). Overlay of Cx43 (red), GFP (green) and GFAP (blue) (d). Scale bar, 100  $\mu$ m.

## 4.2 Generation of CPEB3-GFAP transgenic mice

For studying the role of CPEB3 in astrocytes, transgenic mice over expressing CPEB3 in astrocytes were generated.

### 4.2.1 Transgenic mouse generation

To study the functional role of CPEB3 in astrocytes, transgenic mouse over expressing CPEB3-EGFP fusion protein in astrocytes were generated. The expression of CPEB3 was driven by the human GFAP (hGFAP) promoter (Fig. 11) specifically in astrocytes (Fiacco et al., 2007). These mice were generated using the Tet-Off system (Gossen and Bujard, 1992). In the absence of Dox, tTA binds to the TetO and drives the expression of the gene under the control of hGFAP promoter. CPEB3-EGFP was cloned downstream of TetO sequences in a pMM403-400 vector which has a SV40 poly (A) (Fig. 11). The resulting vector was linearized with *Sfi*I to isolate the transgene (TetO-CPEB3-EGFP) from the plasmid backbone and the transgene was injected into zygotes; the embryos were later transplanted into a foster mother. The litters obtained from these mice were genotyped and the positive founders with TetO-CPEB3 were further bred with hGFAP-tTA mice (Fiacco et al., 2007) to get astrocytic specific expression. The astrocytic tTA binds to TetO and drives CPEB3 expression in astrocytes.

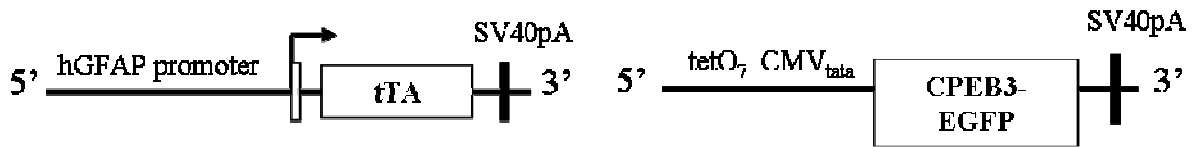


Figure 11: Schematic showing the Tet-Off system. hGFAP promoter, SV40pA: Simian virus 40 polyadenylation signal, TetO7: seven repeats of tetracycline operator, CMV tata: cytomegalovirus minimal promoter and TATA box.

#### 4.2.2 Genotyping of mice

To analyze if the litter from breedings of hGFAP-tTA and TetO-CPEB3 mice were carrying single (hGFAP-tTA or TetO-CPEB3) or double transgenes (hGFAP-tTA: TetO-CPEB3), mice were genotyped by extracting tail tip DNA and amplification with primers specific to the TetO and tTA transgenes. Fig. 12 shows an example of the result obtained from a genotyping PCR with both TetO and tTA PCR for hGFAP-tTA: tetO-CPEB3-EGFP mice. Two bands were observed at a size of approximately 419 bp and 395 bp for the TetO transgene and a single band of size 318 bp for the tTA transgene (represented by circles). The TetO primers for genotyping always yielded two bands for CPEB3-GFAP mice, this may be due to a head to head integration of the transgene. Only DT mice which were positive for both the PCRs were considered for further analysis along with single transgenic littermate controls.

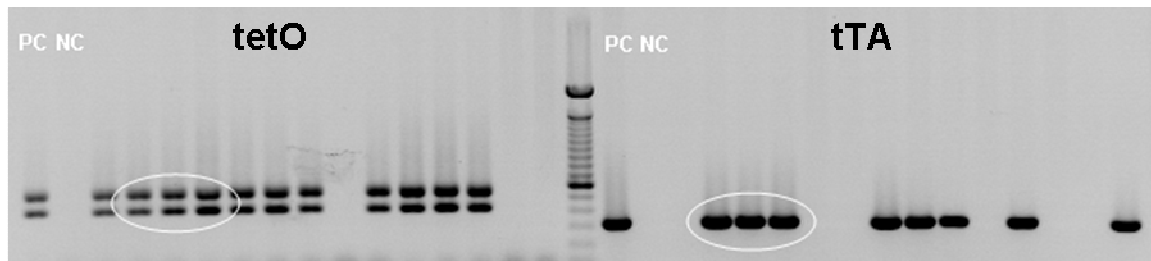


Figure 12: Representative gel image showing the genotyping PCR for TetO and tTA transgenes. TetO PCR yields 419 bp and tTA PCR yields 318 bp, represented by circles. PC – positive control, NC – negative control.

#### 4.2.3 Screening of lines

Single transgenic mice carrying the TetO-CPEB3-EGFP transgene were bred with hGFAP-tTA mice. The litters obtained from breeding were considered as individual lines and the expression was tested by staining for GFP in DT mice, after genotyping (4.2.2). Among the various lines analyzed (# 1, 6, 23, 28, and 40) for expression of CPEB3-EGFP in astrocytes, mice from line #28 were found to show expression specifically in astrocytes. This mouse line was selected for all the studies performed.

### 4.3 Characterization of CPEB3-GFAP transgenic mice

CPEB3 mice were characterized by immunohistochemical techniques. The localization of CPEB3 protein was visualized by staining for GFP, as GFP was tagged to the CPEB3 at the C-terminus of the CPEB3 coding region.

#### 4.3.1 Expression of CPEB3 across brain regions

Upon staining with GFP, expression of CPEB3 was observed in many of the astrocytes in the hippocampus (Fig. 13). Apart from the expression in hippocampus, a spotty expression pattern of CPEB3-EGFP was also observed in some regions of cortex and thalamus. Notably, CPEB3 overexpression led to a decreased GFAP protein content (Fig. 13c, f, i).

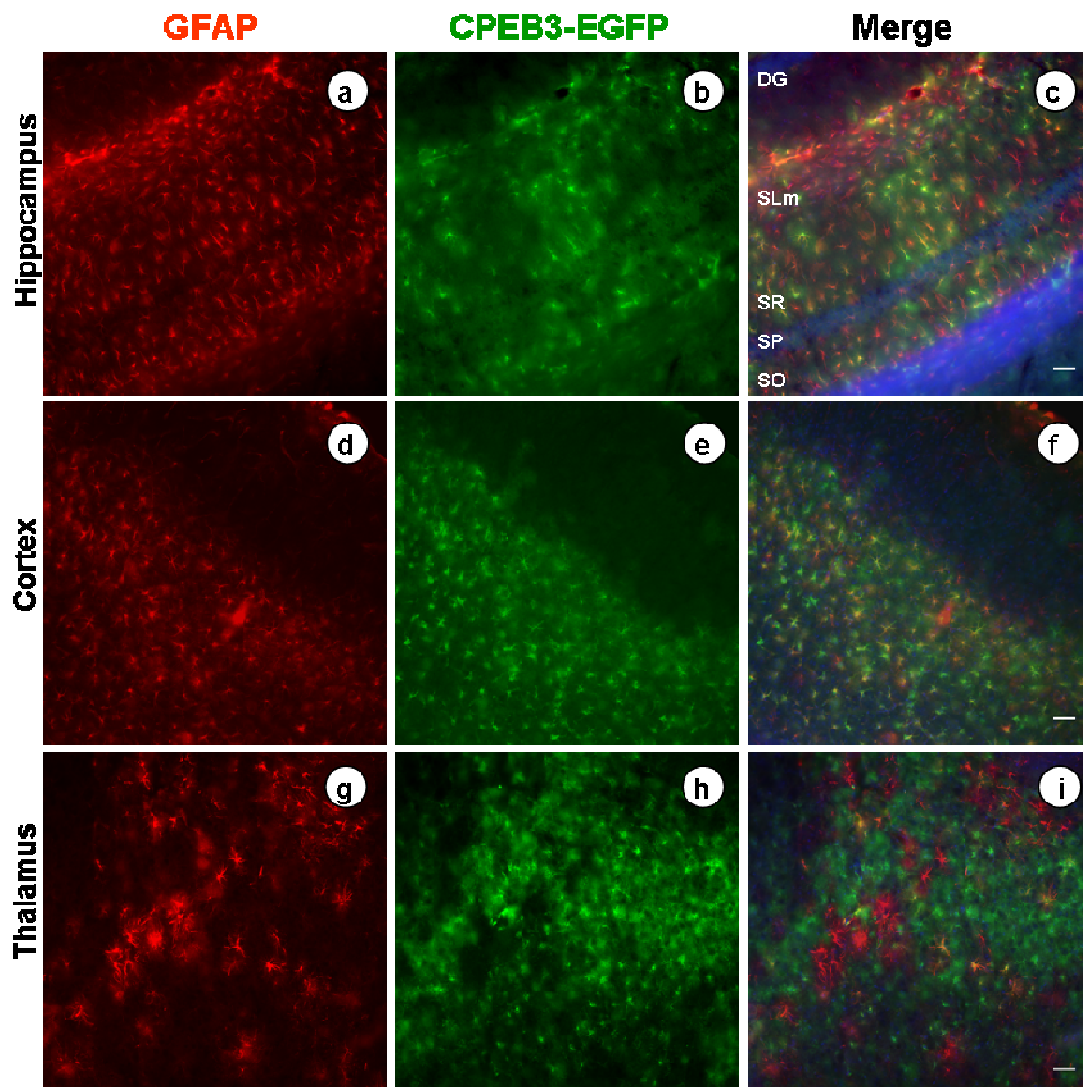


Figure 13: Representative images showing the expression of CPEB3-EGFP across brain regions. Hippocampus (a-c), cortex (d-f) and thalamus (g-i). Scale bar, 25  $\mu$ m. DG- dentate gyrus, SR – stratum radiatum, SO – stratum oriens, SLm – stratum lacunosum moleculare.



### 4.3.2 Localization of CPEB3 within astrocytes

To check for the localization of CPEB3-EGFP in astrocytes, mice overexpressing CPEB3 were perfused and expression was studied after postnatal 21 (p21) days. CPEB3 protein was localized in the cytoplasm and also in peripheral astrocytic processes (Fig. 14A). The identity of the astrocytes was confirmed by co-staining with the astrocytic marker GFAP. Co-localization of CPEB3-EGFP with the astrocytic marker GFAP was clearly visible (Fig. 14A). Overexpression was also confirmed by immunoblotting for CPEB3-EGFP protein by probing the hippocampal protein lysates with GFP antibody (Fig. 14B).

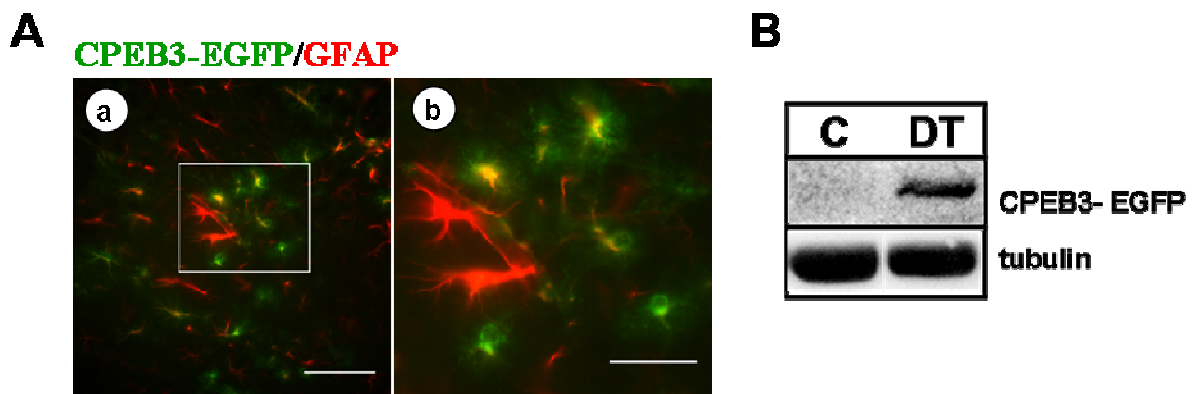


Figure 14: A) Representative image showing localization of CPEB3-EGFP in astrocytes. GFP (green), GFAP (red), co-localization is in yellow. Scale bars, 50  $\mu$ m (a), 20  $\mu$ m (b). B) Immunoblot image showing the overexpressed CPEB3-EGFP protein in DT mice.

### 4.3.3 Developmental deficit in CPEB3-GFAP mice

Mice overexpressing CPEB3 in astrocytes exhibit developmental deficits i.e., they have enlarged ventricles as shown in Fig. 15. The DT mouse brains were morphologically larger (hydrocephalus) and had a different, much more fragile consistency than their control littermates. The 3<sup>rd</sup> ventricle and the lateral ventricles of the brain were enlarged. The reason for this enlargement is not known. However, not all DT mice showed enlarged ventricles (62.5%, n= 8 mice).

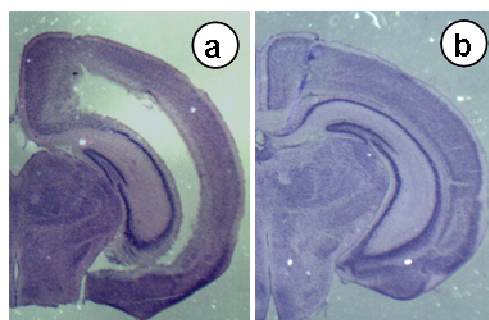


Figure 15: Nissl stained coronal section of CPEB3-GFAP (a) mice showing an enlarged ventricle compared to control mice (b).

#### 4.3.4 Doxycycline treatment

As these mice were generated using the inducible Tet system, transgene expression can be turned off by giving Dox in the food. To rescue the mice from developmental defects and to study the role of CPEB3 in adult astrocytes, these mice and their parents were given Dox in their food during birth and until the age of weaning. Application of Dox blocks the tTA from binding TetO and prevents expression of the CPEB3 transgene. So, transgene expression was turned off until the age of weaning and the mice were analyzed later at different time points to check for optimum expression levels. Mice were analyzed at 4 weeks and 7 weeks after removing Dox. When the mice were analyzed after 4 weeks of Dox removal, enlarged ventricles were not observed, and CPEB3-EGFP expression was prominent in astrocytes (Fig. 16). The 7 weeks time point was selected for all experiments, as maximum expression levels were observed.

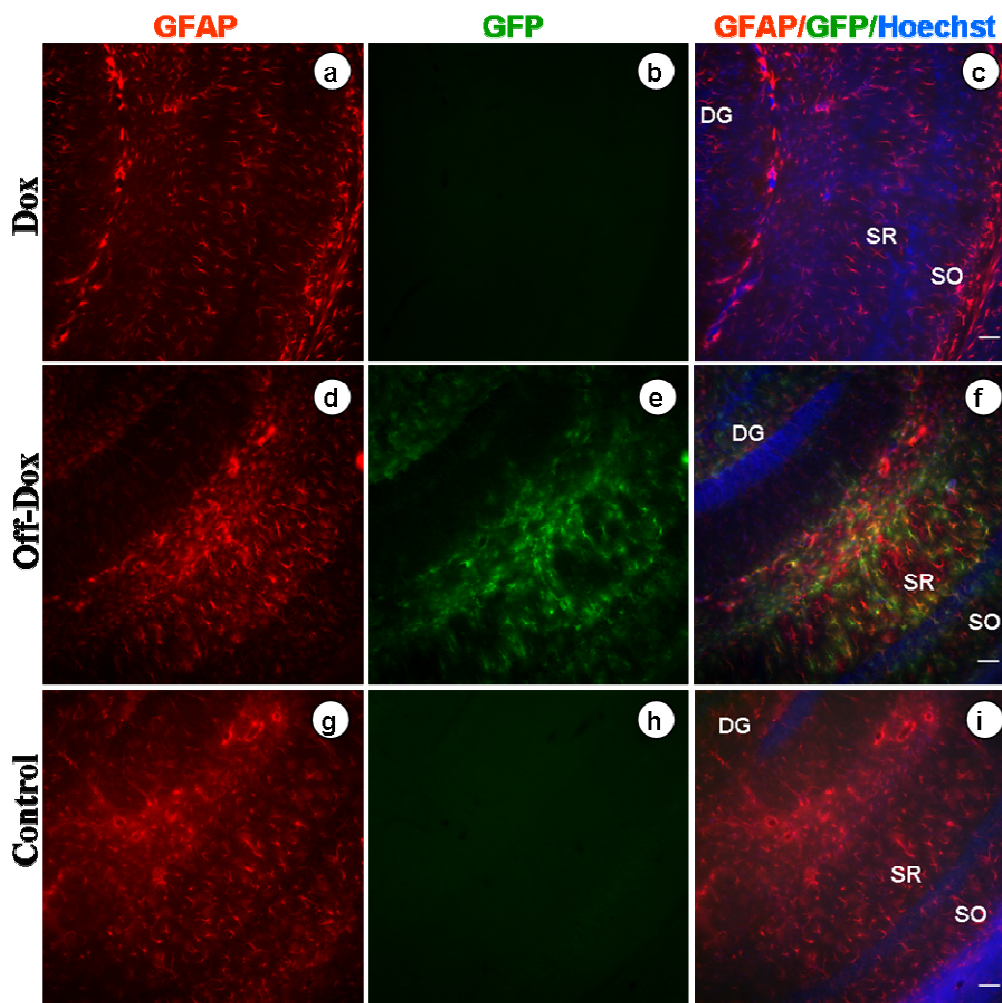


Figure 16: Image showing the comparison of CPEB3-EGFP expression during (a-c) after withdrawal of Dox (d-f) and in control mice (g-i). GFAP in red, GFP in green and Hoechst in blue. Scale bar, 25  $\mu$ m. DG- dentate gyrus, SR – stratum radiatum, SO – stratum oriens.

### 4.3.5 Extent of CPEB3 overexpression in astrocytes

For estimating the extent of CPEB3-EGFP overexpression in the hippocampus, cells expressing EGFP and GFAP were counted in the CA1 region. 50% of the GFAP positive cells were expressing CPEB3-EGFP (Fig. 17A). Almost 90% of these GFP positive cells co-expressed GFAP. To further confirm the extent of overexpression, the specificity of CPEB3-EGFP expression was also checked by co-staining with S100 $\beta$  where a similar 90% of the cells expressing CPEB3-EGFP were also positive for S100 $\beta$  (Fig. 17B). It is at present unclear which cell type the remaining 10% of the CPEB3-EGFP positive cells represent.

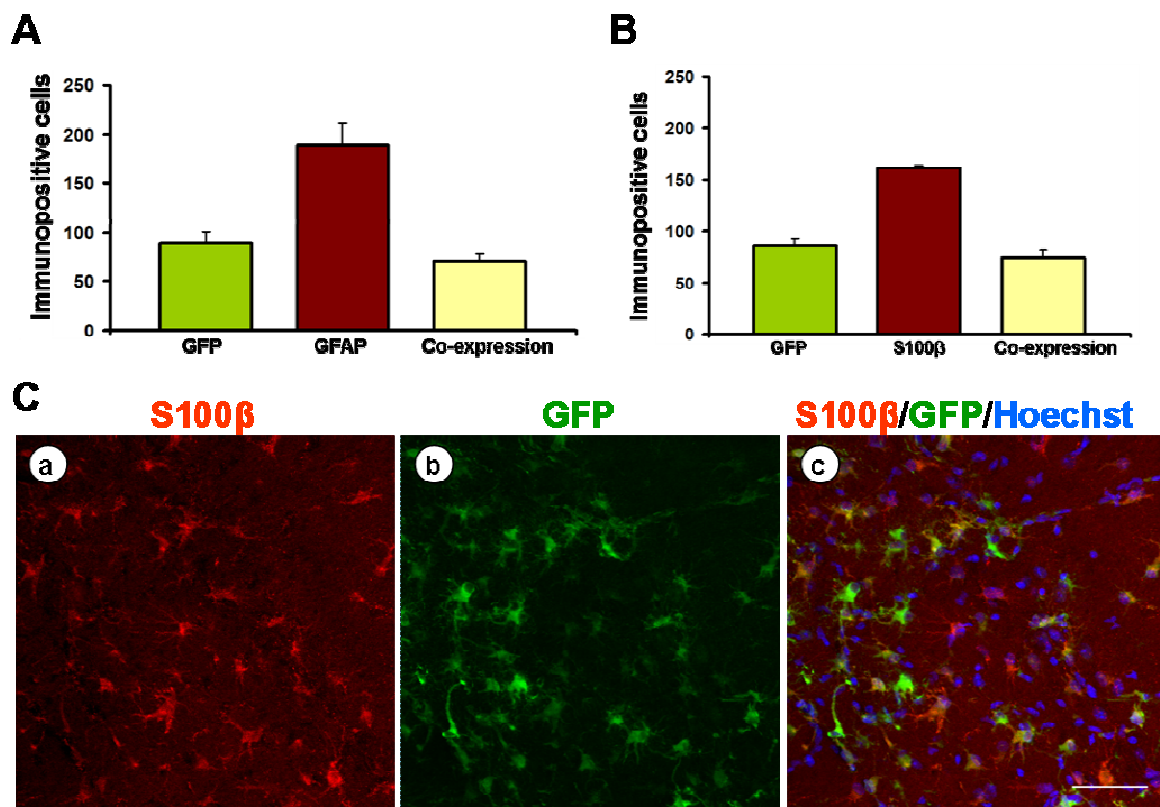


Figure 17: A) Histogram showing the extent of overexpression. Approximately 50% of the GFAP positive cells were overexpressing CPEB3-EGFP in the hippocampus (n=3, 4 sections/mouse). B) Histogram showing the extent of overexpression, quantified for S100 $\beta$  and GFP, (n=3, 4 sections/mouse). Error bars represent SEM. C) Representative image showing staining for S100 $\beta$  and GFP. Scale bar, 50  $\mu$ m.

### 4.3.6 Specificity of CPEB3 expression

To determine the specificity of CPEB3-EGFP expression, the sections were stained with other cell type specific markers such as NG2 (NG2 glia), Iba1 (microglia) and NeuN (neurons) (Fig. 18). Cells expressing GFP and the respective cell type markers were counted to check if there was any co-expression of CPEB3 with the above mentioned cell type. CPEB3-EGFP expression was found to be not co-localized with NG2, Iba1 or NeuN (n= 3 mice, 4

sections/mouse). This shows that the expression of CPEB3-EGFP driven by hGFAP-tTA promoter was specifically in astrocytes.

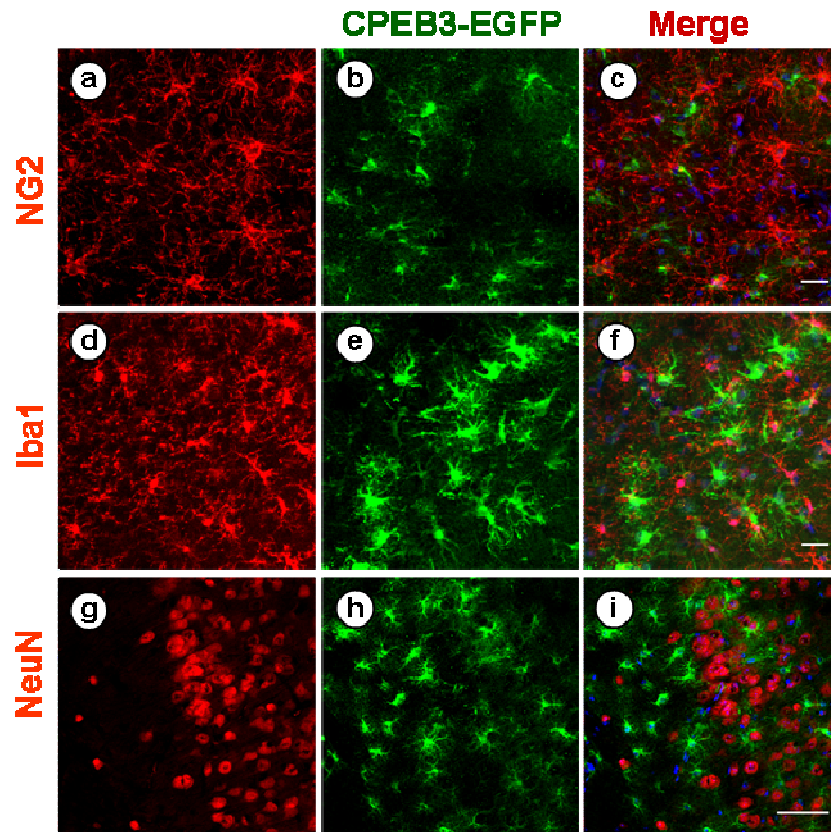


Figure 18: Representative image showing that CPEB3-EGFP is not co-expressed with cell type specific markers of NG2 cells (a-c), microglial (d-f) or with neurons (g-i). Scale bar, 20  $\mu$ m.

#### 4.3.7 Increase in GFAP immunoreactivity

In constitutively overexpressing CPEB3-EGFP mice, an enhanced immunoreactivity for GFAP was observed around the cells expressing CPEB3-EGFP in hippocampus (Fig. 14). To clarify whether this enhanced GFAP expression was due to developmental disturbances or whether it reflected an acute reaction in adult hippocampal astrocytes, double immunofluorescence stainings with EGFP and GFAP were performed in mice after Dox withdrawal (Fig. 19). In areas of the cortex where occasionally a region of EGFP expression was observed, a strong expression of endogenous GFAP was found, which is normally not prominent in adult cortex (Fig. 19 a-c). The increased GFAP immunoreactivity was locally confined to the region of CPEB3-EGFP overexpression. Similarly, in the thalamus of mice overexpressing CPEB3-EGFP, strong GFAP expression was observed (Fig. 19 d-f), whereas in control animals thalamic GFAP expression was weak to non-existent.

Most intriguingly, endogenous GFAP expression was weak in the very cells which expressed CPEB3-EGFP, while it was increased in the neighboring cells not expressing CPEB3-EGFP (figure 19c, f). Although GFAP is a non-CPE containing mRNA in mouse (unlike in humans and rats), there could be an indirect effect on GFAP protein expression by CPEB3.

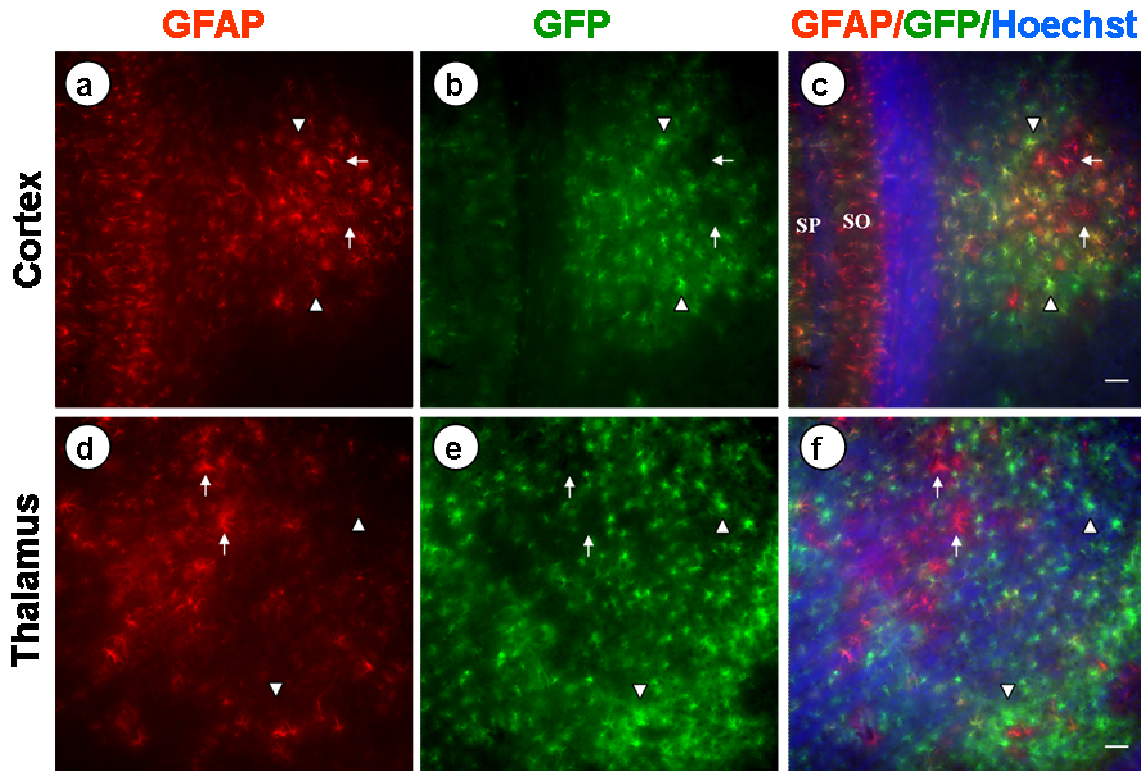


Figure 19: hGFAP-tTA driven overexpression of CPEB3 in astrocytes leads to increased immunoreactivity of GFAP in cortex (a-c) and thalamus (d-f). Paradoxically, there is a negative correlation between the expression of CPEB3 (shown by arrowheads) and GFAP (shown by arrows) in individual cells of these mice. SP – stratum pyramidale, SO – stratum oriens. Scale bar, 25  $\mu$ m.

#### 4.3.8 No change in GFAP protein levels

As reduced immunoreactivity for GFAP was observed in those cells expressing CPEB3-EGFP (4.3.7), immunoblotting was performed with hippocampal protein lysates of CPEB3-GFAP mice and probed for GFAP. Upon quantification, no change in the protein levels for GFAP was observed between controls and DT mice (Fig. 20). The CPEB3-EGFP expressing cells were showing reduced immunoreactivity for GFAP, whereas the non-CPEB3 expressing cells showed enhanced reactivity (Fig. 19). Due to this, there might be no overall alteration in hippocampal protein levels of GFAP observed in immunoblotting. Moreover the expression of CPEB3-EGFP was only in the 50% of the GFAP positive cells; this might be not enough to observe an effect on overall GFAP protein levels. The most prominent changes in GFAP immunoreactivity *in situ* were consistently observed in cortex and thalamus.

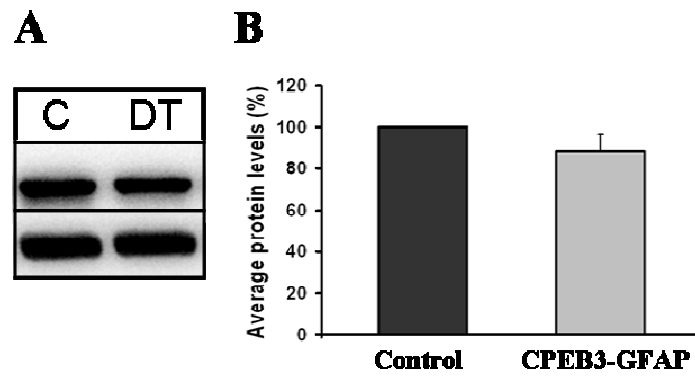


Figure 20: Representative immunoblot image (A) and histogram (B) showing the quantification for hippocampal GFAP protein levels in CPEB3-GFAP mice. n=5 mice/genotype, Error bars represent SEM.

#### 4.3.9 CPEB3 overexpression did not affect the number of astrocytes

To address the question if the overexpression of CPEB3 in astrocytes has any detrimental effects on the number of astrocytes, stainings for S100 $\beta$  were performed. S100 $\beta$  is an astrocytic marker and has no binding sites for CPEB. Quantification was done by counting the number of S100 $\beta$  and Hoechst (nuclei staining) positive cells in the SR and SLM regions in the CA1 region of the hippocampus. There was no difference observed in the number and density of astrocytes between CPEB3-GFAP mice and their control littermates in both regions (Fig. 21).

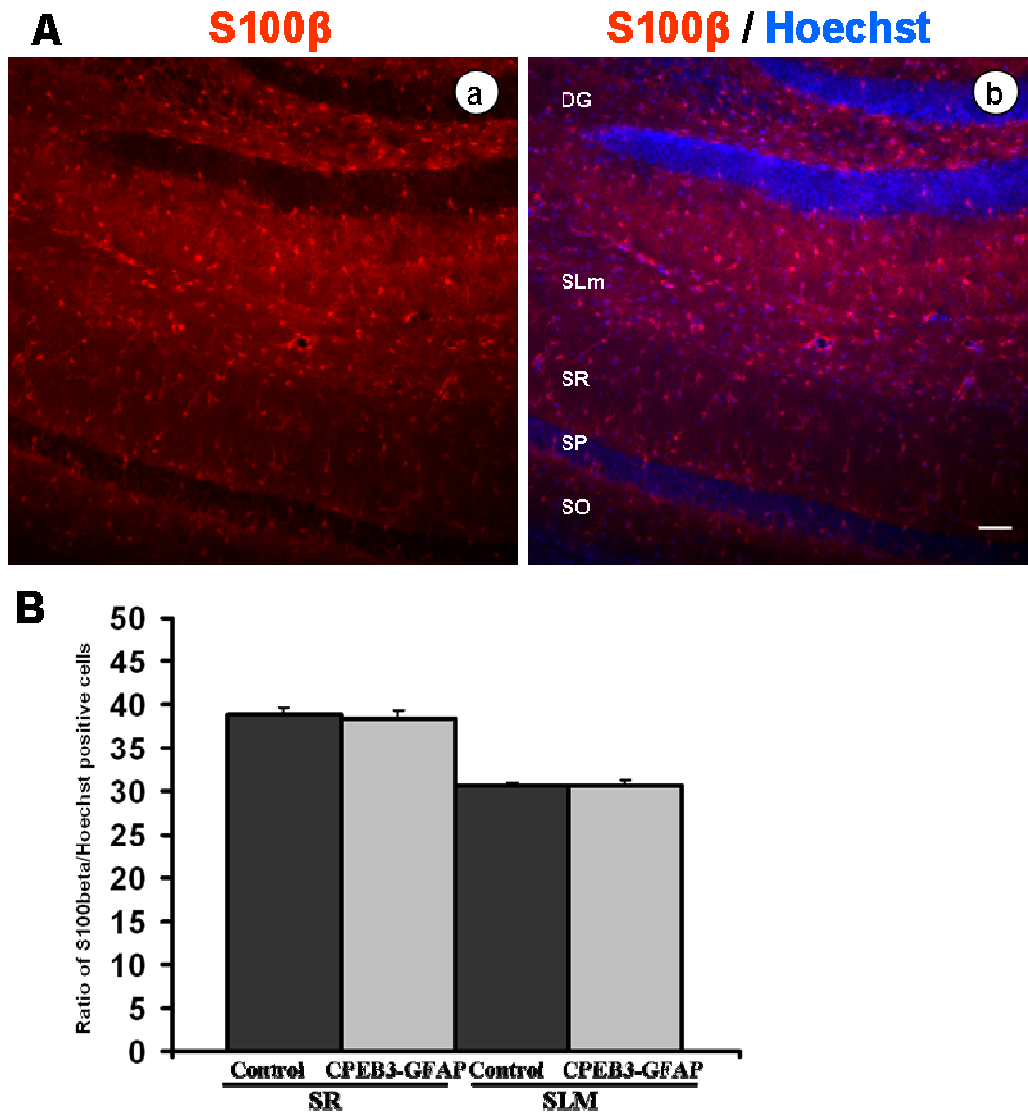


Figure 21: A) Representative image showing staining for S100β and Hoechst in the hippocampus. Scale bar, 25 μm. B) Histogram showing the ratio of astrocytes in SR and SLM regions (n= 5 mice/genotype, 4 sections/mice), Error bars represent SEM. DG- dentate gyrus, SR – stratum radiatum, SO – stratum oriens, SLM – stratum lacunosum moleculare.

#### 4.3.10 TUNEL staining

TUNEL staining was performed to test if overexpression of CPEB3-EGFP has led to cell death. No significant difference in the number of TUNEL positive cells was observed in DT mice compared to their control litters. The positive control (TUNEL staining performed after DNase treatment) showed a very strong signal (Fig. 22). We conclude that overexpression of CPEB3 does not lead to apoptotic cell death.

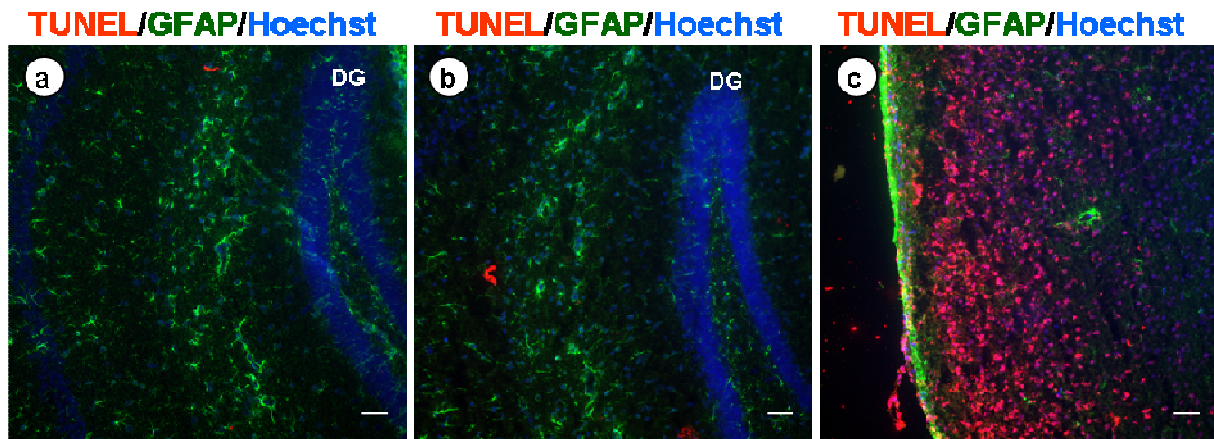


Figure 22: Representative image with the staining for TUNEL. No significant staining was observed in DT (a) and control littermates (b) mice compared to the positive controls (c). Scale bar, 25  $\mu$ m. DG: dentate gyrus.

#### 4.4 Putative astrocytic mRNA targets

The expression of mRNAs can be modulated by regulatory elements present in either 5' or 3' UTR of the mRNAs. These regulatory elements can be the binding sites for microRNAs or for RNA binding proteins. CPEBs are one class of RNA binding proteins which bind to CPEs present in the 3' UTR and regulate the translation of several mRNAs (Richter, 2007). Many mRNAs present in neurons contain CPEs in their 3' UTRs (Du and Richter, 2005). Recent reports show the expression of CPEB1 protein in distal processes of astrocytes, where it regulates the translation of  $\beta$ -catenin mRNA present at the leading edge of migrating astrocyte in an *in vitro* wound healing assay (Jones et al., 2008). CPEB1 also regulates the translation of cyclin B1 mRNA in rat astrocytes thereby controlling the cell cycle (Kim et al., 2011). The presence of CPEBs in astrocytes (4.1.1 and 4.1.2) indicates their possible role in regulating the translation of astrocytic mRNAs. Bioinformatics analysis was performed to screen for new CPEB targets in astrocytes. The 3' UTRs of several astrocytic mRNAs which are involved in key cellular processes were analyzed. Table 23 summarizes different astrocytic mRNAs across species which contain CPEs in their 3' UTR.



mRNAs	Number of CPEs in the 3' UTR across species			Function
	HUMAN	RAT	MOUSE	
Connexin 43	3	2	2	Gap junctional coupling (Nagy and Rash, 2003)
Connexin 30	3	3	4	
Connexin 26	2	2	2	
GS	2	3	3	Glutamate metabolizing enzyme (Martinez-Hernandez et al., 1977)
GLAST (EAAT1)	4	3	2	Glutamate transporters (Rothstein et al., 1994)
GLT-1 (EAAT2)	8	NA	11	
$\beta$ -catenin	3	2	3	Migration of astrocyte (Jones et al., 2008)
Cyclin B1	2	NA	4	Cell cycle (Kim et al., 2011)
GFAP	1	1	---	Intermediate filament protein (Bignami et al., 1972)
Dystrophin	5	NA	6	Anchoring AQP4 (Amiry-Moghaddam et al., 2003)
AQP4	8	4	4	Water channel (Badaut et al., 2002)

Table 23: Putative CPEB targets expressed in astrocytes and the number of CPEs in their 3' UTR present among different species. NA- complete sequence information not available.

## 4.5 Interaction of CPEB3 with target mRNAs

Bioinformatics show that several astrocytic target mRNAs contain CPEB binding sites in their 3' UTR regions (Table 23). To determine if these mRNAs are interacting with CPEB3 protein, RNA Co-IP experiments were performed. Therefore, a luciferase vector pGL4.75 [*hRluc*/CMV] (where the renilla luciferase was replaced with firefly luciferase) containing UTR fragments with and without the CPEs of the targets were generated. A vector containing CPEB3a appended with the FLAG epitope was also generated to be used as a bait.

### 4.5.1 Co-IP of Cx43 mRNA

The distal part of the Cx43 3' UTR containing one CPE (220 bp) (Fig. 23A) was cloned into the pGL4.75 vector. A mutant version, where the CPE was mutated was also cloned in a similar way. HeLa cells were co-transfected with the CPEB3-FLAG (bait) and Cx43wt-pGL or Cx43mut-pGL (prey) plasmids. The CPEB3 interacting with Cx43 mRNA was co-immunoprecipitated using FLAG antibodies. The precipitated mRNA was detected by real time PCR using luciferase-gene specific primers. A clear interaction between the Cx43 3' UTR and CPEB3 was observed, whereas this interaction was strongly diminished almost to control levels when the CPE was mutated. Fig. 23B shows a three fold increase in CPEB3 binding to WT Cx43 UTR in comparison with the mutant. The interaction of CPEB3 with

Cx43 was found to be CPE specific while the interaction with a non-CPE containing UTR, GAPDH (Fig. 23B) was unspecific. There was no interaction observed when FLAG-GFP was used as bait to Co-IP the Cx43 UTR which further showed the specificity of the interaction between Cx43 UTR and CPEB3.

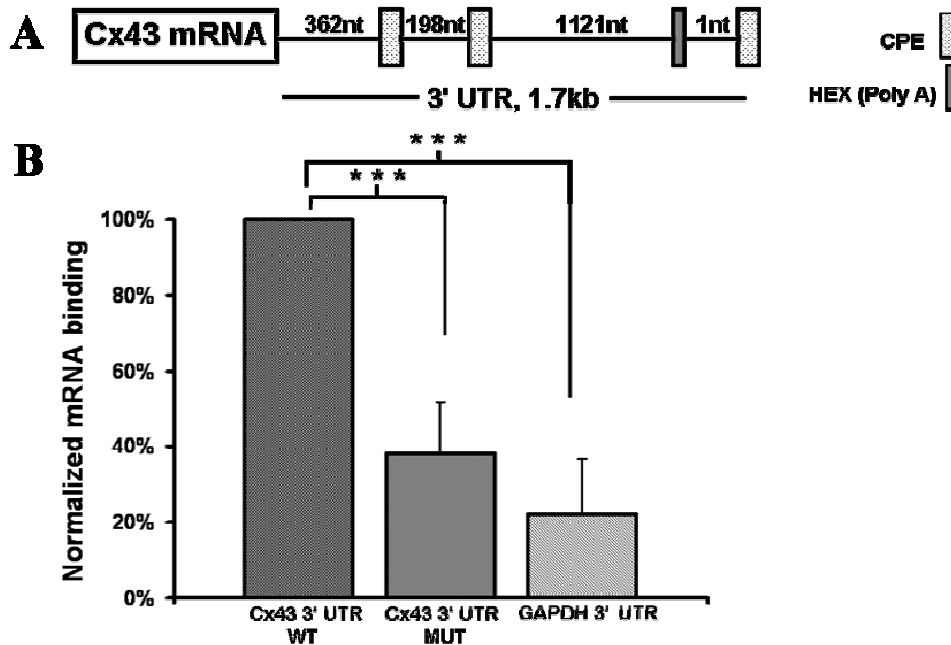


Figure 23: A) Schematic of Cx43 mRNA 3' UTR with binding sites for CPEBs and poly (A) sequences marked. B) Co-IP of overexpressed luciferase reporter mRNA appended with wild-type (WT) or mutated (MUT) 3'UTR derived from Cx43 mRNA or GAPDH 3' UTR (as control); FLAG-CPEB3 fusion protein was used as bait; precipitated mRNA was detected by real time PCR using luciferase-gene specific primers: Values were normalized with the average Ct values obtained for FLAG-GFP using GAPDH as a reference gene. \*\*\* P<0.0001 (student's t-test). n = 3 independent transfections, error bars are SEM.

#### 4.5.2 Co-IP of Cx30 mRNA

The distal 3' UTR of Cx30 bearing a single CPE (183 bp) and poly (A) signal (Fig. 24A) was cloned into a pGL vector (Cx30WT). HeLa cells were co-transfected with either CPEB3-FLAG or CPEB1-FLAG together with the Cx30WT-pGL vector. Using FLAG antibody, CPEB3 or CPEB1 interacting with Cx30 mRNA was co-immunoprecipitated. The precipitated mRNA was detected by real time PCR using luciferase-gene specific primers. The interaction of Cx30 mRNA with CPEB3 was significantly higher compared to its interaction with CPEB1 (Fig. 24B). It could be that similar target mRNAs can be bound by different CPEBs with different affinities. CamKII $\alpha$  mRNA is preferentially bound by CPEB1 in comparison with CPEB2 (Turimella et al., in revision).

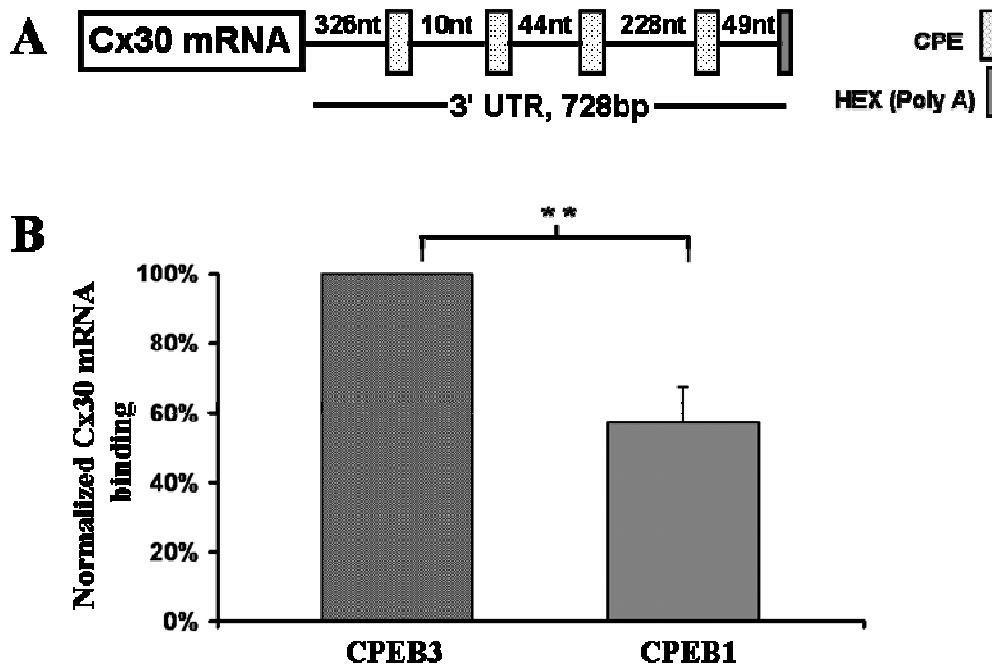


Figure 24: A) Schematic of Cx30 mRNA 3' UTR with binding sites for CPEBs and poly (A) sequences marked. B) Co-IP of overexpressed luciferase reporter mRNA with wild-type (WT) 3'UTR derived from Cx30 mRNA; FLAG-CPEB3 or FLAG-CPEB1 fusion protein were used as baits; precipitated mRNA was detected by real time PCR using luciferase-gene specific primers: Values were normalized with the average Ct values obtained for FLAG-GFP using GAPDH as reference gene. \*\*P<0.0001 (student's t-test), n = 3 independent transfections, error bars are SEM.

#### 4.5.3 Co-IP of GS mRNA

The 3' end of GS mRNA was isolated by 3' RACE of mouse brain cDNA. It was found that mouse GS 3' UTR contains four CPEs and two non-consensus overlapping poly (A) sequences (UAUAAA, AAUCAA) unlike the consensus poly (A) sequence observed in rat GS (AAUAAA) (Du and Richter, 2005) (Fig. 25A). The distal parts of the GS 3' UTR containing WT and MUT versions with one CPE (281 bp) were isolated and cloned into the pGL vector. CPEB3 interaction with GS 3' UTR was tested with Co-IP assay using FLAG antibodies as in 4.5.1. Interaction between the GS 3' UTR and CPEB3 was observed, whereas this interaction was significantly reduced when the CPE was mutated (Fig. 25B).

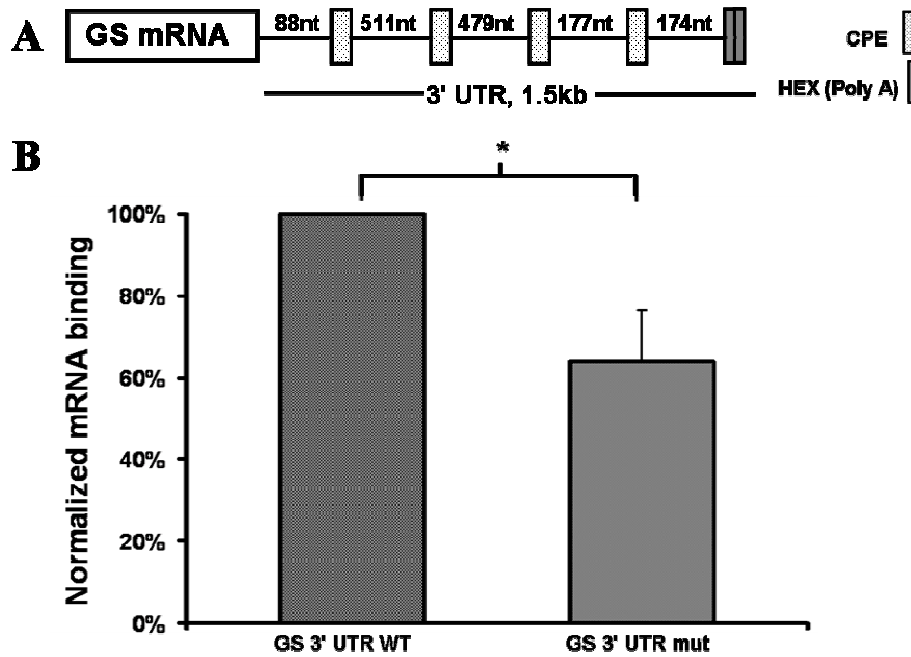


Figure 25: A) Schematic of GS mRNA 3' UTR with binding sites for CPEBs and poly (A) sequences marked. B) Co-IP of overexpressed luciferase reporter mRNA with wild-type (WT) or mutated (mut) 3'UTR derived from GS mRNA: FLAG-CPEB3 fusion protein was used as bait; precipitated mRNA was detected by Real Time PCR using luciferase-gene specific primers; Values were normalized with the average Ct values obtained for FLAG-GFP using GAPDH as reference gene. \* P<0.001 (student's t-test), n = 3 independent transfections, error bars are SEM.

## 4.6 CPEB3 downregulates major astrocytic connexins

The major astrocytic gap junctional proteins Cx43 and Cx30 are involved in metabolite supply to neurons (Rouach et al., 2008), ion homeostasis, potassium buffering (Wallraff et al., 2006) and adult neurogenesis (Kunze et al., 2009). A bioinformatics search and Co-IP identified Cx43 and Cx30 mRNAs as potential targets for CPEBs due to the presence of CPEs in the 3' UTR (Figs. 23A, 24A).

### 4.6.1 Downregulation of Cx43

The astrocytic gap junction protein Cx43 is expressed abundantly in astrocytes both *in situ* and in culture (Theis et al., 2003c; Theis et al., 2004). The interaction of Cx43 with CPEB3 was verified by Co-IP assay (4.5.1), which showed a specific CPE dependent interaction between CPEB3 and Cx43 mRNA. To examine any effect on the expression of Cx43 protein in mice overexpressing CPEB3, antibody staining for Cx43 was performed. A strong reduction in the immunoreactivity for Cx43 was observed in the regions of CPEB3 overexpression (Fig. 26A). In addition, the hippocampal protein levels of Cx43 in CPEB3 mice showed a significant 25% reduction (p<0.05) compared to their control littermates (Fig. 26B, C).

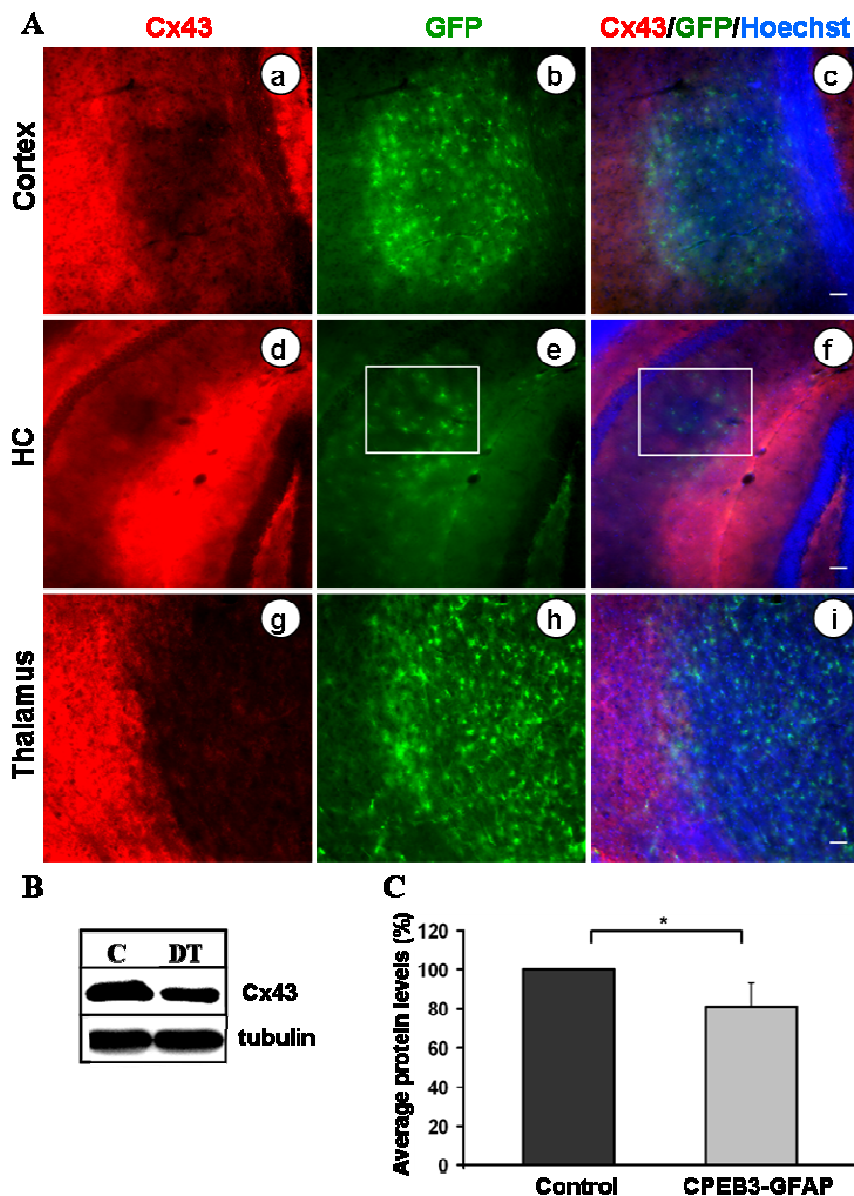


Figure 26: A) Loss of Cx43 protein in the cortex, hippocampus (HC - boxed region) and in thalamus. Scale bar, 25  $\mu$ m. B) Representative image from the immunoblotting of hippocampal lysates shows a significant reduction in the Cx43 protein levels between DT and control mice, also shown in the histogram (C) \* $p < 0.05$  (student's t-test),  $n = 6$  mice/genotype. Error bars are SEM.

#### 4.6.2 Downregulation of Cx30

Cx30 is another important astrocytic protein expressed in the mouse hippocampus and is involved in interastrocytic gap junctional coupling (Gosejacob et al., 2011). To test if CPEB3 overexpression has any impact on Cx30 protein in the hippocampus of CPEB3-GFAP mice, antibody staining was performed. A reduced Cx30 immunoreactivity was observed around the blood vessels in the CA1 region (Fig. 27A, a-c). Typically Cx30 surrounds the blood vessels, where the astrocytic endfeet enwrap the vessel (Rouach et al., 2008; Gosejacob et al., 2011) (Fig. 27g). Cx30 staining in CPEB3-GFAP mice (Fig. 27A, a-c) was almost as pronounced as

the staining in Cx30 knockout mice (Teubner et al., 2003) (Fig. 27A, d-f). The absence of staining in Cx30KO mice shows also the specificity of the antibody used. Control mice show WT levels of Cx30 (Fig. 27A, g, i). Immunoblots were performed for the total protein content of Cx30 from the hippocampal lysates which showed a significant 45% reduction ( $p < 0.05$ ) in the CPEB3-GFAP mice in comparison to their control littermates (Fig. 27B, C).

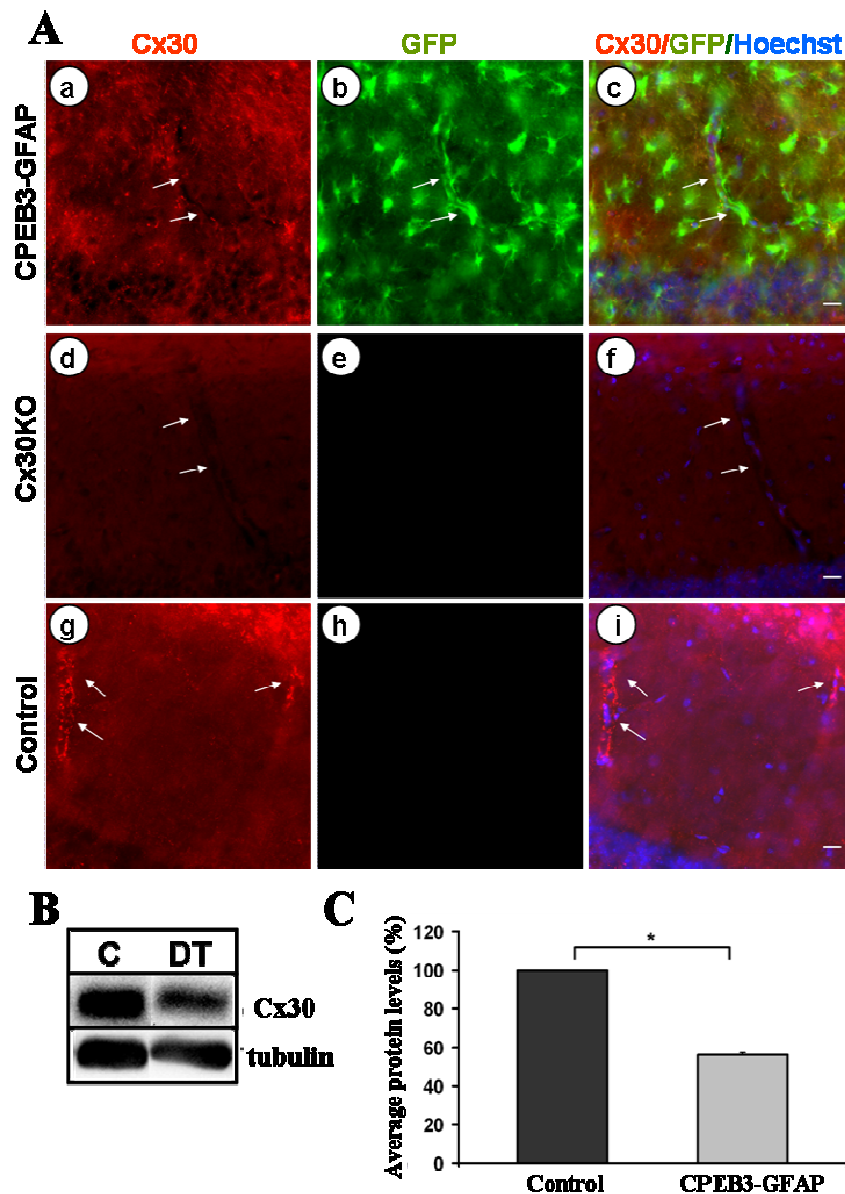


Figure 27: A) Reduced expression of Cx30 protein in the CPEB3-GFAP mice which is similar to Cx30 KO mice (shown by arrows). Staining for Cx30 in WT control gives a strong signal around the vessel in the CA1 region. Scale bar, 10  $\mu$ m. B) Representative image from the immunoblotting of the hippocampal lysates shows a significant reduction in the Cx30 protein levels, also shown in the histogram (C) \* $p < 0.05$  (student's t-test),  $n = 5$  mice/genotype. Error bars are SEM.

#### 4.6.3 Interastrocytic coupling is reduced in CPEB3 mice

Connexins are involved in interastrocytic gap junctional communication (Theis et al., 2003a; Wallraff et al., 2006; Rouach et al., 2008; Gosejacob et al., 2011). As there was a reduction in

the expression of both connexins in CPEB3 mice (4.6.1 - 4.6.2), tracer coupling studies were performed, as described previously (Wallraff et al., 2004). Biocytin was filled for 20 min into astrocytes in the CA1 region of the hippocampus and the sections were then analyzed. Upon staining for biocytin and quantifying the number of cells coupled from the Z-stack images, a significant 40% reduction (Fig. 28B) in the interastrocytic coupling was observed. Fig. 28A shows a representative image with the reduced number of coupled cells in the CPEB3-GFAP mice compared to control. Notably, in these mice, expression is observed in roughly 50% of all astrocytes (Fig. 17A).

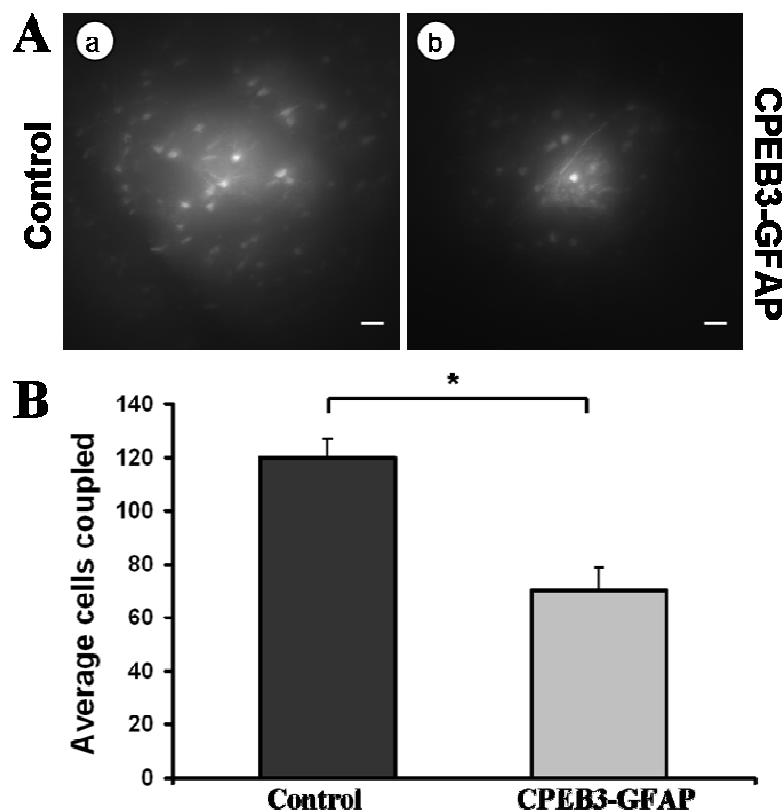


Figure 28: A) Representative image showing the extent of coupling in CPEB3-GFAP mice compared to controls. Scale bar, 10  $\mu$ m. B) The quantification shows that the average numbers of coupled cells were reduced by 40% in DT mice compared to controls. Mice were on Dox until p21. Seven weeks after removal of Dox, mice were analyzed for coupling. \* $p < 0.05$  (student's t-test),  $n = 12$  sections/genotype and 3 mice/genotype respectively. Error bars are SEM.

Interestingly in these DT mice, when biocytin was injected into a CPEB3-EGFP expressing astrocyte, the diffusion of tracer was confined to very few cells and moreover the tracer was taken up specifically by cells which were not expressing CPEB3 (Fig. 29). This further indicates the inhibitory role of CPEB3 on connexin expression.

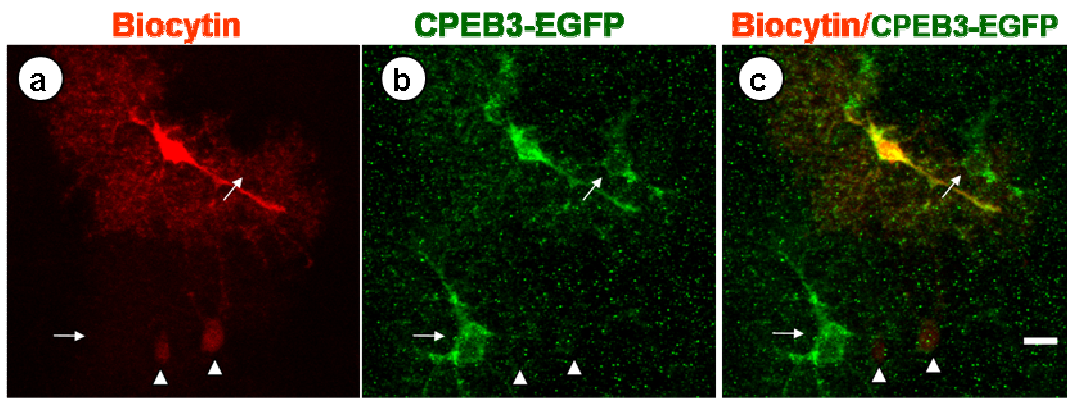


Figure 29: A GFP positive astrocyte filled with biocytin shows gap junctional coupling selectively with the neighboring non GFP astrocytes (arrowhead) and at the same time there was no coupling observed with the neighbouring GFP positive astrocytes (arrow) which could reflect the inhibitory role of CPEB3 upon Cx43. Scale bar, 10  $\mu$ m.

### 4.7 Role of CPEB3 in adult neurogenesis

Connexin expression in radial glia (RG) -like cells is required for adult neurogenesis in the DG of the subgranular zone (SGZ) of mouse hippocampus (Kunze et al., 2009). RG-like cells in the DG were shown to be coupled via gap junctions (Kunze et al., 2009). In mice constitutively overexpressing CPEB3-EGFP, a reduced expression of connexins (4.6.1 - 4.6.2) and significant reduction in interastrocytic gap junctional coupling (4.6.3) was observed. Since endogenous GFAP is expressed in RG-like cells, we wondered whether adult neurogenesis may likewise be impaired in mice overexpressing CPEB3. Together with Mr. Jiong Zhang, these mice were also analyzed for any impact on adult neurogenesis due to impaired connexin expression.

#### 4.7.1 Reduced proliferation

The proliferation marker Ki-67 was used for assessment of proliferating cells in the SGZ of CPEB3 mice. Upon quantifying the number of Ki-67 positive cells (Table 24, Fig. 30A) a significant reduction in the number of proliferating cells was observed in CPEB3 mice compared to the control mice (Fig. 30B) which accounts up to 40%. A complete loss of connexins (DKO mice lacking Cx43 and Cx30) has led to a stronger reduction (87%) in the number of Ki-67 positive cells in the SGZ (Kunze et al., 2009).

Mouse line	Total number of Ki67 positive cells	Total number of DG sections analyzed	Ki-67 positive nuclei per DG section (mean $\pm$ SD)
Control (n =3)	292	30	9.7 $\pm$ 3.0
CPEB3-GFAP (n =3)	194	30	6.5 $\pm$ 2.4

Table 24: Quantitative evaluation of Ki67 expression in the SGZ of the DG.



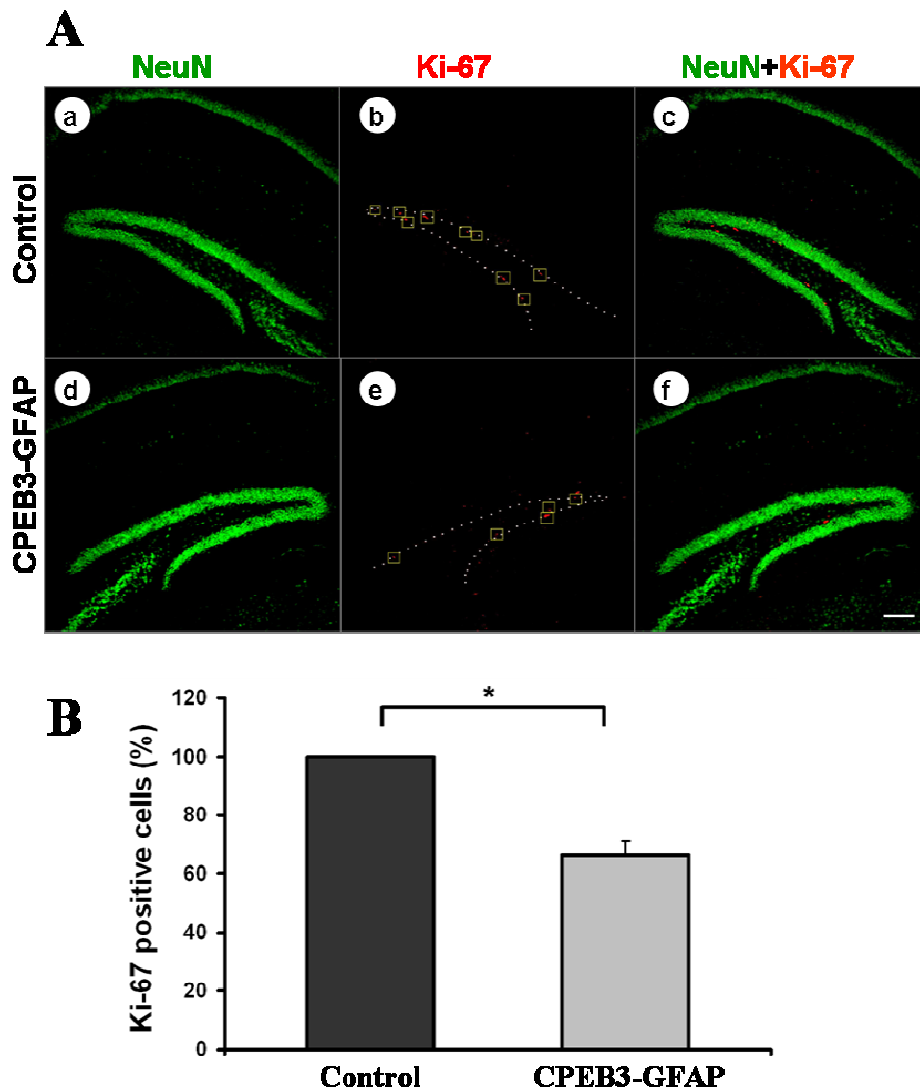


Figure 30: A) Confocal images of the DG of WT mice (a-c) and CPEB3-GFAP mice (d-f). (red- Ki-67, green- NeuN). Ki-67 positive cells are framed with yellow boxes and the dotted lines indicate the border between SGZ and GCL. Upon quantifying, a 40% reduction was observed in the number of Ki-67 positive cells indicating a low proliferative activity in CPEB3-GFAP mice. B) Histogram showing the reduction in the number of Ki-67 positive cells. \* $p < 0.05$  (student's t-test),  $n = 3$  mice/genotype. Error bars are SEM. Scale bar, 100  $\mu\text{m}$ .

#### 4.7.2 Decreased number of granule neurons

In the adult SGZ, RG-like cells give rise to granule neurons which differentiate and migrate to the granule cell layer (Zhao et al., 2008). To find out if the translational inhibition of connexins by CPEB3 has any effect on the number of granule neurons in SGZ, stainings for Prox1 and NeuN were done. Confocal Z-stack images were taken and counting boxes were used to estimate the number of Prox1 positive cells. A significant 10% reduction in the number of granule neurons was observed (Table 25 and Fig. 31A, B) in DT mice compared to control mice. In the DKO mice, a 21% reduction in the number of Prox1 positive granule neurons in the DG was reported (Kunze et al., 2009).

Mouse line	Total number of Prox1 positive cells	Total number of counting boxes analyzed	Prox1 positive cells per counting box (mean $\pm$ SD)
Control (n =3)	2582	60	43 $\pm$ 7.5
CPEB3-GFAP (n =3)	2368	60	39 $\pm$ 6.8

Table 25: Quantitative evaluation of Prox1 expression in the DG.

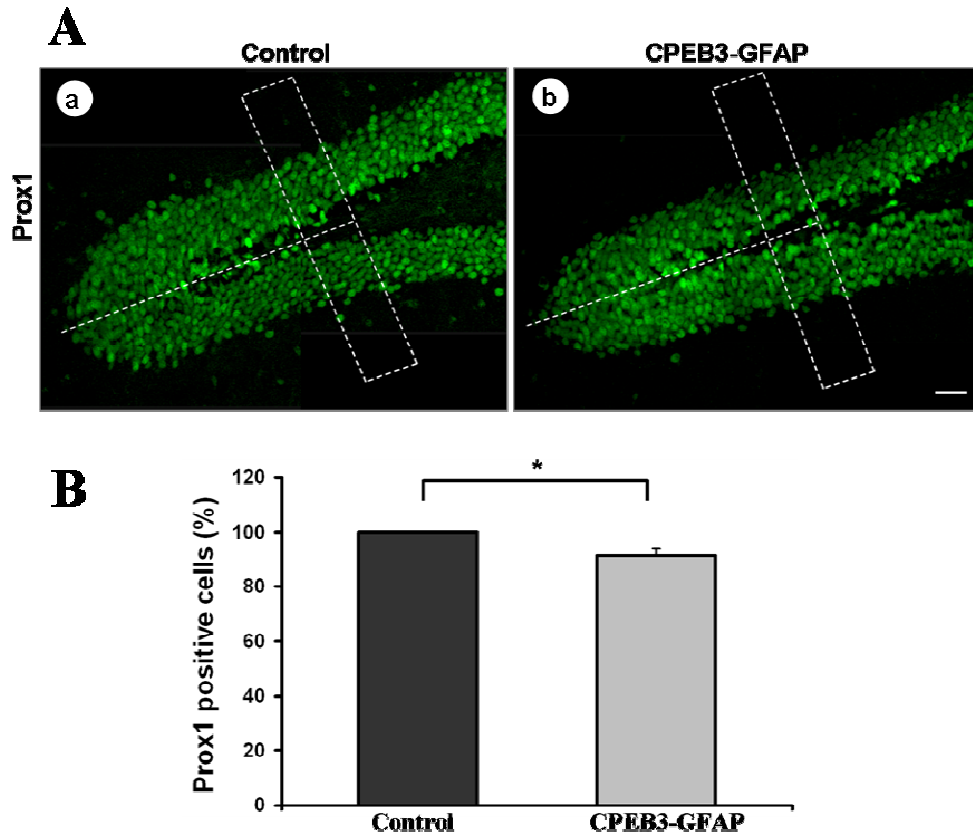


Figure 31: A) Prox1 staining for granule neurons of the DG (p76). B) Histogram showing a significant reduction of Prox1 positive cells. \* $p < 0.01$  (student's t-test),  $n = 3$  mice/genotype and 60 counting boxes/genotype. Scale bar, 100  $\mu$ m. Error bars are SEM.

#### 4.7.3 Reduction in the number of BLBP positive cells

To identify if there was any change in the number and the arrangement of the RG-like cells in the SGZ, expression of brain lipid binding protein (BLBP) an RG marker was assessed in mice overexpressing CPEB3. There was a strong reduction in the number of RG-like cells in CPEB3 mice (Fig. 32A). We observed a 50% reduction in BLBP positive cells in the SGZ of DT mice compared to the controls (Fig. 32B, Table 26).

Mouse line	Total number of BLBP positive cells	Total number of counting boxes analyzed	BLBP positive cells per DG section (mean $\pm$ SD)
Control (n =4)	356	39	9.1 $\pm$ 3.2
CPEB3-GFAP (n =4)	203	40	5.1 $\pm$ 2.9

Table 26: Quantitative evaluation of BLBP expression in the DG.

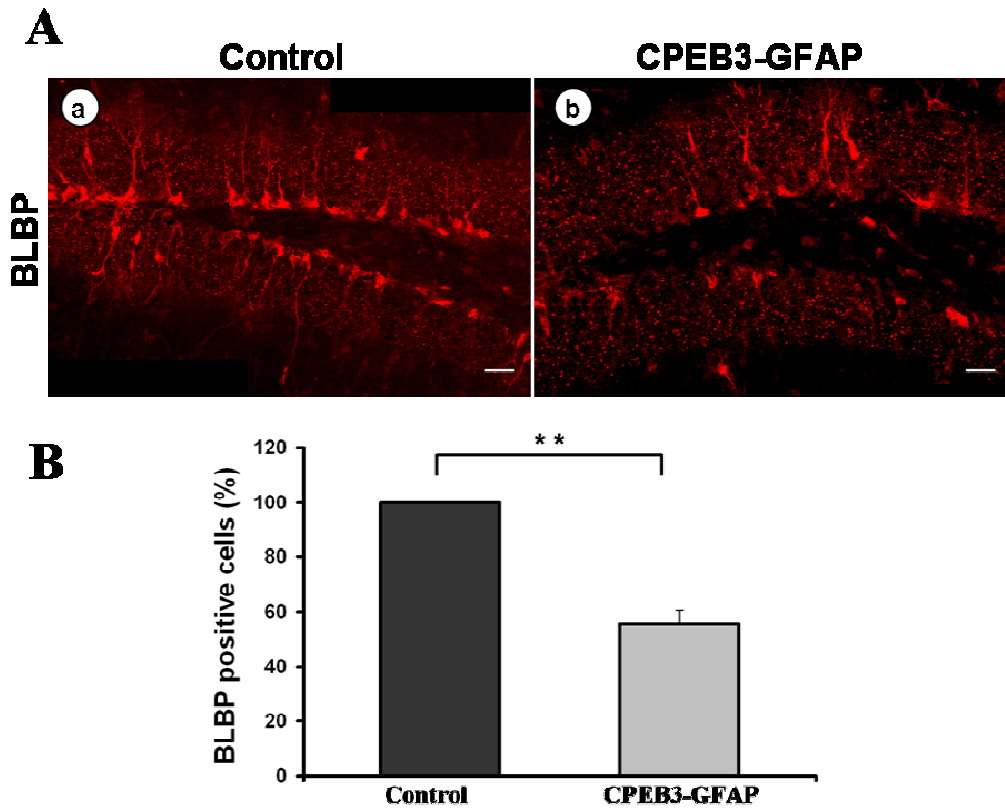


Figure 32: A) BLBP staining showing a strong reduction of BLBP positive RG-like cells in CPEB3 mice compared to control mice. B) Histogram showing the quantification of BLBP positive cells. \*\* $p < 0.001$  (student's t-test). (n= 3 mice/genotype, p76). Scale bar, 100  $\mu$ m. Error bars are SEM.

## 4.8 Analysis of other targets in CPEB3 mice

The other astrocytic proteins that were found to be regulated in these mice overexpressing CPEB3 were GS and EAAT2 (GLT-1).

### 4.8.1 Downregulation of GS

GS is an enzyme converting the excitatory amino acid glutamate to glutamine and is expressed in astrocytes. GS is downregulated during epilepsy (Eid et al., 2004). The 3' UTR of GS contains CPEs (Fig. 25A); hence CPEBs could possibly bind and regulate its translation. The Co-IP showed a CPE specific interaction of CPEB3 with GS mRNA (4.5.3). Upon staining for GS in CPEB3-GFAP mice, a strong reduction in the immunoreactivity for GS was observed in regions of CPEB3 overexpression (Fig. 33A). Immunoblots from hippocampal protein lysates showed a significant reduction of GS protein levels in DT mice compared to their control litters (Fig. 33B, C).

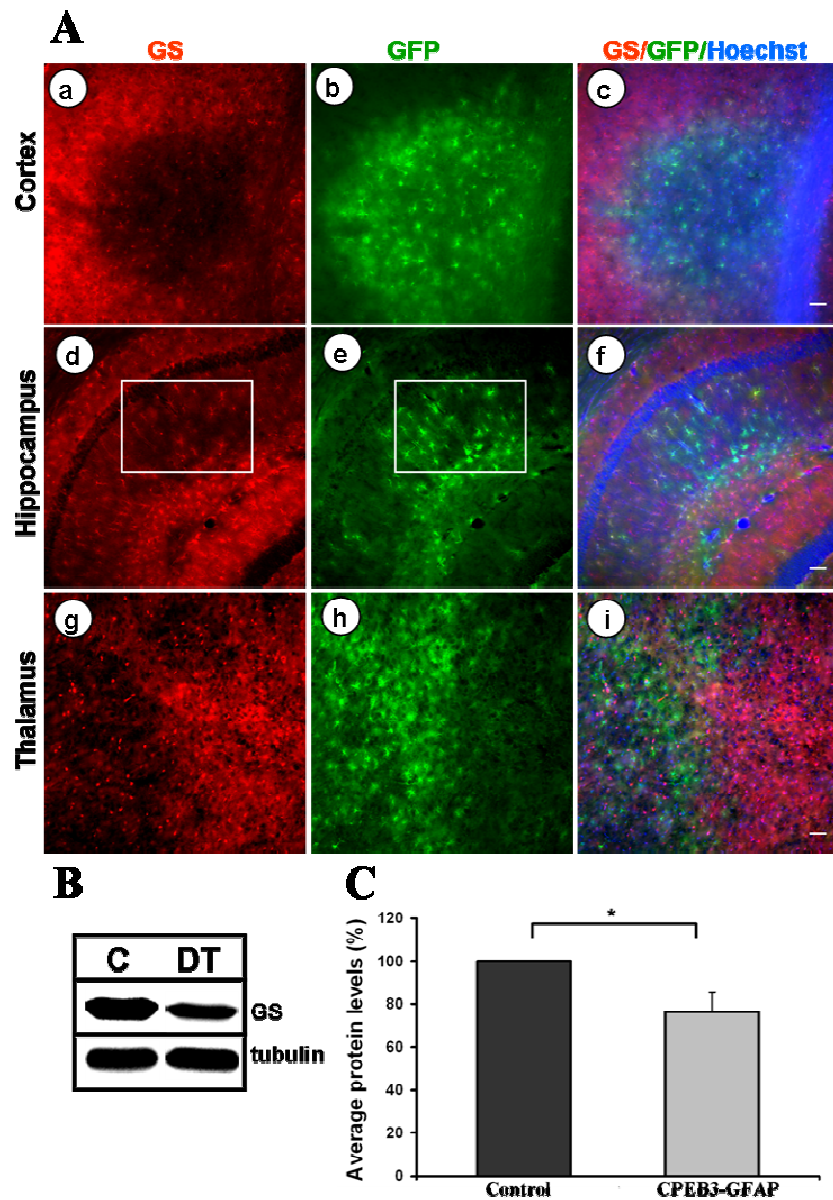


Figure 33: A) Representative picture showing the loss of GS protein in cortex, hippocampus and thalamus of CPEB3-GFAP mice. Scale bar, 25  $\mu$ m. B-C) Representative WB image and histogram showing a significant reduction in the GS protein levels in the hippocampus of the DT mice compared to the controls. \* $p < 0.05$  (student's t-test),  $n = 5$  mice/genotype. Error bars are SEM.

#### 4.8.2 Downregulation of GLT-1

GLT-1 is an astrocytic protein involved in the glutamate uptake of astrocytes which contains several CPEs in its 3' UTR (Table 23). The expression of GLT-1 was reduced in the regions of CPEB3 overexpression in CPEB3-GFAP mice compared to the control staining (Fig. 34A). Immunoblots of hippocampal protein lysates showed a significant reduction in GLT-1 protein levels in DT mice compared to controls (Fig. 34B, C).

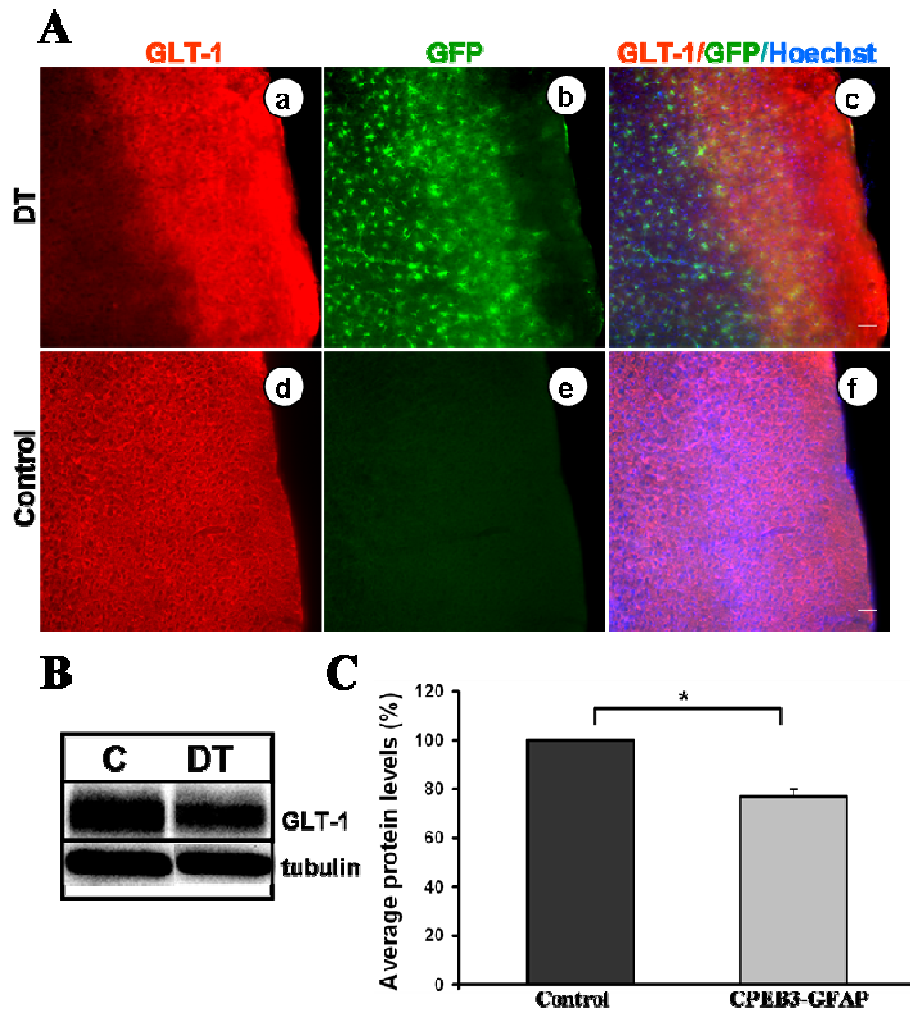


Figure 34: A) Representative image showing the loss of GLT-1 protein in cortex of the DT mice (a-c) compared to the control (d-f) staining. Scale bar, 25  $\mu$ m. B) WB image showing the reduction in protein levels of GLT-1 in DT mice compared to control mice and the corresponding histogram (C). \* $p < 0.05$  (student's t-test).  $n = 5$  mice/genotype. Error bars are SEM.

#### 4.9 No significant change in the transcript levels of CPEB3 targets

As a significant reduction in the hippocampal protein levels of Cx43, Cx30 and GS were observed, the mRNA levels of the targets were checked by quantitative real time PCR. Taqman based assays were used. The efficiency of the taqman primers was calculated (methods section 3.2.8.3). Figure 35A, 35B shows the slope, linear equation and correlation co-efficient for Cx30 and GLT-1 taqman primers respectively. The efficiency of the primers was calculated with the formula given below.

$$E = [10^{(-1/\text{slope})}] - 1 \text{ (Dorak, 2006)}$$

The efficiency (E) for Cx30 was estimated as 1.83, with 82.5% efficiency and for GLT-1 as 1.90, with 90% efficiency. The efficiency of the other primers was also quantified in a similar

way (data not shown, Cx43: E= 1.83, S100β: E= 1.83, GS: E= 1.83). There was a minor decrease in the mRNA levels of the target proteins in CPEB3 mice compared to their control litters (Fig. 35C, D), which was not significant.

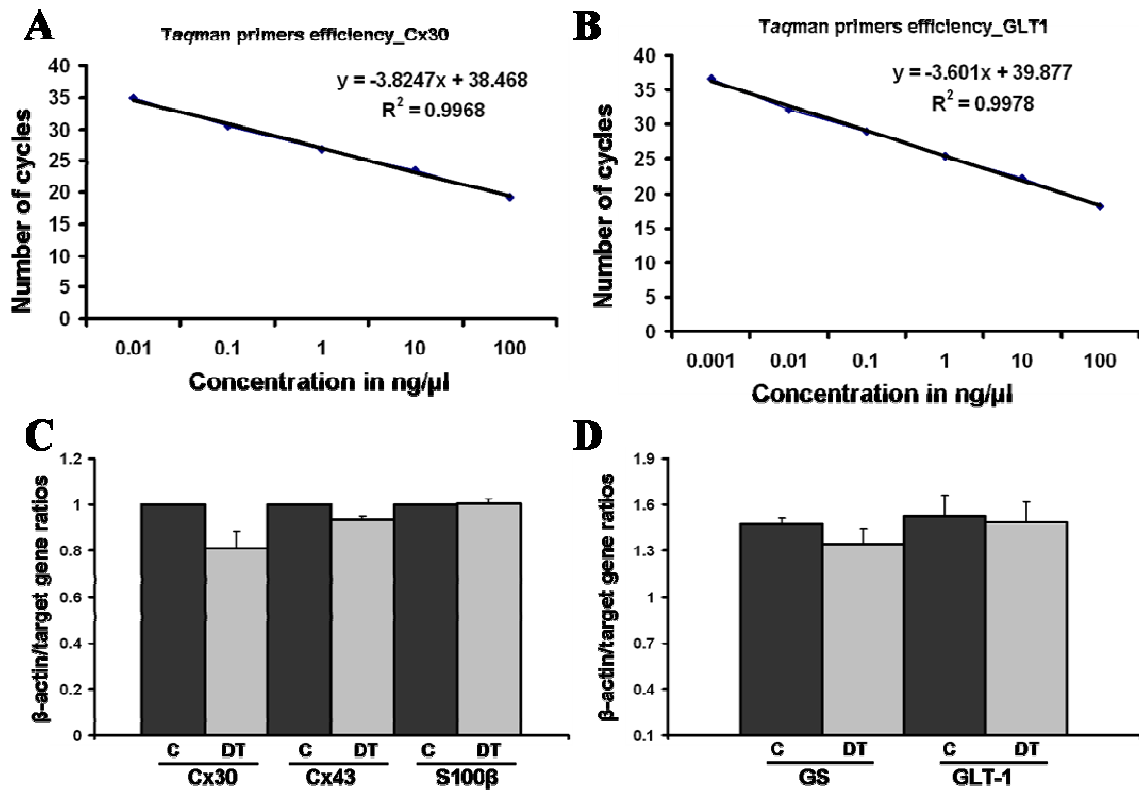


Figure 35: A-B) Standard curves showing the efficiency of Cx30 and GLT-1 primers. E= 1.83 for Cx30 and E= 1.90 for GLT-1 primers. C) Transcript levels of Cx30, Cx43 were not changed between control mice (C) and CPEB3-GFAP mice (DT). S100β was used as a non-CPE containing mRNA control. D) Transcript levels of GS and GLT-1 were not changed between C and DT mice. The transcript levels were normalized to β actin. Five mice/genotype were used for the study.

#### 4.10 Endogenous expression of CPEB3 in WT and transgenic mice

Co-localization of the endogenous CPEB3 and overexpressing CPEB3-EGFP protein was observed in the astrocytes of CPEB3-GFAP mice (Fig. 36). The antibodies used against CPEB3 also recognized the overexpressed protein.

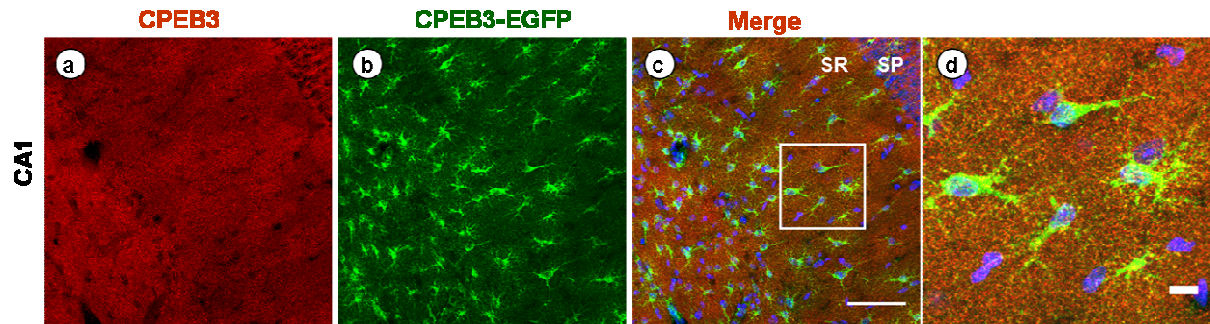


Figure 36: Representative image showing the co-localization of CPEB3 protein with the overexpressed CPEB3-EGFP positive cells in the CA1 region of hippocampus. SP- stratum pyramidale, SR – stratum radiatum. Scale bars, (c) 20  $\mu$ m, (d) 10  $\mu$ m.

The localization of the endogenous CPEB3 protein in astrocytes was also studied using transgenic mice in which astrocytes are fluorescently labeled. Cx43ki-ECFP mice (Degen et al., 2012) were used where astrocytes are labeled with ECFP. Upon staining for CPEB3 and GFP, CPEB3 was found to be co-localized with the CFP signal (Fig. 37) which confirms the *in vivo* localization of CPEB3 protein in astrocytes. Localization of CPEB3 is observed in the fine processes of astrocytes (Fig. 37a). In the SGZ of the DG there was an increased immunoreactivity observed for CPEB3 (Fig. 37 b-d) where it might be localized in RG-like cells and be involved in adult neurogenesis, as overexpression of CPEB3 has a negative impact on adult neurogenesis (4.7). Only 50% of RG-like cells were gap junction coupled. Also, transient amplifying cells and neuroblasts were not coupled (Kunze et al., 2009). It is possible that strong expression of CPEB3 in these cells provides a fast cut-off in gap junctional coupling by translational repression.

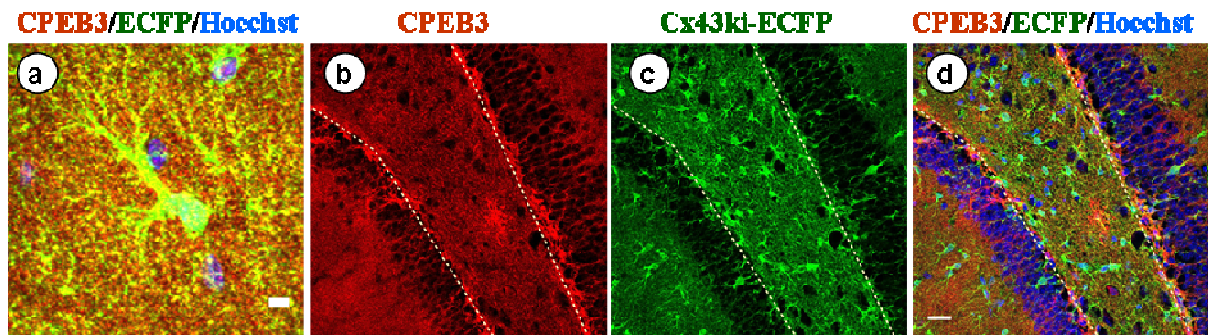


Figure 37: a) Representative image showing the immunolocalization of CPEB3 in fine processes of a CFP labeled astrocyte in hippocampus. b) Immunostaining showing a strong labeling of endogenous CPEB3 in the SGZ of DG, represented by dotted lines. c) Immunostaining for ECFP representing Cx43 expression. d) merged image. Scale bars, (a) 5  $\mu$ m, (d) 25  $\mu$ m.

#### 4.11 CPEB3 constructs for transgenic mice

For comparing the individual effects of the different regulatory elements present in the CPEB3 gene, different transgenic mice were generated.

#### 4.11.1 Investigation of the 3' end of CPEB3

Northern blot analysis revealed two brain specific isoforms for CPEB3: a short version of 4.8 kb and a long version of 6.9 kb (Theis et al., 2003b). The short (sh) version contains a UTR of 927 bp and the long (lg) version contains a ~3.5 kb fragment at the 3' end of CPEB3 mRNA (Theis et al., 2003b). To verify this and further prove that this 3.5 kb fragment was the real end of CPEB3 transcript, a 3' RACE was performed using commercial mouse brain cDNA. The RACE products obtained were sequence analyzed. The UTR of 3.5 kb in size was found to be the end of CPEB3 mRNA. There were several CPEs and poly (A) sequences present in the 3' UTR (Fig. 38), but only sh and lg UTR were functionally verified as true 3' ends.

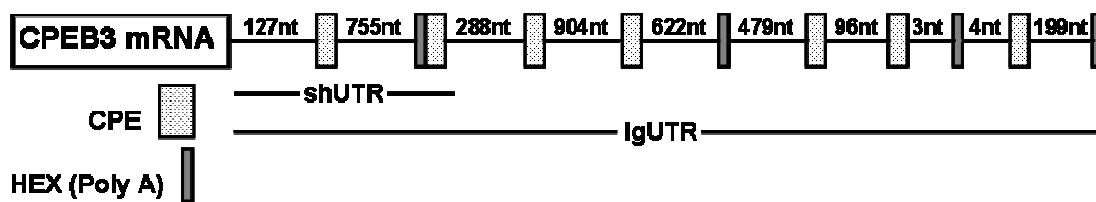


Figure 38: A schematic of CPEB3 3' UTR with CPEs and poly (A) sequences. shUTR – short untranslated region, lgUTR – long untranslated region.

#### 4.11.2 Constructs generated with 3' regulatory elements of CPEB3

From published results (Theis et al., 2003b) and the RACE experiments (4.11.1), the 3' end of CPEB3 mRNA transcript was confirmed with two types of UTRs: 0.9 kb and 3.5 kb with consensus poly (A) signal in both the variants (Fig. 37). These UTRs contain several CPEs to which other CPEBs could bind and regulate the expression of CPEB3, an auto-regulatory effect among CPEB proteins themselves (Theis et al., 2003b). The vectors were generated successfully by cloning the different UTRs (shUTR, lgUTR) into the CPEB3-pMM403-400 vector. The TetOff system was used in generating these mice. The transgenes (TetO:CPEB3shUTR, TetO:CPEB3lgUTR) were isolated from the vector and zygote injected for generating new transgenic mice. These mice were used to compare expression and localization of CPEB3 with UTRs in various cell types and also comparing the regulatory effects of CPEB3 on the target proteins with CPEB3 mice without UTRs. The positive founders carrying the transgenes were identified with genotyping PCR for the TetO transgene. These mice are currently screened for expression using GFAP-tTA (Fiacco et al., 2007) and CamKII-tTA mice (Mayford et al., 1996).



#### 4.11.3 CPEB3d and CPEB3aKD constructs for transgenic mice

The CPEB3 full length isoform, CPEB3a contains the so called B-region with putative phosphorylation sites for CamKII, p70S6 kinase, PKA (Theis et al., 2003b). Indeed, CPEB3 was found to be phosphorylated at S419/S420 residues in the B-region by both PKA and CamKII (Lech Kaczmarczyk., unpublished). To study the expression pattern among CPEB3 isoforms *in vivo* and also the CPEB3 targets, an isoform lacking the B- region (CPEB3d) was cloned into the pMM403-400 vector for generating transgenic mice. Similarly, a mutant form of CPEB3a in the B-region where two serines in the phosphorylation site were mutated to alanines (kinase dead), named CPEB3aKD was cloned into the pMM403-400 vector. These two transgenes (TetO:CPEB3d, TetO:CPEB3aKD) were digested from the pMM vector and used for zygote injection to generate transgenic mice using TetOff system. The positive founders carrying the transgenes were identified with genotyping PCR for tetO transgene and are currently screened for expression using GFAP-tTA (Fiacco et al., 2007) and CamKII-tTA mice (Mayford et al., 1996).

## 5 Discussion

### 5.1 Expression of CPEBs in astrocytes

CPEBs are expressed in different cell types of the CNS. While most of the work was done on CPEBs in neurons, recent reports showed CPEB1 expression in astrocytes (Jones et al., 2008). In the present study, all four CPEB transcripts (CPEB 1-4) were found to be expressed (Fig. 8) in astrocytes *in vitro*. Mainly, isoforms lacking the B-region were abundantly expressed compared to the isoforms containing the B-region. The B-region contains putative phosphorylation sites for various kinases such as CamKII $\alpha$ , S6 kinase and PKA (Theis et al., 2003b). The authors reported that only isoforms containing the B-region were expressed in principal cell layers of the hippocampus and also hypothesized that the B-region lacking isoforms might be expressed in non neuronal cells. The current findings of B-region lacking isoforms in astrocytes is consistent with the published results (Theis et al., 2003b). In primary astrocyte cultures, all CPEBs (1-4) were found to be localized in the cytoplasm and the expression was diffusely present throughout the cytoplasm (Fig. 9). Notably, CPEB3 was observed in astrocytic processes (Fig. 8g), similar to the localization of CPEB3 protein in the neuronal processes (Huang et al., 2006). Expression of CPEB3 and CPEB4 in hippocampal astrocytes was confirmed by non-radioactive *in situ* hybridization with probes specific to each CPEB (Vangoor et al., in revision). The localization of CPEB3 protein *in vivo* in hippocampal astrocytes is further confirmed by the co-expression of CPEB3 protein with ECFP in fine processes in Cx43ki-ECFP transgenic mice (Fig. 37). The distinct localization of CPEB3 in astrocytic processes might indicate its role in local protein synthesis.

A high complexity of expression of CPEBs is observed among glial cells (astrocytes and NG2 cells) similar to that of neurons (Turimella et al., in revision). Among different CPEBs, CPEB3 was more abundantly expressed in NG2 cells (Turimella et al., in revision) compared to astrocytes (Vangoor et al., in revision). Several mRNAs which contain CPEs in their 3'UTRs are expressed in NG2 cells, for example Cx43 and GLT-1; but unlike in astrocytes, they are not able to form functional proteins (Seifert et al., unpublished). So, in NG2 cells, CPEB3 might regulate the translation of these NG2-specific mRNAs.

### 5.2 CPEB3-GFAP transgenic mice

For studying the role of CPEB3 in astrocytes and to identify new putative target proteins transgenic mice were generated. Mice expressing CPEB3 in astrocytes were generated where

the expression of CPEB3-EGFP was driven by the hGFAP promoter (hGFAP-tTA: TetO-CPEB3EGFP). These mice were generated using the Tet-Off system in which the transgene expression can be controlled at any time by Dox. Transgene expression was observed in GFAP positive astrocytes. These mice overexpressing CPEB3 develop enlarged ventricles during postnatal brain development (Fig. 15). This developmental deficit (hydrocephalus) could be due to several reasons. Due to interruption in the flow of the cerebrospinal fluids (CSF) or alterations in the synthesis or absorption of CSF, leading to accumulation of CSF in these ventricles (Bruni et al., 1988; Koh et al., 2005). The cells lining the ventricles of the brain are the ependymal cells (cells of the glial lineage) which regulate CSF flow and facilitate the circulation of brain CSF in between ventricles (Cathcart and Worthington, 1964). Loss of polarity of these cells could lead to hydrocephalus as this causes disturbances in the flow of the brain CSF (Kobayashi et al., 2002). There are studies showing that genetic ablation of the  $\beta$ -catenin gene could also lead to hydrocephalus in mice (Ohtoshi, 2008).  $\beta$ -catenin is an important component of the Wnt-1 signalling pathway (Butz et al., 1992) and was shown to be a CPEB1 target in astrocytes (Jones et al., 2008). Wnt signalling is involved in many developmental processes such as proliferation, migration, polarity and cell fate specification (Cadigan and Nusse, 1997). Wnt-1/ $\beta$ -catenin signalling is required for brain morphogenesis (Brault et al., 2001). So, the developmental deficit observed in CPEB3-GFAP mice could be due to any of the reasons mentioned above and could be a direct or indirect effect of CPEB3 overexpression in astrocytes.

Mice were on Dox until weaning to prevent developmental deficit, and after removing Dox the mice were analyzed for transgene expression. 50% of the GFAP positive cells in the hippocampus were expressing CPEB3 and 90% of the GFP positive cells co-express GFAP (Fig. 17A). As not all astrocytes in the hippocampus are GFAP positive (Verkhatsky and Butt, 2007), it could be that indeed all GFP positive cells were astrocytes. The specificity of CPEB3 expression was also verified with co-staining for S100 $\beta$  and GFP, where a similar number of cells (90%) co-expressed both markers. There was no co-localization of CPEB3-EGFP with non-astrocytic markers such as NG2 (for NG2 glia), NeuN (neurons) and Iba1 (microglia), showing the specificity of CPEB3 expression. CPEB3-EGFP protein was often localized in the distal processes of astrocytes in hippocampus, where it might modulate local protein synthesis.

### 5.3 Bimodal impact on GFAP protein expression

In regions of cortex and thalamus, local CPEB3 overexpression was observed. Surrounding these overexpressing cells, there was an increase in GFAP immunoreactivity, whereas in control mice GFAP expression was not observed in cortex and thalamus (not shown). Paradoxically, in those very regions of cortex and thalamus the very cells overexpressing CPEB3 showed weak or no expression of endogenous GFAP. However, the neighbouring cells which were weakly positive or negative for CPEB3 showed strong GFAP expression. Similarly, reduced immunoreactivity for GFAP was observed in cells transfected with CPEB3 while no change was found in the GFAP protein amount in the untransfected cells. This reflects a negative impact of CPEB3 on GFAP expression. So far GFAP was considered as a non-CPEB target, as mouse GFAP mRNA does not contain CPEs (but CPEs are present in human and rat versions, verified with the sequences from Ensembl.org). In fact, it has been utilized as an mRNA which is explicitly not subject to stimulated polyadenylation (Huang et al., 2002; Huang et al., 2003). However, it is possible that manipulation of CPEB-mediated translational control changes other CPEB targets which are required to maintain the cellular phenotype of astrocytes thereby indirectly causing GFAP downregulation. But, in contrast there was no difference in the hippocampal protein levels of GFAP in CPEB3-GFAP mice compared to the control litters. This could be due to overexpression of CPEB3 in only 50% of the astrocytes and could be also compensated by the upregulation of GFAP in non-CPEB3 overexpressing cells in the hippocampus. We refrained from immunoblot analysis of cortex and thalamus, as the overexpression of CPEB3 in astrocytes was confined to very local areas. Interestingly, the number of S100 $\beta$  positive cells was not affected in mice overexpressing CPEB3 in astrocytes.

### 5.4 Downregulation of astrocytic connexins by CPEB3

CPEB3 acts as a basal repressor of translation of its target proteins (Huang et al., 2006). Si-RNA mediated knockdown of CPEB3 in primary neuronal cultures showed an increase in GluR2 protein levels (Huang et al., 2006). This was confirmed by the finding that mice overexpressing CPEB3 in neurons show a reduction of GluR2 protein levels (Lech Kaczmarczyk., unpublished). To find out more targets for CPEB3, a screening for putative astrocytic targets was carried out which yielded connexins (Cx43 and Cx30) as possible targets. Both Cx43 and Cx30, the major astrocytic connexins which form gap junctions in the hippocampus possess CPEs in their 3' UTRs (Table 23). RNA Co-IP showed an interaction of

CPEB3 protein with Cx43 UTR in a CPE dependent fashion, and the interaction was significantly reduced upon mutating CPEs. Moreover, CPEB3 protein is binding Cx30 mRNA with high affinity compared to CPEB1 (Fig. 24). It could be that similar target mRNAs are bound by different CPEBs with varying affinities. For example, cyclinB1 mRNA is bound by CPEB1 with high affinity compared to other CPEBs (Novoa et al., 2010). We investigated the impact of CPEB3 on the translation of Cx43 and Cx30 in astrocytes. As a first hint, the immunoreactivity of Cx43 in the primary astrocyte cultures transfected with CPEB3-EGFP vector was reduced (Fig. 10). Similarly, in mice overexpressing CPEB3 in astrocytes the immunoreactivity for Cx43 protein was reduced in regions of overexpression in cortex, thalamus and hippocampus. Immunoblots of hippocampal protein lysates from CPEB3-GFAP mice showed a significant reduction of Cx43 protein levels compared to their control litters. Similarly Cx30 immunoreactive puncta which are more prominently observed around the blood vessels of the hippocampus (Gosejacob et al., 2011) are strongly reduced in CPEB3-GFAP mice (Fig. 27A). This reduced immunoreactivity for Cx30 around vessels was also observed in thalamus and cortex (not shown). Immunoblots from total hippocampal protein also showed a reduction of Cx30 in comparison with the controls.

The most important function of connexins in the hippocampus is forming functional intracellular gap junctions between astrocytes which mediate the exchange of small molecules, metabolites and ions (Giaume and Theis, 2010). Gap junctional coupling can be assessed electrophysiologically by injecting tracers (e.g., biocytin, sulforhodamine B, Lucifer yellow, Alexa dyes, neurobiotin) with low molecular weights (<1 kDa) into a single astrocyte with the patch clamp technique and analysing the extent of tracer spread (Giaume and Theis, 2010). As both connexins (Cx43, Cx30) were downregulated in mice overexpressing CPEB3, biocytin tracer injections were performed which revealed an approximate 40% reduction in the number of coupled cells compared to the control litters. Interestingly, the tracer was spreading preferentially through the non-CPEB3 overexpressing cells, showing the strong inhibition of connexins by CPEB3. In Cx43 deficient mice (Cx43KO), 50% reduction of tracer coupling was observed (Theis et al., 2003a). In Cx30KO mice, 22% reduction of the tracer coupling in the hippocampus was observed (Gosejacob et al., 2011). However, genetic ablation of both connexins resulted in a complete inhibition of tracer spread between astrocytes in the hippocampus (Wallraff et al., 2006; Rouach et al., 2008). Similarly, as both connexins are CPEB targets and were downregulated in CPEB3-GFAP mice, a strong reduction in astrocytic coupling has been observed.

Connexins form HCs and at the unapposed cell surface enable diffusion of ions and small molecules between the intra- and extracellular space and thereby support autocrine/paracrine actions (Spray et al., 2006; Saez et al., 2010). HCs are oligomerized in the golgi/trans-golgi network (Musil and Goodenough, 1991; Koval et al., 1997; George et al., 1999) and after assembling they are transported to the non-junctional plasma-membrane through a cytoskeleton-mediated route (Jordan et al., 1999; Giepmans et al., 2001; Martin et al., 2001). After insertion in the plasma membrane they diffuse laterally to join gap junctional plaques and are docked with HCs from neighbouring cells to form intercellular channels (Lauf et al., 2002). Moreover Cx43 HCs are directly targeted to the region of gap junctional plaques via a microtubule/N-cadherin-dependent pathway (Shaw et al., 2007). But, recently it was shown that HCs formed by Cx43 are also delivered at all cell surface domains that lack contacting cells, and the authors speculate that this might be due to differences in either channel packing or due to the interactions of Cx43 with its binding partners (Simek et al., 2009). Similarly, overexpression of CPEB3 in astrocytes which downregulates Cx43 could also lead to the mislocalization of connexins. For example, the presence of CPEB3 could lead to production of Cx43 protein in the soma or in the proximal processes. This may favour the presence of Cx43 as HCs instead of gap junction channels in the fine processes. This could also be one of the reasons which resulted in reduced coupling between hippocampal astrocytes in CPEB3-GFAP mice.

Astrocytic connexins form gap junctions and mediate spatial buffering of potassium (Orkand, 1986; Wallraff et al., 2006), and metabolite supply to neurons (Rouach et al., 2008). Most importantly both astrocytic connexins are expressed and mediate gap junctional coupling also in RG-like cells in the SGZ of the hippocampus and their function is required for adult neurogenesis (Kunze et al., 2009). In mice lacking both connexins, a strong inhibition of cell proliferation and a reduction in the granule cell number (Prox1 positive cells) was observed (Kunze et al., 2009). In mice overexpressing CPEB3 in astrocytes connexin expression was reduced which has resulted in inhibition of gap junctional coupling. So, we decided to study the role of CPEB3 in adult neurogenesis. Staining for Ki-67 revealed a reduction in the number of proliferating cells in the SGZ and Prox1 staining demonstrated a significant reduction of granule neurons. Furthermore, a reduction in the number of RG-like cells, the neural stem cells itself, was also observed upon staining for BLBP. The actual underlying mechanism of decreased proliferation and neurogenesis is not known. Studies performed on Cx43KO mice show that the absence of Cx43 leads to effects on cell proliferation (Wiencken-

Barger et al., 2007) and moreover gap junction coupling has an important role in modifying neurogenesis (Sutor and Hagerty, 2005). In various studies Cx43 was shown to form cell-cell adhesion contacts either independent or dependent on gap junctional coupling (Theis et al., 2005). However recent studies performed by Mr. Jiong Zhang (unpublished), indicate that coupling rather than adhesion is required for adult neurogenesis. The present study proves connexins as new targets of CPEB3, and the involvement of CPEB3 in adult neurogenesis via regulating connexins.

## 5.5 Downregulation of GLT-1 and GS

Glutamate is the major excitatory neurotransmitter expressed in the mammalian CNS. An equilibrium of the glutamate levels in the extracellular space has to be maintained to prevent excitotoxicity, which otherwise leads to cell death (Sheldon and Robinson, 2007). Glutamate released from neurons into the extracellular space is cleared by Na<sup>+</sup>-dependent high affinity glutamate transporters family (Shigeri et al., 2004). GLAST and GLT-1 are the glutamate transporters which belong to this family and are primarily expressed by astrocytes (Rothstein et al., 1994; Lehre et al., 1995). GLT-1 has a predominant role in the clearance of extracellular glutamate (Danbolt, 2001). These transporters were found to be deregulated in several neurodegenerative disorders. There are several reports showing that these transporters were regulated by both transcriptional and post-transcriptional mechanisms (Sheldon and Robinson, 2007). As the mRNA encoding GLT-1 contain CPEs in its 3' UTR (Table 23), the impact of CPEB3 overexpression on GLT-1 was studied. Immunoreactivity for GLT-1 was reduced in regions of CPEB3 overexpression in cortex and hippocampus (not shown). Moreover, there was a significant reduction in the hippocampal protein levels of GLT-1 protein in CPEB3 mice compared to controls. CPEB3 regulates the translation of GLT-1 in astrocytes possibly by binding to CPEs present in the 3' UTR of GLT-1 mRNA, but this has still to be confirmed. The decrease in the protein levels of GLT-1 could lead to accumulation of glutamate in the extracellular space and thereby causing excitotoxicity, as the inhibition of GLT-1 and GLAST by antisense oligonucleotides leads to neurodegeneration characteristic of excitotoxicity (Rothstein et al., 1996). Even though endogenous expression of CPEB3 in astrocytes is low, mRNA levels of CPEB3 were upregulated 2 hr post injection of kainate, a glutamate receptor agonist (Theis et al., 2003b). The possible upregulation of CPEB3 in disease conditions such as epilepsy could downregulate GLT-1, which has yet to be studied. A second possible mechanism for GLT-1 decrease could be via Eph-ephrin signalling: The Eph family of receptors (receptor tyrosine kinases) binds to ephrin ligands by cell surface association with

neighbouring cells. This complex of Eph-ephrins has the ability of generating bidirectional signalling which effects both receptor expressing and ephrin expressing cells (Pasquale, 2008). EphA4 is involved in neuron to glia signalling via interacting with glial ephrinA3 ligand and is a negative regulator of glutamate transporters, GLT-1 and GLAST (Carmona et al., 2009). EphA4 receptor is also found in reactive astrocytes (Goldshmit et al., 2006). In the present study, overexpression of CPEB3 leads to reactive nature of astrocytes. Hence, EphA4 which might be present in the reactive astrocytes of CPEB3-GFAP mice may downregulate GLT-1. Indeed, one of the CPEB family members, CPEB2 regulates EphA4 translation in neurons (Turimella et al., unpublished). Glutamate released from neuronal synapses is taken up by astrocytes mainly through glutamate transporters GLT-1 and GLAST (Rothstein et al., 1996; Gegelashvili et al., 2000) and converted into glutamine by GS. GS converts the glutamate to the receptor-inactive substrate glutamine upon consuming ATP and ammonia (Seifert et al., 2010). GS protein was downregulated in astrocytes of human patients with hippocampal sclerosis and MTLE thereby impairing the glutamate-glutamine cycle (Eid et al., 2004; van der Hel et al., 2005). The mRNA encoding GS was polyadenylated after kainate induced seizures in rat brain (Du and Richter, 2005). As GS contains four CPEs in its 3' UTR it could be a putative target for CPEBs. The Co-IP studies showed an interaction of GS mRNA with CPEB3 protein in a CPE dependent fashion. Furthermore, in mice overexpressing CPEB3 in astrocytes immunoreactivity for GS was reduced in the regions of CPEB3 overexpression. In addition a significant reduction in the total protein levels of GS was observed in the hippocampus of CPEB3 mice (Fig. 33B, C). The impairment of GS could disturb the glutamate-glutamine cycle and lead to the accumulation of extracellular glutamate levels. This could eventually lead to excitotoxicity and seizure activity, which is observed in patients with MTLE (Eid et al., 2008a). Seizure activity in CPEB3-GFAP mice should be analyzed by performing telemetric EEG measurements.

### **5.6 CPEB3 regulation does not induce cell death or affects astrocyte identity**

TUNEL staining was used to check if there was cell death as an adverse effect of CPEB3 overexpression in astrocytes. No apoptotic cells were observed in the regions of CPEB3 overexpression and no change in the number and the density of astrocytes in the hippocampus was found. Thus the effects observed in mice overexpressing CPEB3 in astrocytes are translational, by directly binding to the CPEs present in the 3' UTRs of the target mRNAs. There was no change in the immunoreactivity for NeuN in cortex, thalamus and hippocampus, and no change in the number of S100 $\beta$  positive astrocytes. Moreover the transcript levels of



the altered proteins (Cx43, Cx30, GS and GLT-1) tested was not altered, confirming the translational effect of CPEB3.

### 5.7 Upregulation of CPEB3 leads to astrocyte dysfunction

Astrocyte dysfunction is a key feature observed in brain disorders, especially in epilepsy (Seifert et al., 2010) during which several of the key proteins involved in the normal cellular functions are dysregulated. CPEB3 overexpression in astrocytes has led to the downregulation of connexins, GS and GLT-1. These studies also raise the possibility of translational regulation by CPEB3 being involved in astrocytic dysfunction in epilepsy. The functions of all these proteins are found to be altered in diseased condition and are hallmarks of TLE (Seifert et al., 2010). Hence it can be speculated that the expression of CPEB3 might be upregulated and involved in the progression of epilepsy by contributing to astrocyte dysfunction. The expression of another astrocytic protein, a water channel protein (AQP4) is reduced at the endfeet in patients presenting with MTLE with hippocampal sclerosis (Eid et al., 2005; Binder and Steinhauser, 2006), this could be due to the disruption of the dystrophin complex (Amiry-Moghaddam et al., 2003). But, both AQP4 and dystrophin in the dystrophin complex are CPE containing mRNAs (Table 23) and are influenced by CPEB3 as well (not shown). By leading to decreased and/or mislocalized expression of all these astrocytic proteins, CPEBs might contribute to astrocytic dysfunction. Studies should be performed by subjecting CPEB3-GFAP mice to the kainate model of epilepsy (TLE animal model established in the institute by Dr. Peter Bedner) and analyzing the changes of the target gene proteins and compare with their expression in normal conditions.

### 5.8 Regulation of CPEB3 activity

Two brain specific isoforms were identified for CPEB3, a short version of 4.8 kb and a long version of 6.9 kb. The short version contains a 3' UTR of 927 bp and the long version contains a 3' UTR of ~3.5 kb (Theis et al., 2003b). RACE experiments were performed to further confirm this and the isolated UTR fragments were sequence analyzed. The 3.5 kb fragment of the 3' UTR contains several CPEs to which other CPEB proteins could bind and regulate their own translation by an autoregulatory feedback loop (Theis et al., 2003b). The autoregulatory feedback mechanism of CPEB was shown previously with *Drosophila* CPEB protein *orb*, in directing the on-site accumulation of *orb* protein in developing *Drosophila* oocyte (Tan et al., 2001). CPEB proteins could also be regulated by miRNAs. Recently it was predicted that the

CPEB 2-4 subfamily possess miRNA binding sites for miR-92 and miR-26 in their 3' UTRs. The binding and the regulation of CPEB 2-4 by these miRNAs was validated by luciferase reporter gene assays (Morgan et al., 2010). Recently CPEB1 in astrocytes was shown to be phosphorylated by Aurora A kinase and to regulate the translation of cyclin B1 mRNA (Kim et al., 2011). As CPEB3 contains recognition sites for CamKII, S6 kinase and PKA (Theis et al., 2003b), the activity of CPEB3 can be also regulated by phosphorylation through these kinases depending on their presence in astrocytes. CPEB3 is indeed proven to be phosphorylated by PKA and by CamKII at S419/S420 residues in the B-region (Lech Kaczmarczyk, unpublished), and so the regulatory activity of CPEB3 can be affected by the presence of these kinases in astrocytes.

## 6 Future outlook

All the four CPEB proteins (CPEB 1-4) were expressed in primary astrocyte cultures. CPEB3 was localized in the fine processes of astrocytes similar to neurons where it can modulate local protein synthesis. The overexpression of CPEB3 in astrocytes downregulated two major astrocytic connexins (Cx43 and Cx30). Consistently, with the astrocytic overexpression of CPEB3, interastrocytic gap junctional communication was also reduced. Thus, CPEBs may play a role in astrocytic heterogeneity. For example, in the somatosensory cortex (barrel cortex), Cx43 and Cx30 together with GLT-1 and GS are differentially expressed: In the so-called barrel fields, connexins, GLT-1 and GS expression is strong, while in the septal regions between the barrels, the expression of all four proteins is weak (Voutsinos-Porche et al., 2003; Houades et al., 2008). The same applies to the neurogenic niche of the hippocampus, where a strong expression of CPEB3 is observed. Only 50% of the neural stem cells are coupled, while transient amplifying cells and neuroblasts are not coupled (Kunze et al., 2009). Since we observed a negative correlation between CPEB3 and connexin expression, high expression of CPEB3 in half of the neural stem cells and possibly in precursor cells could be directly related to lack of coupling in this cell population. This would be consistent with the requirement of connexin expression for adult neurogenesis (Kunze et al., 2009) and with the effect of CPEB3 expression on adult neurogenesis observed in this study. In addition, both NG2 cells and astrocytes express mRNA for Cx43 and the glutamate transporters GLAST and GLT-1, but only astrocytes show the corresponding protein functions. The mRNA levels for connexins and glutamate transporters in NG2 cells are much lower compared to astrocytes (Gerald Seifert, unpublished), while NG2 cells express much higher levels of CPEBs compared to astrocytes. Maybe the strong expression of CPEBs prevents the translation of typical astrocytic mRNAs expressed at low levels in NG2 cells, just like myc mRNA translation was prevented by CPEB1 in cultured fibroblasts (Groisman et al., 2006). The hypothesis that astrocyte heterogeneity and glial identity is based on differential CPEB expression should be investigated further in various brain regions and cell types.

In a mouse model of TLE, a reduction in astrocytic gap junctional coupling was observed before the onset of spontaneous seizures, indicating that the loss of astrocytic connexins may play a role in the progression of epilepsy (Bedner et al., unpublished). Is the loss of connexin expression due to translational regulation by CPEB3? To investigate this, Cx43ki-ECFP mice should be brought into the epilepsy model, and expression changes for CPEBs should be investigated by antibody stainings and FACS purification followed by WB analysis for

CPEBs. One possibility is that the expression of CPEB3 is upregulated and causes downregulation of connexins during epilepsy. Loss of interastrocytic gap junctional coupling leads to hyperexcitability in acute hippocampal slices (Wallraff et al., 2006). The reduced interastrocytic gap junctional coupling observed in CPEB3-GFAP mice could also be due to the mislocalization of the HCs formed by Cx43 and Cx30 proteins. HC activity of astrocytes in CPEB3-GFAP mice can be determined by performing electrophysiology and measuring HC currents and comparing them with astrocytes in the DKO mice (Giaume and Theis, 2010). Further experiments are required to examine the impact of CPEBs for connexin expression in astrocytes.

The overexpression of CPEB3 in astrocytes reduced GLT-1 and GS levels. This could lead to accumulation of glutamate in the extracellular space and in turn to seizure activity, a common feature in patients with MTLE (Eid et al., 2008a). Both of these findings predict a predisposition of CPEB3-GFAP mice towards epilepsy. The susceptibility of these mice to epileptiform activity can be tested by various stimulation protocols using hippocampal slices. The following parameters can be checked: 1) spontaneous epileptiform activity, 2) epileptiform activity induced by electrical stimulation, and 3) epileptiform activity in the zero magnesium model (Wallraff et al., 2006). In addition, spontaneous seizure activity can be measured by telemetric EEG recordings. Upon subjecting CPEB3-GFAP to the model of TLE, the severity of status epilepticus, duration of latency, seizure activity at different time point's post-injection of kainate should be studied. Morphological changes such as neuronal loss, granule cell dispersion, and astrogliosis should also be studied. Target gene expression can also be analyzed in the TLE model of CPEB3-GFAP mice. In an independent approach, Cx43ki-ECFP mice (Degen et al., 2012) can be brought into the TLE model, the ECFP labelled astrocytes can be isolated using FACS and the expression levels of CPEBs can be investigated by reverse transcription PCR and WB. The expression levels should be compared between the injected and non-injected side of the hippocampus at different stages of epilepsy.

By downregulating various proteins (Cx43, Cx30, GS and GLT-1), CPEB3 might be one of the factors contributing to astrocyte dysfunction observed during epilepsy (Seifert et al., 2010). The other putative targets of CPEBs which are altered in astrocytes are: 1) AQP4, a water channel expressed in astrocytes (Badaut et al., 2002), 2) dystrophin which helps in anchoring AQP4 to the membrane (Amiry-Moghaddam et al., 2003), 3) Kir4.1, a potassium channel subunit expressed in astrocytes which is overlapping with AQP4 at the astrocytic end

feet (Higashi et al., 2001), and 4) the other astrocytic glutamate transporter, GLAST. Even though Kir4.1 does not contain CPEs, CPEBs might have an indirect effect via dystrophin, which anchors Kir4.1 to endfeet (Connors et al., 2004). The translation of all the above mentioned targets should be tested in CPEB3-GFAP mice. In addition, the 3' UTRs containing CPEs of the respective target mRNAs should be isolated and the interaction of CPEB3 with them studied by RNA Co-IP.

## 7 Summary

CPEBs regulate the translation of mRNAs encoding key players involved in synaptic plasticity (Richter, 2007). CPEB1 in neurons is involved in synaptic plasticity (Alarcon et al., 2004), learning and memory (Berger-Sweeney et al., 2006). Several studies were focused on the role of CPEBs in neurons, but not much is known about the role of CPEB 2-4 subfamily in astrocytes. Hence the present study was aimed to investigate the expression of CPEBs in astrocytes and also to study the functional role of CPEB3 in astrocytes.

In the present work, the expression of CPEB (1-4) proteins in astrocytes was investigated. All CPEB transcripts and proteins were found to be expressed in astrocytes. CPEB3 was localized to the distal processes of astrocytes compared to the other CPEBs, similar to the localization observed in primary neuronal cultures. To study the functional role of CPEB3, transgenic mice were generated using the Tet-off system. Overexpression of CPEB3-EGFP in astrocytes during development caused enlarged ventricles, and acute overexpression in adult mice induced increased immunoreactivity for GFAP in cortex, hippocampus and thalamus, while in cells overexpressing CPEB3, GFAP protein content was decreased. In these brain areas, CPEB3 overexpression also led to downregulation of the protein levels for Cx43 and Cx30, two major astrocytic gap junction proteins involved in extracellular ion homeostasis and metabolite supply to neurons. Consistently, in the hippocampus of CPEB3 overexpressing mice, intercellular gap junction coupling was strongly impaired. Connexin function in RG-like cells is required for adult neurogenesis in the SGZ, a neurogenic niche in the hippocampus. In the SGZ of CPEB3 overexpressing mice, a significant reduction in the number of proliferating cells, reduced granule neurons and RG-like cells was observed. Altogether, the present study showed a negative correlation between CPEB3 expression and gap junctional coupling, which might be responsible for astrocyte heterogeneity. All these results confirm that astrocytic connexins are CPEB3 targets. CPEB3 overexpression also led to downregulation of GLT-1 and GS, key players involved in extracellular glutamate clearance. Since interastrocytic coupling and astrocytic GLT-1 and GS activities are downregulated in epilepsy patients presenting with hippocampal sclerosis, it can be hypothesised that upregulation of CPEBs in astrocytes may contribute to the pathogenesis of epilepsy.

## 8 References

- Abramoff, M.D., Magalhaes, P.J., and Ram, S.J. (2004). "Image Processing with ImageJ". *Biophotonics International volume 11*, pp. 36-42.
- Alarcon, J.M., Hodgman, R., Theis, M., Huang, Y.S., Kandel, E.R., and Richter, J.D. (2004). Selective modulation of some forms of schaffer collateral-CA1 synaptic plasticity in mice with a disruption of the CPEB-1 gene. *Learn Mem 11*, 318-327.
- Alev, C., Urschel, S., Sonntag, S., Zoidl, G., Fort, A.G., Hoher, T., Matsubara, M., Willecke, K., Spray, D.C., and Dermietzel, R. (2008). The neuronal connexin36 interacts with and is phosphorylated by CaMKII in a way similar to CaMKII interaction with glutamate receptors. *Proc Natl Acad Sci U S A 105*, 20964-20969.
- Altevogt, B.M., Kleopa, K.A., Postma, F.R., Scherer, S.S., and Paul, D.L. (2002). Connexin29 is uniquely distributed within myelinating glial cells of the central and peripheral nervous systems. *J Neurosci 22*, 6458-6470.
- Altevogt, B.M., and Paul, D.L. (2004). Four classes of intercellular channels between glial cells in the CNS. *J Neurosci 24*, 4313-4323.
- Amiry-Moghaddam, M., Otsuka, T., Hurn, P.D., Traystman, R.J., Haug, F.M., Froehner, S.C., Adams, M.E., Neely, J.D., Agre, P., Ottersen, O.P., and Bhardwaj, A. (2003). An alpha-syntrophin-dependent pool of AQP4 in astroglial end-feet confers bidirectional water flow between blood and brain. *Proc Natl Acad Sci U S A 100*, 2106-2111.
- Anderson, C., Catoe, H., and Werner, R. (2006). MIR-206 regulates connexin43 expression during skeletal muscle development. *Nucleic Acids Res 34*, 5863-5871.
- Arriza, J.L., Eliasof, S., Kavanaugh, M.P., and Amara, S.G. (1997). Excitatory amino acid transporter 5, a retinal glutamate transporter coupled to a chloride conductance. *Proc Natl Acad Sci U S A 94*, 4155-4160.
- Arriza, J.L., Fairman, W.A., Wadiche, J.I., Murdoch, G.H., Kavanaugh, M.P., and Amara, S.G. (1994). Functional comparisons of three glutamate transporter subtypes cloned from human motor cortex. *J Neurosci 14*, 5559-5569.
- Aschner, M. (2000). Neuron-astrocyte interactions: implications for cellular energetics and antioxidant levels. *Neurotoxicology 21*, 1101-1107.
- Atkins, C.M., Nozaki, N., Shigeri, Y., and Soderling, T.R. (2004). Cytoplasmic polyadenylation element binding protein-dependent protein synthesis is regulated by calcium/calmodulin-dependent protein kinase II. *J Neurosci 24*, 5193-5201.
- Badaut, J., Lasbennes, F., Magistretti, P.J., and Regli, L. (2002). Aquaporins in brain: distribution, physiology, and pathophysiology. *J Cereb Blood Flow Metab 22*, 367-378.
- Balcar, V.J. (2002). Molecular pharmacology of the Na<sup>+</sup>-dependent transport of acidic amino acids in the mammalian central nervous system. *Biol Pharm Bull 25*, 291-301.

- Baranova, A., Ivanov, D., Petrash, N., Pestova, A., Skoblov, M., Kelmanson, I., Shagin, D., Nazarenko, S., Geraymovych, E., Litvin, O., Tiunova, A., Born, T.L., Usman, N., Staroverov, D., Lukyanov, S., and Panchin, Y. (2004). The mammalian pannexin family is homologous to the invertebrate innexin gap junction proteins. *Genomics* 83, 706-716.
- Barkoff, A.F., Dickson, K.S., Gray, N.K., and Wickens, M. (2000). Translational control of cyclin B1 mRNA during meiotic maturation: coordinated repression and cytoplasmic polyadenylation. *Dev Biol* 220, 97-109.
- Bashirullah, A., Cooperstock, R.L., and Lipshitz, H.D. (1998). RNA localization in development. *Annu Rev Biochem* 67, 335-394.
- Bedner, P., Steinhauser, C., and Theis, M. (2012). Functional redundancy and compensation among members of gap junction protein families? *Biochim Biophys Acta* 1818, 1971-1984.
- Bennett, M.V., and Zukin, R.S. (2004). Electrical coupling and neuronal synchronization in the Mammalian brain. *Neuron* 41, 495-511.
- Berger-Sweeney, J., Zearfoss, N.R., and Richter, J.D. (2006). Reduced extinction of hippocampal-dependent memories in CPEB knockout mice. *Learn Mem* 13, 4-7.
- Bignami, A., Eng, L.F., Dahl, D., and Uyeda, C.T. (1972). Localization of the glial fibrillary acidic protein in astrocytes by immunofluorescence. *Brain Res* 43, 429-435.
- Binder, D.K., and Steinhauser, C. (2006). Functional changes in astroglial cells in epilepsy. *Glia* 54, 358-368.
- Binder, D.K., Yao, X., Zador, Z., Sick, T.J., Verkman, A.S., and Manley, G.T. (2006). Increased seizure duration and slowed potassium kinetics in mice lacking aquaporin-4 water channels. *Glia* 53, 631-636.
- Blumcke, I., Beck, H., Lie, A.A., and Wiestler, O.D. (1999). Molecular neuropathology of human mesial temporal lobe epilepsy. *Epilepsy Res* 36, 205-223.
- Boassa, D., Ambrosi, C., Qiu, F., Dahl, G., Gaietta, G., and Sosinsky, G. (2007). Pannexin1 channels contain a glycosylation site that targets the hexamer to the plasma membrane. *J Biol Chem* 282, 31733-31743.
- Brault, V., Moore, R., Kutsch, S., Ishibashi, M., Rowitch, D.H., McMahon, A.P., Sommer, L.,
- Boussadia, O., and Kemler, R. (2001). Inactivation of the beta-catenin gene by Wnt1-Cre-mediated deletion results in dramatic brain malformation and failure of craniofacial development. *Development* 128, 1253-1264.
- Bruni, J.E., Del Bigio, M.R., Cardoso, E.R., and Persaud, T.V. (1988). Hereditary hydrocephalus in laboratory animals and humans. *Exp Pathol* 35, 239-246.
- Bruzzone, R., Hormuzdi, S.G., Barbe, M.T., Herb, A., and Monyer, H. (2003). Pannexins, a family of gap junction proteins expressed in brain. *Proc Natl Acad Sci U S A* 100, 13644-13649.



Bushong, E.A., Martone, M.E., and Ellisman, M.H. (2004). Maturation of astrocyte morphology and the establishment of astrocyte domains during postnatal hippocampal development. *Int J Dev Neurosci* 22, 73-86.

Butt, A.M., and Ransom, B.R. (1989). Visualization of oligodendrocytes and astrocytes in the intact rat optic nerve by intracellular injection of lucifer yellow and horseradish peroxidase. *Glia* 2, 470-475.

Butz, S., Stappert, J., Weissig, H., and Kemler, R. (1992). Plakoglobin and beta-catenin: distinct but closely related. *Science* 257, 1142-1144.

Cacheaux, L.P., Ivens, S., David, Y., Lakhter, A.J., Bar-Klein, G., Shapira, M., Heinemann, U., Friedman, A., and Kaufer, D. (2009). Transcriptome profiling reveals TGF-beta signaling involvement in epileptogenesis. *J Neurosci* 29, 8927-8935.

Cadigan, K.M., and Nusse, R. (1997). Wnt signaling: a common theme in animal development. *Genes Dev* 11, 3286-3305.

Cahoy, J.D., Emery, B., Kaushal, A., Foo, L.C., Zamanian, J.L., Christopherson, K.S., Xing, Y., Lubischer, J.L., Krieg, P.A., Krupenko, S.A., Thompson, W.J., and Barres, B.A. (2008). A transcriptome database for astrocytes, neurons, and oligodendrocytes: a new resource for understanding brain development and function. *J Neurosci* 28, 264-278.

Cao, Q., and Richter, J.D. (2002). Dissolution of the maskin-eIF4E complex by cytoplasmic polyadenylation and poly(A)-binding protein controls cyclin B1 mRNA translation and oocyte maturation. *EMBO J* 21, 3852-3862.

Carmona, M.A., Murai, K.K., Wang, L., Roberts, A.J., and Pasquale, E.B. (2009). Glial ephrin-A3 regulates hippocampal dendritic spine morphology and glutamate transport. *Proc Natl Acad Sci U S A* 106, 12524-12529.

Cathcart, R.S., 3rd, and Worthington, W.C., Jr. (1964). Ciliary Movement in the Rat Cerebral Ventricles: Clearing Action and Directions of Currents. *J Neuropathol Exp Neurol* 23, 609-618.

Cina, C., Maass, K., Theis, M., Willecke, K., Bechberger, J.F., and Naus, C.C. (2009). Involvement of the cytoplasmic C-terminal domain of connexin43 in neuronal migration. *J Neurosci* 29, 2009-2021.

Clelland, C.D., Choi, M., Romberg, C., Clemenson, G.D., Jr., Fagniere, A., Tyers, P., Jessberger, S., Saksida, L.M., Barker, R.A., Gage, F.H., and Bussey, T.J. (2009). A functional role for adult hippocampal neurogenesis in spatial pattern separation. *Science* 325, 210-213.

Colak, D., Mori, T., Brill, M.S., Pfeifer, A., Falk, S., Deng, C., Monteiro, R., Mummery, C., Sommer, L., and Gotz, M. (2008). Adult neurogenesis requires Smad4-mediated bone morphogenic protein signaling in stem cells. *J Neurosci* 28, 434-446.

Collignon, F., Wetjen, N.M., Cohen-Gadol, A.A., Cascino, G.D., Parisi, J., Meyer, F.B., Marsh, W.R., Roche, P., and Weigand, S.D. (2006). Altered expression of connexin subtypes in mesial temporal lobe epilepsy in humans. *J Neurosurg* 105, 77-87.

- Condorelli, D.F., Trovato-Salinaro, A., Mudo, G., Mirone, M.B., and Belluardo, N. (2003). Cellular expression of connexins in the rat brain: neuronal localization, effects of kainate-induced seizures and expression in apoptotic neuronal cells. *Eur J Neurosci* *18*, 1807-1827.
- Connors, N.C., Adams, M.E., Froehner, S.C., and Kofuji, P. (2004). The potassium channel Kir4.1 associates with the dystrophin-glycoprotein complex via alpha-syntrophin in glia. *J Biol Chem* *279*, 28387-28392.
- Curtis, M.A., Kam, M., Nannmark, U., Anderson, M.F., Axell, M.Z., Wikkelso, C., Holtas, S., van Roon-Mom, W.M., Bjork-Eriksson, T., Nordborg, C., Frisen, J., Dragunow, M., Faull, R.L., and Eriksson, P.S. (2007). Human neuroblasts migrate to the olfactory bulb via a lateral ventricular extension. *Science* *315*, 1243-1249.
- D'Hondt, C., Ponsaerts, R., De Smedt, H., Bultynck, G., and Himpens, B. (2009). Pannexins, distant relatives of the connexin family with specific cellular functions? *Bioessays* *31*, 953-974.
- Danbolt, N.C. (2001). Glutamate uptake. *Prog Neurobiol* *65*, 1-105.
- Degen, J., Dublin, P., Zhang, J., Dobrowolski, R., Jokwitz, M., Karram, K., Trotter, J., Jabs, R., Willecke, K., Steinhauser, C., and Theis, M. (2012). Dual reporter approaches for identification of Cre efficacy and astrocyte heterogeneity. *FASEB J* *26*, 4576-4583.
- Degen, J., Meier, C., Van Der Giessen, R.S., Sohl, G., Petrasch-Parwez, E., Urschel, S., Dermietzel, R., Schilling, K., De Zeeuw, C.I., and Willecke, K. (2004). Expression pattern of lacZ reporter gene representing connexin36 in transgenic mice. *J Comp Neurol* *473*, 511-525.
- Dermietzel, R., Gao, Y., Scemes, E., Vieira, D., Urban, M., Kremer, M., Bennett, M.V., and Spray, D.C. (2000). Connexin43 null mice reveal that astrocytes express multiple connexins. *Brain Res Brain Res Rev* *32*, 45-56.
- Derouiche, A., and Frotscher, M. (1991). Astroglial processes around identified glutamatergic synapses contain glutamine synthetase: evidence for transmitter degradation. *Brain Res* *552*, 346-350.
- Derouiche, A., and Frotscher, M. (2001). Peripheral astrocyte processes: monitoring by selective immunostaining for the actin-binding ERM proteins. *Glia* *36*, 330-341.
- Dickson, K.S., Bilger, A., Ballantyne, S., and Wickens, M.P. (1999). The cleavage and polyadenylation specificity factor in *Xenopus laevis* oocytes is a cytoplasmic factor involved in regulated polyadenylation. *Mol Cell Biol* *19*, 5707-5717.
- Dingledine, R., Borges, K., Bowie, D., and Traynelis, S.F. (1999). The glutamate receptor ion channels. *Pharmacol Rev* *51*, 7-61.
- Djukic, B., Casper, K.B., Philpot, B.D., Chin, L.S., and McCarthy, K.D. (2007). Conditional knock-out of Kir4.1 leads to glial membrane depolarization, inhibition of potassium and glutamate uptake, and enhanced short-term synaptic potentiation. *J Neurosci* *27*, 11354-11365.

- Don, R.H., Cox, P.T., Wainwright, B.J., Baker, K., and Mattick, J.S. (1991). 'Touchdown' PCR to circumvent spurious priming during gene amplification. *Nucleic Acids Res* *19*, 4008.
- Dorak, M.T. (2006). *Real-time PCR*. Taylor & Francis: New York.
- Du, L., and Richter, J.D. (2005). Activity-dependent polyadenylation in neurons. *RNA* *11*, 1340-1347.
- Eberhart, D.E., Malter, H.E., Feng, Y., and Warren, S.T. (1996). The fragile X mental retardation protein is a ribonucleoprotein containing both nuclear localization and nuclear export signals. *Hum Mol Genet* *5*, 1083-1091.
- Eiberger, J., Kibschull, M., Strenzke, N., Schober, A., Bussow, H., Wessig, C., Djahed, S., Reucher, H., Koch, D.A., Lautermann, J., Moser, T., Winterhager, E., and Willecke, K. (2006). Expression pattern and functional characterization of connexin29 in transgenic mice. *Glia* *53*, 601-611.
- Eid, T., Ghosh, A., Wang, Y., Beckstrom, H., Zaveri, H.P., Lee, T.S., Lai, J.C., Malthankar-Phatak, G.H., and de Lanerolle, N.C. (2008a). Recurrent seizures and brain pathology after inhibition of glutamine synthetase in the hippocampus in rats. *Brain* *131*, 2061-2070.
- Eid, T., Lee, T.S., Thomas, M.J., Amiry-Moghaddam, M., Bjornsen, L.P., Spencer, D.D., Agre, P., Ottersen, O.P., and de Lanerolle, N.C. (2005). Loss of perivascular aquaporin 4 may underlie deficient water and K<sup>+</sup> homeostasis in the human epileptogenic hippocampus. *Proc Natl Acad Sci U S A* *102*, 1193-1198.
- Eid, T., Thomas, M.J., Spencer, D.D., Runden-Pran, E., Lai, J.C., Malthankar, G.V., Kim, J.H., Danbolt, N.C., Ottersen, O.P., and de Lanerolle, N.C. (2004). Loss of glutamine synthetase in the human epileptogenic hippocampus: possible mechanism for raised extracellular glutamate in mesial temporal lobe epilepsy. *Lancet* *363*, 28-37.
- Eid, T., Williamson, A., Lee, T.S., Petroff, O.A., and de Lanerolle, N.C. (2008b). Glutamate and astrocytes--key players in human mesial temporal lobe epilepsy? *Epilepsia* *49 Suppl 2*, 42-52.
- Eng, L.F., Vanderhaeghen, J.J., Bignami, A., and Gerstl, B. (1971). An acidic protein isolated from fibrous astrocytes. *Brain Res* *28*, 351-354.
- Eriksson, P.S., Perfilieva, E., Bjork-Eriksson, T., Alborn, A.M., Nordborg, C., Peterson, D.A., and Gage, F.H. (1998). Neurogenesis in the adult human hippocampus. *Nat Med* *4*, 1313-1317.
- Favaro, R., Valotta, M., Ferri, A.L., Latorre, E., Mariani, J., Giachino, C., Lancini, C., Tosetti, V., Ottolenghi, S., Taylor, V., and Nicolis, S.K. (2009). Hippocampal development and neural stem cell maintenance require Sox2-dependent regulation of Shh. *Nat Neurosci* *12*, 1248-1256.
- Fiacco, T.A., Agulhon, C., Taves, S.R., Petravic, J., Casper, K.B., Dong, X., Chen, J., and McCarthy, K.D. (2007). Selective stimulation of astrocyte calcium in situ does not affect neuronal excitatory synaptic activity. *Neuron* *54*, 611-626.

- Filippov, M.A., Hormuzdi, S.G., Fuchs, E.C., and Monyer, H. (2003). A reporter allele for investigating connexin 26 gene expression in the mouse brain. *Eur J Neurosci* *18*, 3183-3192.
- Fonseca, C.G., Green, C.R., and Nicholson, L.F. (2002). Upregulation in astrocytic connexin 43 gap junction levels may exacerbate generalized seizures in mesial temporal lobe epilepsy. *Brain Res* *929*, 105-116.
- Fukuda, S., Kato, F., Tozuka, Y., Yamaguchi, M., Miyamoto, Y., and Hisatsune, T. (2003). Two distinct subpopulations of nestin-positive cells in adult mouse dentate gyrus. *J Neurosci* *23*, 9357-9366.
- Fushiki, D., Hamada, Y., Yoshimura, R., and Endo, Y. (2010). Phylogenetic and bioinformatic analysis of gap junction-related proteins, innexins, pannexins and connexins. *Biomed Res* *31*, 133-142.
- Gao, X., Kemper, A., and Popko, B. (1999). Advanced transgenic and gene-targeting approaches. *Neurochem Res* *24*, 1181-1188.
- Gebauer, F., and Richter, J.D. (1995). Cloning and characterization of a *Xenopus* poly(A) polymerase. *Mol Cell Biol* *15*, 1422-1430.
- Gebauer, F., and Richter, J.D. (1996). Mouse cytoplasmic polyadenylation element binding protein: an evolutionarily conserved protein that interacts with the cytoplasmic polyadenylation elements of *c-mos* mRNA. *Proc Natl Acad Sci U S A* *93*, 14602-14607.
- Gegelashvili, G., Dehnes, Y., Danbolt, N.C., and Schousboe, A. (2000). The high-affinity glutamate transporters GLT1, GLAST, and EAAT4 are regulated via different signalling mechanisms. *Neurochem Int* *37*, 163-170.
- George, C.H., Kendall, J.M., and Evans, W.H. (1999). Intracellular trafficking pathways in the assembly of connexins into gap junctions. *J Biol Chem* *274*, 8678-8685.
- Giaume, C., Koulakoff, A., Roux, L., Holcman, D., and Rouach, N. (2010). Astroglial networks: a step further in neuroglial and gliovascular interactions. *Nat Rev Neurosci* *11*, 87-99.
- Giaume, C., and Theis, M. (2010). Pharmacological and genetic approaches to study connexin-mediated channels in glial cells of the central nervous system. *Brain Res Rev* *63*, 160-176.
- Giaume, C., and Venance, L. (1998). Intercellular calcium signaling and gap junctional communication in astrocytes. *Glia* *24*, 50-64.
- Giepmans, B.N., Verlaan, I., Hengeveld, T., Janssen, H., Calafat, J., Falk, M.M., and Moolenaar, W.H. (2001). Gap junction protein connexin-43 interacts directly with microtubules. *Curr Biol* *11*, 1364-1368.
- Gingras, A.C., Raught, B., and Sonenberg, N. (2001). Regulation of translation initiation by FRAP/mTOR. *Genes Dev* *15*, 807-826.

- Gingrich, J.R., and Roder, J. (1998). Inducible gene expression in the nervous system of transgenic mice. *Annu Rev Neurosci* 21, 377-405.
- Glass, M., and Dragunow, M. (1995). Neurochemical and morphological changes associated with human epilepsy. *Brain Res Brain Res Rev* 21, 29-41.
- Goldshmit, Y., Galea, M.P., Bartlett, P.F., and Turnley, A.M. (2006). EphA4 regulates central nervous system vascular formation. *J Comp Neurol* 497, 864-875.
- Gordon, G.R., Mulligan, S.J., and MacVicar, B.A. (2007). Astrocyte control of the cerebrovasculature. *Glia* 55, 1214-1221.
- Gosejacob, D., Dublin, P., Bedner, P., Huttmann, K., Zhang, J., Tress, O., Willecke, K., Pfrieger, F., Steinhauser, C., and Theis, M. (2011). Role of astroglial connexin30 in hippocampal gap junction coupling. *Glia* 59, 511-519.
- Gossen, M., and Bujard, H. (1992). Tight control of gene expression in mammalian cells by tetracycline-responsive promoters. *Proc Natl Acad Sci U S A* 89, 5547-5551.
- Gossen, M., Freundlieb, S., Bender, G., Muller, G., Hillen, W., and Bujard, H. (1995). Transcriptional activation by tetracyclines in mammalian cells. *Science* 268, 1766-1769.
- Gould, E. (2007). How widespread is adult neurogenesis in mammals? *Nat Rev Neurosci* 8, 481-488.
- Groisman, I., Huang, Y.S., Mendez, R., Cao, Q., and Richter, J.D. (2001). Translational control of embryonic cell division by CPEB and maskin. *Cold Spring Harb Symp Quant Biol* 66, 345-351.
- Groisman, I., Huang, Y.S., Mendez, R., Cao, Q., Theurkauf, W., and Richter, J.D. (2000). CPEB, maskin, and cyclin B1 mRNA at the mitotic apparatus: implications for local translational control of cell division. *Cell* 103, 435-447.
- Groisman, I., Ivshina, M., Marin, V., Kennedy, N.J., Davis, R.J., and Richter, J.D. (2006). Control of cellular senescence by CPEB. *Genes Dev* 20, 2701-2712.
- Groisman, I., Jung, M.Y., Sarkissian, M., Cao, Q., and Richter, J.D. (2002). Translational control of the embryonic cell cycle. *Cell* 109, 473-483.
- Guthrie, P.B., Knappenberger, J., Segal, M., Bennett, M.V., Charles, A.C., and Kater, S.B. (1999). ATP released from astrocytes mediates glial calcium waves. *J Neurosci* 19, 520-528.
- Hagele, S., Kuhn, U., Boning, M., and Katschinski, D.M. (2009). Cytoplasmic polyadenylation-element-binding protein (CPEB)1 and 2 bind to the HIF-1alpha mRNA 3'-UTR and modulate HIF-1alpha protein expression. *Biochem J* 417, 235-246.
- Hake, L.E., Mendez, R., and Richter, J.D. (1998). Specificity of RNA binding by CPEB: requirement for RNA recognition motifs and a novel zinc finger. *Mol Cell Biol* 18, 685-693.
- Hake, L.E., and Richter, J.D. (1994). CPEB is a specificity factor that mediates cytoplasmic polyadenylation during *Xenopus* oocyte maturation. *Cell* 79, 617-627.

- Halassa, M.M., Fellin, T., and Haydon, P.G. (2007). The tripartite synapse: roles for gliotransmission in health and disease. *Trends Mol Med* 13, 54-63.
- Hertz, L., and Zielke, H.R. (2004). Astrocytic control of glutamatergic activity: astrocytes as stars of the show. *Trends Neurosci* 27, 735-743.
- Higashi, K., Fujita, A., Inanobe, A., Tanemoto, M., Doi, K., Kubo, T., and Kurachi, Y. (2001). An inwardly rectifying K(+) channel, Kir4.1, expressed in astrocytes surrounds synapses and blood vessels in brain. *Am J Physiol Cell Physiol* 281, C922-931.
- Hombach, S., Janssen-Bienhold, U., Sohl, G., Schubert, T., Bussow, H., Ott, T., Weiler, R., and Willecke, K. (2004). Functional expression of connexin57 in horizontal cells of the mouse retina. *Eur J Neurosci* 19, 2633-2640.
- Hosoda, N., Funakoshi, Y., Hirasawa, M., Yamagishi, R., Asano, Y., Miyagawa, R., Ogami, K., Tsujimoto, M., and Hoshino, S. (2011). Anti-proliferative protein Tob negatively regulates CPEB3 target by recruiting Caf1 deadenylase. *EMBO J* 30, 1311-1323.
- Houades, V., Koulakoff, A., Ezan, P., Seif, I., and Giaume, C. (2008). Gap junction-mediated astrocytic networks in the mouse barrel cortex. *J Neurosci* 28, 5207-5217.
- Huang, Y.S., Carson, J.H., Barbarese, E., and Richter, J.D. (2003). Facilitation of dendritic mRNA transport by CPEB. *Genes Dev* 17, 638-653.
- Huang, Y.S., Jung, M.Y., Sarkissian, M., and Richter, J.D. (2002). N-methyl-D-aspartate receptor signaling results in Aurora kinase-catalyzed CPEB phosphorylation and alpha CaMKII mRNA polyadenylation at synapses. *EMBO J* 21, 2139-2148.
- Huang, Y.S., Kan, M.C., Lin, C.L., and Richter, J.D. (2006). CPEB3 and CPEB4 in neurons: analysis of RNA-binding specificity and translational control of AMPA receptor GluR2 mRNA. *EMBO J* 25, 4865-4876.
- Huber, K.M., Gallagher, S.M., Warren, S.T., and Bear, M.F. (2002). Altered synaptic plasticity in a mouse model of fragile X mental retardation. *Proc Natl Acad Sci U S A* 99, 7746-7750.
- Huttelmaier, S., Zenklusen, D., Lederer, M., Dichtenberg, J., Lorenz, M., Meng, X., Bassell, G.J., Condeelis, J., and Singer, R.H. (2005). Spatial regulation of beta-actin translation by Src-dependent phosphorylation of ZBP1. *Nature* 438, 512-515.
- Huttmann, K., Sadgrove, M., Wallraff, A., Hinterkeuser, S., Kirchhoff, F., Steinhäuser, C., and Gray, W.P. (2003). Seizures preferentially stimulate proliferation of radial glia-like astrocytes in the adult dentate gyrus: functional and immunocytochemical analysis. *Eur J Neurosci* 18, 2769-2778.
- Iglesias, R., Dahl, G., Qiu, F., Spray, D.C., and Scemes, E. (2009). Pannexin 1: the molecular substrate of astrocyte "hemichannels". *J Neurosci* 29, 7092-7097.

- Jones, K.J., Korb, E., Kundel, M.A., Kochanek, A.R., Kabraji, S., McEvoy, M., Shin, C.Y., and Wells, D.G. (2008). CPEB1 regulates beta-catenin mRNA translation and cell migration in astrocytes. *Glia* 56, 1401-1413.
- Jordan, K., Solan, J.L., Dominguez, M., Sia, M., Hand, A., Lampe, P.D., and Laird, D.W. (1999). Trafficking, assembly, and function of a connexin43-green fluorescent protein chimera in live mammalian cells. *Mol Biol Cell* 10, 2033-2050.
- Jung, M.Y., Lorenz, L., and Richter, J.D. (2006). Translational control by neuroguidin, a eukaryotic initiation factor 4E and CPEB binding protein. *Mol Cell Biol* 26, 4277-4287.
- Karram, K., Goebbels, S., Schwab, M., Jennissen, K., Seifert, G., Steinhauser, C., Nave, K.A., and Trotter, J. (2008). NG2-expressing cells in the nervous system revealed by the NG2-EYFP-knockin mouse. *Genesis* 46, 743-757.
- Kempermann, G., Jessberger, S., Steiner, B., and Kronenberg, G. (2004). Milestones of neuronal development in the adult hippocampus. *Trends Neurosci* 27, 447-452.
- Kiebler, M.A., Jansen, R.P., Dahm, R., and Macchi, P. (2005). A putative nuclear function for mammalian Staufen. *Trends Biochem Sci* 30, 228-231.
- Kim, K.C., Oh, W.J., Ko, K.H., Shin, C.Y., and Wells, D.G. (2011). Cyclin B1 expression regulated by cytoplasmic polyadenylation element binding protein in astrocytes. *J Neurosci* 31, 12118-12128.
- Kimelberg, H.K., Biddlecome, S., and Bourke, R.S. (1979). SITS-inhibitable Cl<sup>-</sup> transport and Na<sup>+</sup>-dependent H<sup>+</sup> production in primary astroglial cultures. *Brain Res* 173, 111-124.
- Kimelberg, H.K., and Nedergaard, M. (2010). Functions of astrocytes and their potential as therapeutic targets. *Neurotherapeutics* 7, 338-353.
- Kobayashi, Y., Watanabe, M., Okada, Y., Sawa, H., Takai, H., Nakanishi, M., Kawase, Y., Suzuki, H., Nagashima, K., Ikeda, K., and Motoyama, N. (2002). Hydrocephalus, situs inversus, chronic sinusitis, and male infertility in DNA polymerase lambda-deficient mice: possible implication for the pathogenesis of immotile cilia syndrome. *Mol Cell Biol* 22, 2769-2776.
- Koh, L., Zakharov, A., and Johnston, M. (2005). Integration of the subarachnoid space and lymphatics: is it time to embrace a new concept of cerebrospinal fluid absorption? *Cerebrospinal Fluid Res* 2, 6.
- Kohan, D.E. (2008). Progress in gene targeting: using mutant mice to study renal function and disease. *Kidney Int* 74, 427-437.
- Koval, M., Harley, J.E., Hick, E., and Steinberg, T.H. (1997). Connexin46 is retained as monomers in a trans-Golgi compartment of osteoblastic cells. *J Cell Biol* 137, 847-857.
- Kucheryavykh, Y.V., Kucheryavykh, L.Y., Nichols, C.G., Maldonado, H.M., Baksi, K., Reichenbach, A., Skatchkov, S.N., and Eaton, M.J. (2007). Downregulation of Kir4.1 inward

rectifying potassium channel subunits by RNAi impairs potassium transfer and glutamate uptake by cultured cortical astrocytes. *Glia* 55, 274-281.

Kumar, N.M., and Gilula, N.B. (1996). The gap junction communication channel. *Cell* 84, 381-388.

Kunze, A., Congreso, M.R., Hartmann, C., Wallraff-Beck, A., Huttmann, K., Bedner, P., Requardt, R., Seifert, G., Redecker, C., Willecke, K., Hofmann, A., Pfeifer, A., Theis, M., and Steinhauser, C. (2009). Connexin expression by radial glia-like cells is required for neurogenesis in the adult dentate gyrus. *Proc Natl Acad Sci U S A* 106, 11336-11341.

Kunzelmann, P., Schroder, W., Traub, O., Steinhauser, C., Dermietzel, R., and Willecke, K. (1999). Late onset and increasing expression of the gap junction protein connexin30 in adult murine brain and long-term cultured astrocytes. *Glia* 25, 111-119.

Kurihara, Y., Tokuriki, M., Myojin, R., Hori, T., Kuroiwa, A., Matsuda, Y., Sakurai, T., Kimura, M., Hecht, N.B., and Uesugi, S. (2003). CPEB2, a novel putative translational regulator in mouse haploid germ cells. *Biol Reprod* 69, 261-268.

Laird, P.W., Zijderveld, A., Linders, K., Rudnicki, M.A., Jaenisch, R., and Berns, A. (1991). Simplified mammalian DNA isolation procedure. *Nucleic Acids Res* 19, 4293.

Langer, J., Stephan, J., Theis, M., and Rose, C.R. (2012). Gap junctions mediate intercellular spread of sodium between hippocampal astrocytes in situ. *Glia* 60, 239-252.

Larsen, W.J. (1977). Structural diversity of gap junctions. A review. *Tissue Cell* 9, 373-394.

Lauf, U., Giepmans, B.N., Lopez, P., Braconnot, S., Chen, S.C., and Falk, M.M. (2002). Dynamic trafficking and delivery of connexons to the plasma membrane and accretion to gap junctions in living cells. *Proc Natl Acad Sci U S A* 99, 10446-10451.

Lehre, K.P., and Danbolt, N.C. (1998). The number of glutamate transporter subtype molecules at glutamatergic synapses: chemical and stereological quantification in young adult rat brain. *J Neurosci* 18, 8751-8757.

Lehre, K.P., Levy, L.M., Ottersen, O.P., Storm-Mathisen, J., and Danbolt, N.C. (1995). Differential expression of two glial glutamate transporters in the rat brain: quantitative and immunocytochemical observations. *J Neurosci* 15, 1835-1853.

Levi, G., Wilkin, G.P., Ciotti, M.T., and Johnstone, S. (1983). Enrichment of differentiated, stellate astrocytes in cerebellar interneuron cultures as studied by GFAP immunofluorescence and autoradiographic uptake patterns with [3H]D-aspartate and [3H]GABA. *Brain Res* 312, 227-241.

Liang, S.L., Carlson, G.C., and Coulter, D.A. (2006). Dynamic regulation of synaptic GABA release by the glutamate-glutamine cycle in hippocampal area CA1. *J Neurosci* 26, 8537-8548.



- Lie, D.C., Colamarino, S.A., Song, H.J., Desire, L., Mira, H., Consiglio, A., Lein, E.S., Jessberger, S., Lansford, H., Dearie, A.R., and Gage, F.H. (2005). Wnt signalling regulates adult hippocampal neurogenesis. *Nature* *437*, 1370-1375.
- Magnotti, L.M., Goodenough, D.A., and Paul, D.L. (2011). Functional heterotypic interactions between astrocyte and oligodendrocyte connexins. *Glia* *59*, 26-34.
- Martin, P.E., Errington, R.J., and Evans, W.H. (2001). Gap junction assembly: multiple connexin fluorophores identify complex trafficking pathways. *Cell Commun Adhes* *8*, 243-248.
- Martinez-Hernandez, A., Bell, K.P., and Norenberg, M.D. (1977). Glutamine synthetase: glial localization in brain. *Science* *195*, 1356-1358.
- Mathern, G.W., Mendoza, D., Lozada, A., Pretorius, J.K., Dehnes, Y., Danbolt, N.C., Nelson, N., Leite, J.P., Chimelli, L., Born, D.E., Sakamoto, A.C., Assirati, J.A., Fried, I., Peacock, W.J., Ojemann, G.A., and Adelson, P.D. (1999). Hippocampal GABA and glutamate transporter immunoreactivity in patients with temporal lobe epilepsy. *Neurology* *52*, 453-472.
- Maxeiner, S., Kruger, O., Schilling, K., Traub, O., Urschel, S., and Willecke, K. (2003). Spatiotemporal transcription of connexin45 during brain development results in neuronal expression in adult mice. *Neuroscience* *119*, 689-700.
- Mayford, M., Bach, M.E., Huang, Y.Y., Wang, L., Hawkins, R.D., and Kandel, E.R. (1996). Control of memory formation through regulated expression of a CaMKII transgene. *Science* *274*, 1678-1683.
- McCarthy, K.D., and de Vellis, J. (1980). Preparation of separate astroglial and oligodendroglial cell cultures from rat cerebral tissue. *J Cell Biol* *85*, 890-902.
- McGrew, L.L., and Richter, J.D. (1990). Translational control by cytoplasmic polyadenylation during *Xenopus* oocyte maturation: characterization of cis and trans elements and regulation by cyclin/MPF. *EMBO J* *9*, 3743-3751.
- Mendez, R., Hake, L.E., Andresson, T., Littlepage, L.E., Ruderman, J.V., and Richter, J.D. (2000a). Phosphorylation of CPE binding factor by Eg2 regulates translation of c-mos mRNA. *Nature* *404*, 302-307.
- Mendez, R., Murthy, K.G., Ryan, K., Manley, J.L., and Richter, J.D. (2000b). Phosphorylation of CPEB by Eg2 mediates the recruitment of CPSF into an active cytoplasmic polyadenylation complex. *Mol Cell* *6*, 1253-1259.
- Mendez, R., and Richter, J.D. (2001). Translational control by CPEB: a means to the end. *Nat Rev Mol Cell Biol* *2*, 521-529.
- Mercier, F., and Hatton, G.I. (2001). Connexin 26 and basic fibroblast growth factor are expressed primarily in the subpial and subependymal layers in adult brain parenchyma: roles in stem cell proliferation and morphological plasticity? *J Comp Neurol* *431*, 88-104.

- Morgan, M., Iaconcig, A., and Muro, A.F. (2010). CPEB2, CPEB3 and CPEB4 are coordinately regulated by miRNAs recognizing conserved binding sites in paralog positions of their 3'-UTRs. *Nucleic Acids Res* *38*, 7698-7710.
- Morrens, J., Van Den Broeck, W., and Kempermann, G. (2011). Glial cells in adult neurogenesis. *Glia*.
- Musil, L.S., and Goodenough, D.A. (1991). Biochemical analysis of connexin43 intracellular transport, phosphorylation, and assembly into gap junctional plaques. *J Cell Biol* *115*, 1357-1374.
- Nagy, J.I., Dudek, F.E., and Rash, J.E. (2004). Update on connexins and gap junctions in neurons and glia in the mammalian nervous system. *Brain Res Brain Res Rev* *47*, 191-215.
- Nagy, J.I., Ionescu, A.V., Lynn, B.D., and Rash, J.E. (2003). Coupling of astrocyte connexins Cx26, Cx30, Cx43 to oligodendrocyte Cx29, Cx32, Cx47: Implications from normal and connexin32 knockout mice. *Glia* *44*, 205-218.
- Nagy, J.I., Lynn, B.D., Tress, O., Willecke, K., and Rash, J.E. (2011). Connexin26 expression in brain parenchymal cells demonstrated by targeted connexin ablation in transgenic mice. *Eur J Neurosci* *34*, 263-271.
- Nagy, J.I., and Rash, J.E. (2003). Astrocyte and oligodendrocyte connexins of the glial syncytium in relation to astrocyte anatomical domains and spatial buffering. *Cell Commun Adhes* *10*, 401-406.
- Nakase, T., Sohl, G., Theis, M., Willecke, K., and Naus, C.C. (2004). Increased apoptosis and inflammation after focal brain ischemia in mice lacking connexin43 in astrocytes. *Am J Pathol* *164*, 2067-2075.
- Naus, C.C., Bechberger, J.F., and Paul, D.L. (1991). Gap junction gene expression in human seizure disorder. *Exp Neurol* *111*, 198-203.
- Naus, C.C., Bechberger, J.F., Zhang, Y., Venance, L., Yamasaki, H., Juneja, S.C., Kidder, G.M., and Giaume, C. (1997). Altered gap junctional communication, intercellular signaling, and growth in cultured astrocytes deficient in connexin43. *J Neurosci Res* *49*, 528-540.
- Nedergaard, M., Ransom, B., and Goldman, S.A. (2003). New roles for astrocytes: redefining the functional architecture of the brain. *Trends Neurosci* *26*, 523-530.
- Nielsen, S., Nagelhus, E.A., Amiry-Moghaddam, M., Bourque, C., Agre, P., and Ottersen, O.P. (1997). Specialized membrane domains for water transport in glial cells: high-resolution immunogold cytochemistry of aquaporin-4 in rat brain. *J Neurosci* *17*, 171-180.
- Ninkovic, J., and Gotz, M. (2007). Signaling in adult neurogenesis: from stem cell niche to neuronal networks. *Curr Opin Neurobiol* *17*, 338-344.
- Nishiyama, A., Komitova, M., Suzuki, R., and Zhu, X. (2009). Polydendrocytes (NG2 cells): multifunctional cells with lineage plasticity. *Nat Rev Neurosci* *10*, 9-22.

- Nishiyama, A., Yang, Z., and Butt, A. (2005). Astrocytes and NG2-glia: what's in a name? *J Anat* 207, 687-693.
- Novoa, I., Gallego, J., Ferreira, P.G., and Mendez, R. (2010). Mitotic cell-cycle progression is regulated by CPEB1 and CPEB4-dependent translational control. *Nat Cell Biol* 12, 447-456.
- Oberheim, N.A., Takano, T., Han, X., He, W., Lin, J.H., Wang, F., Xu, Q., Wyatt, J.D., Pilcher, W., Ojemann, J.G., Ransom, B.R., Goldman, S.A., and Nedergaard, M. (2009). Uniquely hominid features of adult human astrocytes. *J Neurosci* 29, 3276-3287.
- Odermatt, B., Wellershaus, K., Wallraff, A., Seifert, G., Degen, J., Euwens, C., Fuss, B., Bussow, H., Schilling, K., Steinhauser, C., and Willecke, K. (2003). Connexin 47 (Cx47)-deficient mice with enhanced green fluorescent protein reporter gene reveal predominant oligodendrocytic expression of Cx47 and display vacuolized myelin in the CNS. *J Neurosci* 23, 4549-4559.
- Ohtoshi, A. (2008). Hydrocephalus caused by conditional ablation of the Pten or beta-catenin gene. *Cerebrospinal Fluid Res* 5, 16.
- Olsen, M.L., and Sontheimer, H. (2008). Functional implications for Kir4.1 channels in glial biology: from K<sup>+</sup> buffering to cell differentiation. *J Neurochem* 107, 589-601.
- Orellana, J.A., Saez, P.J., Cortes-Campos, C., Elizondo, R.J., Shoji, K.F., Contreras-Duarte, S., Figueroa, V., Velarde, V., Jiang, J.X., Nualart, F., Saez, J.C., and Garcia, M.A. (2012). Glucose increases intracellular free Ca<sup>2+</sup> in tanycytes via ATP released through connexin 43 hemichannels. *Glia* 60, 53-68.
- Orellana, J.A., Saez, P.J., Shoji, K.F., Schalper, K.A., Palacios-Prado, N., Velarde, V., Giaume, C., Bennett, M.V., and Saez, J.C. (2009). Modulation of brain hemichannels and gap junction channels by pro-inflammatory agents and their possible role in neurodegeneration. *Antioxid Redox Signal* 11, 369-399.
- Orkand, R.K. (1986). Glial-interstitial fluid exchange. *Ann N Y Acad Sci* 481, 269-272.
- Orkand, R.K., Nicholls, J.G., and Kuffler, S.W. (1966). Effect of nerve impulses on the membrane potential of glial cells in the central nervous system of amphibia. *J Neurophysiol* 29, 788-806.
- Pannasch, U., Vargova, L., Reingruber, J., Ezan, P., Holcman, D., Giaume, C., Sykova, E., and Rouach, N. (2011). Astroglial networks scale synaptic activity and plasticity. *Proc Natl Acad Sci U S A* 108, 8467-8472.
- Papageorgiou, I.E., Gabriel, S., Fetani, A.F., Kann, O., and Heinemann, U. (2011). Redistribution of astrocytic glutamine synthetase in the hippocampus of chronic epileptic rats. *Glia* 59, 1706-1718.
- Pascual, O., Casper, K.B., Kubera, C., Zhang, J., Revilla-Sanchez, R., Sul, J.Y., Takano, H., Moss, S.J., McCarthy, K., and Haydon, P.G. (2005). Astrocytic purinergic signaling coordinates synaptic networks. *Science* 310, 113-116.

- Pasquale, E.B. (2008). Eph-ephrin bidirectional signaling in physiology and disease. *Cell* *133*, 38-52.
- Pellerin, L., and Magistretti, P.J. (1996). Excitatory amino acids stimulate aerobic glycolysis in astrocytes via an activation of the Na<sup>+</sup>/K<sup>+</sup> ATPase. *Dev Neurosci* *18*, 336-342.
- Perea, G., Navarrete, M., and Araque, A. (2009). Tripartite synapses: astrocytes process and control synaptic information. *Trends Neurosci* *32*, 421-431.
- Peters, A., Palay, S.L., and Webster, H.D. (1991). The fine structure of the nervous system. New York: Oxford University Press.
- Petito, C.K., Chung, M.C., Verkhovsky, L.M., and Cooper, A.J. (1992). Brain glutamine synthetase increases following cerebral ischemia in the rat. *Brain Res* *569*, 275-280.
- Pique, M., Lopez, J.M., Foissac, S., Guigo, R., and Mendez, R. (2008). A combinatorial code for CPE-mediated translational control. *Cell* *132*, 434-448.
- Polito, A., and Reynolds, R. (2005). NG2-expressing cells as oligodendrocyte progenitors in the normal and demyelinated adult central nervous system. *J Anat* *207*, 707-716.
- Proper, E.A., Hoogland, G., Kappen, S.M., Jansen, G.H., Rensen, M.G., Schrama, L.H., van Veelen, C.W., van Rijen, P.C., van Nieuwenhuizen, O., Gispen, W.H., and de Graan, P.N. (2002). Distribution of glutamate transporters in the hippocampus of patients with pharmacoresistant temporal lobe epilepsy. *Brain* *125*, 32-43.
- Rasband, W.S. (1997-2011). ImageJ, U. S. National Institutes of Health, Bethesda, Maryland, USA, <http://imagej.nih.gov/ij/>.
- Reaume, A.G., de Sousa, P.A., Kulkarni, S., Langille, B.L., Zhu, D., Davies, T.C., Juneja, S.C., Kidder, G.M., and Rossant, J. (1995). Cardiac malformation in neonatal mice lacking connexin43. *Science* *267*, 1831-1834.
- Retamal, M.A., Froger, N., Palacios-Prado, N., Ezan, P., Saez, P.J., Saez, J.C., and Giaume, C. (2007). Cx43 hemichannels and gap junction channels in astrocytes are regulated oppositely by proinflammatory cytokines released from activated microglia. *J Neurosci* *27*, 13781-13792.
- Richter, J.D. (2007). CPEB: a life in translation. *Trends Biochem Sci* *32*, 279-285.
- Richter, J.D., and Lorenz, L.J. (2002). Selective translation of mRNAs at synapses. *Curr Opin Neurobiol* *12*, 300-304.
- Robinson, S.R. (2001). Changes in the cellular distribution of glutamine synthetase in Alzheimer's disease. *J Neurosci Res* *66*, 972-980.
- Rosier, F., Lambert, D., and Mertens-Strijthagen, M. (1996). Effect of glucose deprivation on rat glutamine synthetase in cultured astrocytes. *Biochem J* *315* ( Pt 2), 607-612.

- Rothstein, J.D., Dykes-Hoberg, M., Pardo, C.A., Bristol, L.A., Jin, L., Kuncl, R.W., Kanai, Y., Hediger, M.A., Wang, Y., Schielke, J.P., and Welty, D.F. (1996). Knockout of glutamate transporters reveals a major role for astroglial transport in excitotoxicity and clearance of glutamate. *Neuron* 16, 675-686.
- Rothstein, J.D., Martin, L., Levey, A.I., Dykes-Hoberg, M., Jin, L., Wu, D., Nash, N., and Kuncl, R.W. (1994). Localization of neuronal and glial glutamate transporters. *Neuron* 13, 713-725.
- Rouach, N., Koulakoff, A., Abudara, V., Willecke, K., and Giaume, C. (2008). Astroglial metabolic networks sustain hippocampal synaptic transmission. *Science* 322, 1551-1555.
- Roux, K.H. (1995). Optimization and troubleshooting in PCR. *PCR Methods Appl* 4, S185-194.
- Saez, J.C., Schalper, K.A., Retamal, M.A., Orellana, J.A., Shoji, K.F., and Bennett, M.V. (2010). Cell membrane permeabilization via connexin hemichannels in living and dying cells. *Exp Cell Res* 316, 2377-2389.
- Sambrook, J., and Russell, D.W. (2001). *Molecular cloning : a laboratory manual*. Cold Spring Harbor Laboratory Press: Cold Spring Harbor, N.Y.
- Sarac, S., Afzal, S., Broholm, H., Madsen, F.F., Ploug, T., and Laursen, H. (2009). Excitatory amino acid transporters EAAT-1 and EAAT-2 in temporal lobe and hippocampus in intractable temporal lobe epilepsy. *APMIS* 117, 291-301.
- Scemes, E., Spray, D.C., and Meda, P. (2009). Connexins, pannexins, innexins: novel roles of "hemi-channels". *Pflugers Arch* 457, 1207-1226.
- Scemes, E., Suadicani, S.O., Dahl, G., and Spray, D.C. (2007). Connexin and pannexin mediated cell-cell communication. *Neuron Glia Biol* 3, 199-208.
- Schmechel, D.E., and Rakic, P. (1979). A Golgi study of radial glial cells in developing monkey telencephalon: morphogenesis and transformation into astrocytes. *Anat Embryol (Berl)* 156, 115-152.
- Schousboe, A. (2003). Role of astrocytes in the maintenance and modulation of glutamatergic and GABAergic neurotransmission. *Neurochem Res* 28, 347-352.
- Schousboe, A., Svenneby, G., and Hertz, L. (1977). Uptake and metabolism of glutamate in astrocytes cultured from dissociated mouse brain hemispheres. *J Neurochem* 29, 999-1005.
- Seifert, G., Carmignoto, G., and Steinhauser, C. (2010). Astrocyte dysfunction in epilepsy. *Brain Res Rev* 63, 212-221.
- Seifert, G., Huttmann, K., Binder, D.K., Hartmann, C., Wyczynski, A., Neusch, C., and Steinhauser, C. (2009). Analysis of astroglial K<sup>+</sup> channel expression in the developing hippocampus reveals a predominant role of the Kir4.1 subunit. *J Neurosci* 29, 7474-7488.
- Seifert, G., Schilling, K., and Steinhauser, C. (2006). Astrocyte dysfunction in neurological disorders: a molecular perspective. *Nat Rev Neurosci* 7, 194-206.

- Seifert, G., and Steinhauser, C. (2011). Neuron-astrocyte signaling and epilepsy. *Exp Neurol*.
- Shan, J., Munro, T.P., Barbarese, E., Carson, J.H., and Smith, R. (2003). A molecular mechanism for mRNA trafficking in neuronal dendrites. *J Neurosci* 23, 8859-8866.
- Shaw, R.M., Fay, A.J., Puthenveedu, M.A., von Zastrow, M., Jan, Y.N., and Jan, L.Y. (2007). Microtubule plus-end-tracking proteins target gap junctions directly from the cell interior to adherens junctions. *Cell* 128, 547-560.
- Sheldon, A.L., and Robinson, M.B. (2007). The role of glutamate transporters in neurodegenerative diseases and potential opportunities for intervention. *Neurochem Int* 51, 333-355.
- Sher, P.K., and Hu, S.X. (1990). Increased glutamate uptake and glutamine synthetase activity in neuronal cell cultures surviving chronic hypoxia. *Glia* 3, 350-357.
- Shestopalov, V.I., and Panchin, Y. (2008). Pannexins and gap junction protein diversity. *Cell Mol Life Sci* 65, 376-394.
- Shigeri, Y., Seal, R.P., and Shimamoto, K. (2004). Molecular pharmacology of glutamate transporters, EAATs and VGLUTs. *Brain Res Brain Res Rev* 45, 250-265.
- Shin, C.Y., Kundel, M., and Wells, D.G. (2004). Rapid, activity-induced increase in tissue plasminogen activator is mediated by metabotropic glutamate receptor-dependent mRNA translation. *J Neurosci* 24, 9425-9433.
- Simek, J., Churko, J., Shao, Q., and Laird, D.W. (2009). Cx43 has distinct mobility within plasma-membrane domains, indicative of progressive formation of gap-junction plaques. *J Cell Sci* 122, 554-562.
- Smithies, O. (1993). Animal models of human genetic diseases. *Trends Genet* 9, 112-116.
- Sohl, G., Maxeiner, S., and Willecke, K. (2005). Expression and functions of neuronal gap junctions. *Nat Rev Neurosci* 6, 191-200.
- Sohl, G., Odermatt, B., Maxeiner, S., Degen, J., and Willecke, K. (2004). New insights into the expression and function of neural connexins with transgenic mouse mutants. *Brain Res Brain Res Rev* 47, 245-259.
- Sohl, G., and Willecke, K. (2003). An update on connexin genes and their nomenclature in mouse and man. *Cell Commun Adhes* 10, 173-180.
- Song, H.J., Stevens, C.F., and Gage, F.H. (2002). Neural stem cells from adult hippocampus develop essential properties of functional CNS neurons. *Nat Neurosci* 5, 438-445.
- Spray, D.C., Ye, Z.C., and Ransom, B.R. (2006). Functional connexin "hemichannels": a critical appraisal. *Glia* 54, 758-773.
- Stebbins-Boaz, B., Cao, Q., de Moor, C.H., Mendez, R., and Richter, J.D. (1999). Maskin is a CPEB-associated factor that transiently interacts with eIF-4E. *Mol Cell* 4, 1017-1027.

- Stebbins-Boaz, B., Hake, L.E., and Richter, J.D. (1996). CPEB controls the cytoplasmic polyadenylation of cyclin, Cdk2 and c-mos mRNAs and is necessary for oocyte maturation in *Xenopus*. *EMBO J* 15, 2582-2592.
- Steinhauser, C., and Seifert, G. (2002). Glial membrane channels and receptors in epilepsy: impact for generation and spread of seizure activity. *Eur J Pharmacol* 447, 227-237.
- Steward, O., and Schuman, E.M. (2003). Compartmentalized synthesis and degradation of proteins in neurons. *Neuron* 40, 347-359.
- Suarez, I., Bodega, G., and Fernandez, B. (2002). Glutamine synthetase in brain: effect of ammonia. *Neurochem Int* 41, 123-142.
- Sun, Y., Chen, X., and Xiao, D. (2007). Tetracycline-inducible expression systems: new strategies and practices in the transgenic mouse modeling. *Acta Biochim Biophys Sin (Shanghai)* 39, 235-246.
- Sutor, B., and Hagerty, T. (2005). Involvement of gap junctions in the development of the neocortex. *Biochim Biophys Acta* 1719, 59-68.
- Takano, T., Tian, G.F., Peng, W., Lou, N., Libionka, W., Han, X., and Nedergaard, M. (2006). Astrocyte-mediated control of cerebral blood flow. *Nat Neurosci* 9, 260-267.
- Tan, L., Chang, J.S., Costa, A., and Schedl, P. (2001). An autoregulatory feedback loop directs the localized expression of the *Drosophila* CPEB protein Orb in the developing oocyte. *Development* 128, 1159-1169.
- Tanaka, K., Watase, K., Manabe, T., Yamada, K., Watanabe, M., Takahashi, K., Iwama, H., Nishikawa, T., Ichihara, N., Kikuchi, T., Okuyama, S., Kawashima, N., Hori, S., Takimoto, M., and Wada, K. (1997). Epilepsy and exacerbation of brain injury in mice lacking the glutamate transporter GLT-1. *Science* 276, 1699-1702.
- Tani, H., Dulla, C.G., Huguenard, J.R., and Reimer, R.J. (2010). Glutamine is required for persistent epileptiform activity in the disinhibited neocortical brain slice. *J Neurosci* 30, 1288-1300.
- Tansey, F.A., Farooq, M., and Cammer, W. (1991). Glutamine synthetase in oligodendrocytes and astrocytes: new biochemical and immunocytochemical evidence. *J Neurochem* 56, 266-272.
- Tay, J., Hodgman, R., Sarkissian, M., and Richter, J.D. (2003). Regulated CPEB phosphorylation during meiotic progression suggests a mechanism for temporal control of maternal mRNA translation. *Genes Dev* 17, 1457-1462.
- Tay, J., and Richter, J.D. (2001). Germ cell differentiation and synaptonemal complex formation are disrupted in CPEB knockout mice. *Dev Cell* 1, 201-213.
- Tessler, S., Danbolt, N.C., Faull, R.L., Storm-Mathisen, J., and Emson, P.C. (1999). Expression of the glutamate transporters in human temporal lobe epilepsy. *Neuroscience* 88, 1083-1091.

- Teubner, B., Michel, V., Pesch, J., Lautermann, J., Cohen-Salmon, M., Sohl, G., Jahnke, K., Winterhager, E., Herberhold, C., Hardelin, J.P., Petit, C., and Willecke, K. (2003). Connexin30 (Gjb6)-deficiency causes severe hearing impairment and lack of endocochlear potential. *Hum Mol Genet* *12*, 13-21.
- Theis, M., Jauch, R., Zhuo, L., Speidel, D., Wallraff, A., Doring, B., Frisch, C., Sohl, G., Teubner, B., Euwens, C., Huston, J., Steinhauser, C., Messing, A., Heinemann, U., and Willecke, K. (2003a). Accelerated hippocampal spreading depression and enhanced locomotory activity in mice with astrocyte-directed inactivation of connexin43. *J Neurosci* *23*, 766-776.
- Theis, M., Si, K., and Kandel, E.R. (2003b). Two previously undescribed members of the mouse CPEB family of genes and their inducible expression in the principal cell layers of the hippocampus. *Proc Natl Acad Sci U S A* *100*, 9602-9607.
- Theis, M., Sohl, G., Eiberger, J., and Willecke, K. (2005). Emerging complexities in identity and function of glial connexins. *Trends Neurosci* *28*, 188-195.
- Theis, M., Sohl, G., Speidel, D., Kuhn, R., and Willecke, K. (2003c). Connexin43 is not expressed in principal cells of mouse cortex and hippocampus. *Eur J Neurosci* *18*, 267-274.
- Theis, M., Speidel, D., and Willecke, K. (2004). Astrocyte cultures from conditional connexin43-deficient mice. *Glia* *46*, 130-141.
- van der Hel, W.S., Notenboom, R.G., Bos, I.W., van Rijen, P.C., van Veelen, C.W., and de Graan, P.N. (2005). Reduced glutamine synthetase in hippocampal areas with neuron loss in temporal lobe epilepsy. *Neurology* *64*, 326-333.
- Venance, L., Rozov, A., Blatow, M., Burnashev, N., Feldmeyer, D., and Monyer, H. (2000). Connexin expression in electrically coupled postnatal rat brain neurons. *Proc Natl Acad Sci U S A* *97*, 10260-10265.
- Verkhratsky, A., and Butt, A. (2007). *Glial Neurobiology: A text book*. John Wiley & Sons Ltd, The Atrium, West Sussex, England.
- Villalba, A., Coll, O., and Gebauer, F. (2011). Cytoplasmic polyadenylation and translational control. *Curr Opin Genet Dev* *21*, 452-457.
- Voutsinos-Porche, B., Knott, G., Tanaka, K., Quairiaux, C., Welker, E., and Bonvento, G. (2003). Glial glutamate transporters and maturation of the mouse somatosensory cortex. *Cereb Cortex* *13*, 1110-1121.
- Wallraff, A., Kohling, R., Heinemann, U., Theis, M., Willecke, K., and Steinhauser, C. (2006). The impact of astrocytic gap junctional coupling on potassium buffering in the hippocampus. *J Neurosci* *26*, 5438-5447.
- Wallraff, A., Odermatt, B., Willecke, K., and Steinhauser, C. (2004). Distinct types of astroglial cells in the hippocampus differ in gap junction coupling. *Glia* *48*, 36-43.



- Wang, X., Lou, N., Xu, Q., Tian, G.F., Peng, W.G., Han, X., Kang, J., Takano, T., and Nedergaard, M. (2006). Astrocytic Ca<sup>2+</sup> signaling evoked by sensory stimulation in vivo. *Nat Neurosci* 9, 816-823.
- Wells, D.G. (2006). RNA-binding proteins: a lesson in repression. *J Neurosci* 26, 7135-7138.
- Wells, D.G., Richter, J.D., and Fallon, J.R. (2000). Molecular mechanisms for activity-regulated protein synthesis in the synapto-dendritic compartment. *Curr Opin Neurobiol* 10, 132-137.
- Wiencken-Barger, A.E., Djukic, B., Casper, K.B., and McCarthy, K.D. (2007). A role for Connexin43 during neurodevelopment. *Glia* 55, 675-686.
- Wilczynska, A., Aigueperse, C., Kress, M., Dautry, F., and Weil, D. (2005). The translational regulator CPEB1 provides a link between dcp1 bodies and stress granules. *J Cell Sci* 118, 981-992.
- Wu, L., Wells, D., Tay, J., Mendis, D., Abbott, M.A., Barnitt, A., Quinlan, E., Heynen, A., Fallon, J.R., and Richter, J.D. (1998). CPEB-mediated cytoplasmic polyadenylation and the regulation of experience-dependent translation of alpha-CaMKII mRNA at synapses. *Neuron* 21, 1129-1139.
- Xu, H.F., Ding, Y.J., Shen, Y.W., Xue, A.M., Xu, H.M., Luo, C.L., Li, B.X., Liu, Y.L., and Zhao, Z.Q. (2012). MicroRNA-1 represses Cx43 expression in viral myocarditis. *Mol Cell Biochem* 362, 141-148.
- Zhao, C., Deng, W., and Gage, F.H. (2008). Mechanisms and functional implications of adult neurogenesis. *Cell* 132, 645-660.
- Zonta, M., Angulo, M.C., Gobbo, S., Rosengarten, B., Hossmann, K.A., Pozzan, T., and Carmignoto, G. (2003). Neuron-to-astrocyte signaling is central to the dynamic control of brain microcirculation. *Nat Neurosci* 6, 43-50.

## 9 Appendix

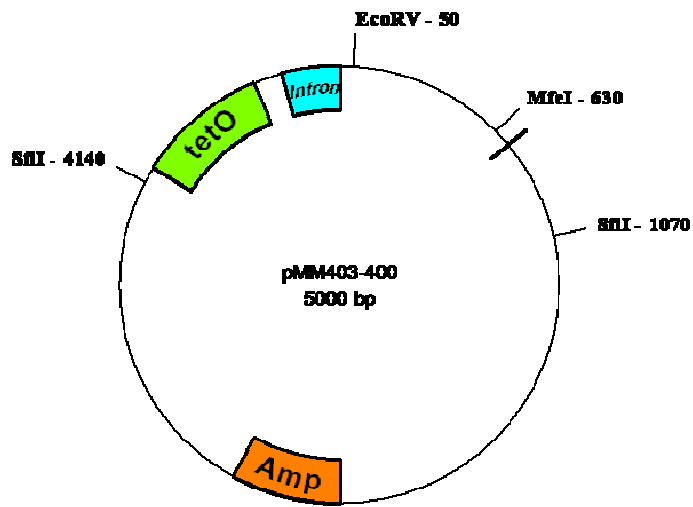
### I. Competent cells preparation for transformation

A sterile loop was used to take cells from a glycerol stock (containing commercially available *E. coli*. K12 cells, Invitrogen), inoculated in 2.5 ml of YT++ medium and incubated by shaking at 37°C/overnight/250 rpm. 200 µl of overnight culture was added to 5 ml of YT++ medium and shaken for 1.5 hr at 37°C (during this time 100 ml of YT++ medium was prewarmed in a flask at 37°C). OD at 600 nm was determined using a spectrophotometer (Eppendorf) which should lie in between 0.7 – 0.8. The complete 5 ml culture was poured into 100 ml of prewarmed YT++ medium and shaken for 2 hr at 37°C. The OD at 600 nm was determined and if it was  $\geq 0.5$ , the growth was stopped by incubating the flask on ice for 5 min. The culture was centrifuged at 3500 rpm for 5 min by aliquoting into two 50 ml falcons. The supernatant was discarded and the pellet was resuspended in 10 ml of TFBI buffer and incubated on ice for 10 min. Following a centrifugation at 3500 rpm for 5 min, the supernatant was discarded and the pellet was resuspended in 2 ml of TFBII buffer. Appropriate amounts of aliquots were prepared in 1.5 ml Eppendorf tubes and frozen immediately in liquid nitrogen. Tubes with cells were stored at -80°C.

#### Buffers:

Medium / Buffer	Contents	Preparation
YT medium	8 g tryptone 5 g yeast extract 5 g NaCl pH - 7.5	Dissolved in 1 l of dH <sub>2</sub> O Sterilization by autoclaving
YT++ medium	YT medium 20 mM MgSO <sub>4</sub> 10 mM KCl	80 ml YT medium 10 ml MgSO <sub>4</sub> (sterile filtered) 10 ml KCl (sterile filtered)
TFBI	30 mM KAC 50 mM MnCl <sub>2</sub> 100 mM RbCl 10 mM CaCl <sub>2</sub> 15 % glycerol in dH <sub>2</sub> O	Sterile filtered
TFBII	10 mM Na MOPS 75 mM CaCl <sub>2</sub> 10 mM RbCl 15 % glycerol in dH <sub>2</sub> O	Sterile filtered

## II. pMM403-400 vector map



## List of Figures

- Figure 1: CPEB general domain structure
- Figure 2: A model of synapse-specific translational control
- Figure 3: CPEB3 domain structure with B and C regions
- Figure 4: Schematic showing the tetracycline based inducible gene expression
- Figure 5: Gap junctional plaque – Molecular organization and schematic topology
- Figure 6: Schematic showing the adult neurogenesis in mammals
- Figure 7: Astrocyte dysfunction in epilepsy
- Figure 8: RT-PCR for CPEBs on primary astrocyte cultures for CPEBs
- Figure 9: Staining for different CPEB (1-4) proteins in primary astrocyte cultures
- Figure 10: Decreased Cx43 and GFAP expression in primary astrocyte cultures
- Figure 11: Schematic showing the Tet-off system.
- Figure 12: Gel image showing the genotyping PCR
- Figure 13: Expression of CPEB3-EGFP across brain regions
- Figure 14: Localization of CPEB3-EGFP in astrocytes
- Figure 15: Nissl stained coronal section of CPEB3-GFAP mice
- Figure 16: Comparison of CPEB3-EGFP expression during and after dox application
- Figure 17: Extent of CPEB3 overexpression in astrocytes
- Figure 18: Specificity of CPEB3 expression
- Figure 19: GFAP immunoreactivity
- Figure 20: No change in GFAP protein levels
- Figure 21: CPEB3 overexpression did not affect the number of astrocytes
- Figure 22: Staining for TUNEL positive cells.
- Figure 23: Co-IP of Cx43 mRNA
- Figure 24: Co-IP of Cx30 mRNA
- Figure 25: Co-IP of GS mRNA
- Figure 26: Downregulation of Cx43
- Figure 27: Downregulation of Cx30
- Figure 28: Interastrocytic coupling is reduced in CPEB3 mice
- Figure 29: Selectivity of biocytin uptake
- Figure 30: Reduced proliferation in SGZ
- Figure 31: Decreased granule neurons
- Figure 32: Reduction in the number of BLBP positive cells

Figure 33: Downregulation of GS

Figure 34: Downregulation of GLT-1

Figure 35: No change in the transcript levels of CPEB3 targets analyzed

Figure 36: Localization of endogenous CPEB3 with overexpressed protein

Figure 37: Localization of endogenous CPEB3 in ECFP positive astrocytes

Figure 38: Schematic of CPEB3 3' UTR with CPEs and poly (A) sequences

## **List of Tables**

Table 1: Classification of mature astrocytes

Table 2: Functions of astrocytes

Table 3: Reverse Transcription reaction mix for astrocyte cultures

Table 4: Primer sequences for splice isoforms of CPEBs (1-4)

Table 5: PCR program for CPEB isoforms

Table 6: Primer used for CPEB3 RACE

Table 7: PCR program for CPEB3 RACE

Table 8: Touchdown PCR program for CPEB3 RACE

Table 9: Two step PCR program for infusion cloning

Table 10: Primer sequences for CPEB3sh and IgUTR amplification

Table 11: Primer sequences for genotyping (TetO and tTA) PCR

Table 12: Reaction mix for genotyping PCR

Table 13: PCR program for genotyping PCR

Table 14: Reverse transcription reaction mix for RNA from mouse brain

Table 15: Real time PCR primer and probe sequences of transcripts

Table 16: Primers for GS 3' RACE

Table 17: PCR program for generating luciferase vectors

Table 18: Primers used for generating GS luciferase vectors

Table 19: Primers used for generating Cx30 luciferase vectors

Table 20: Reverse transcription reaction mix for RNA extracted from Co-IP samples

Table 21: *Taq*-man primer and probe sequences used for Real time of RNA Co-IP samples

Table 22: Distribution CPEB isoforms

Table 23: Putative CPEB targets expressed in astrocytes

Table 24: Quantitative evaluation of Ki-67 expression

Table 25: Quantitative evaluation of Prox1 expression in the dentate gyrus

Table 26: Quantitative evaluation of BLBP expression in the dentate gyrus

## **Curriculum Vitae**

Name : **Vamshidhar Reddy Vangoor**  
 Birth place : Mahabubnagar, India

### **Education:**

- Since June 2012: Working as a **Postdoctoral researcher** at the Department of Neuroscience and Pharmacology, Rudolf Magnus institute, UMC Utrecht, Netherlands.  
 Group leaders: Prof. Dr. Jeroen Pasterkamp and Dr. Pierre de Graan.
- 2007 – 2012: **PhD** in Prof. Martin Theis lab, Institute of Cellular Neurosciences, University of Bonn, Germany.  
 Thesis title: *Overexpression of CPEB3 leads to astrocyte dysfunction.*
- 2006 – 2007: **Masters in Molecular Biology** at University of Skövde, Sweden.  
**Master thesis** in the lab of Prof. Martin Theis, Institute of Cellular Neurosciences, University of Bonn, Germany.  
 Thesis title: *Characterization of normal and mutated forms of CPEB3 and CPEB4 in neural cells.*
- 1999 – 2003: **Bachelor of Pharmacy** from Jawaharlal Nehru Technological University, Hyderabad, India.
- 1996 – 1998: Secondary school education, India.

### **Presentations at Scientific Meetings:**

**Vangoor VR** et al., (2009, 2011). 9<sup>th</sup> and 10<sup>th</sup> European meeting on Glial Cells in Health and Disease.

**Vangoor VR** et al., (2009, 2011). 8<sup>th</sup> and 9<sup>th</sup> Goettingen meeting of the German Neuroscience Society, Germany.

**Vangoor VR** et al., (2010). Society for Neuroscience (SFN) meeting, San Diego, USA.

### **Manuscripts:**

CPEB3 regulates the translation of Cx43 and Cx30, interastrocytic coupling and adult neurogenesis. (*PNAS*, in revision)

**Vangoor VR**, Turimella SL, Zhang J, Kaczmarczyk L, Bedner P, Passlick S, von Staden E, Derouiche A, Jabs R, Seifert G, Steinhäuser C and Theis M.

Expression of new CPEB1 and CPEB2 splice isoforms in hippocampal neurons and their RNA binding activities. (*Journal of Comparative Neurology*, in revision)

Turimella SL, **Vangoor VR**, Kaczmarczyk L, Bedner P, Karl K, Zoidl G, Seifert G, Steinhäuser C, Kandel ER and Theis M.

Expression of Cytoplasmic Polyadenylation Element Binding Proteins 3 and 4 in neurons, microglial cells and NG2 glia. (*Brain Research*, in revision)

Turimella SL\*, **Vangoor VR\***, Bedner P, Kaczmarczyk L, Borojerdi A, Karram K, Trotter J and Theis M.

The impact of Cytoplasmic Polyadenylation Element Binding Protein (CPEB)-mediated translational regulation on development and progression of temporal lobe epilepsy: Evidence from mice expressing a dominant negative CPEB in forebrain neurons (*Manuscript in preparation*).

Bedner P, Dublin P, Turimella SL, **Vangoor VR**, Hüttmann K, Kandel ER, Steinhäuser C and Theis M.